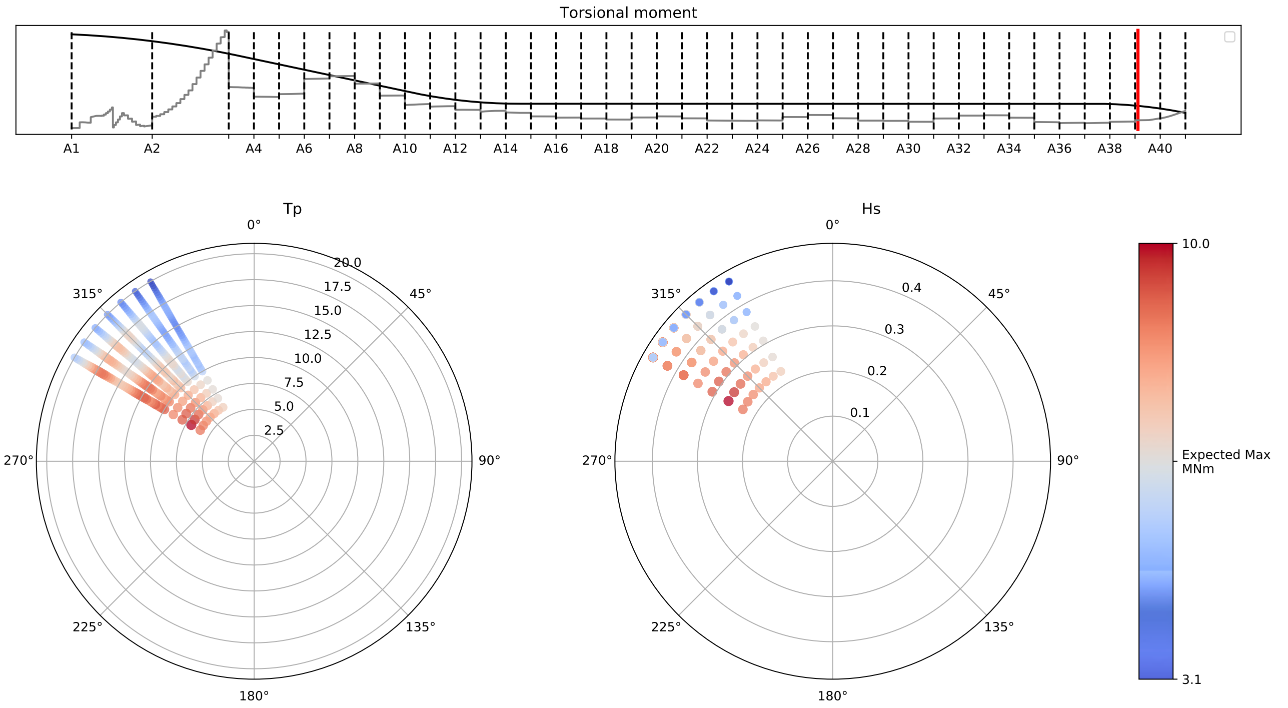
Torsional moment
A1
A2
A4
A6
A8
A10
A12
A14
A16
A18
A20
A22
A24
A26
A28
A30
A32
A34
A36
A38
A40
Tp
Hs
0°
45°
90°
135°
180°
225°
270°
315°
20.0
17.5
15.0
12.5
10.0
7.5
5.0
2.5
0.4
0.3
0.2
0.1
10.0
3.1
Expected Max
MNm

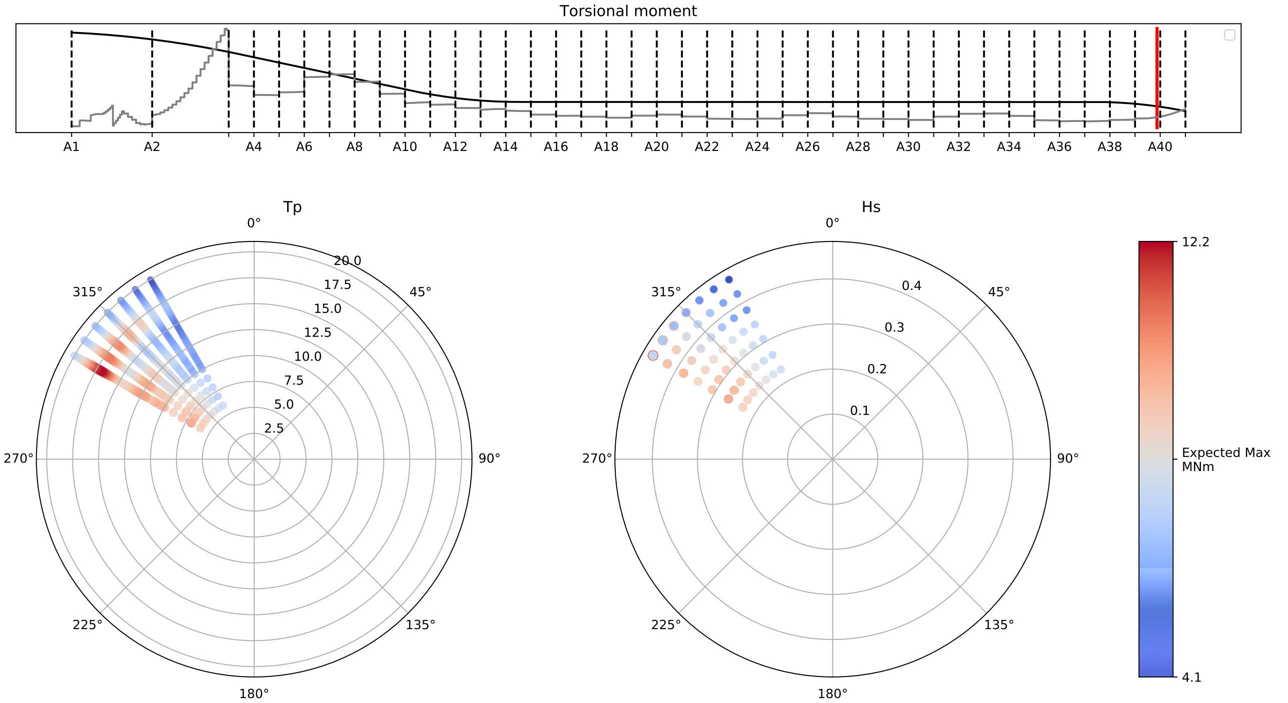
Torsional moment
A1
A2
A4
A6
A8
A10
A12
A14
A16
A18
A20
A22
A24
A26
A28
A30
A32
A34
A36
A38
A40
Tp
Hs
0°
45°
90°
135°
180°
225°
270°
315°
20.0
17.5
15.0
12.5
10.0
7.5
5.0
2.5
0.4
0.3
0.2
0.1
12.2
4.1
Expected Max
MNm

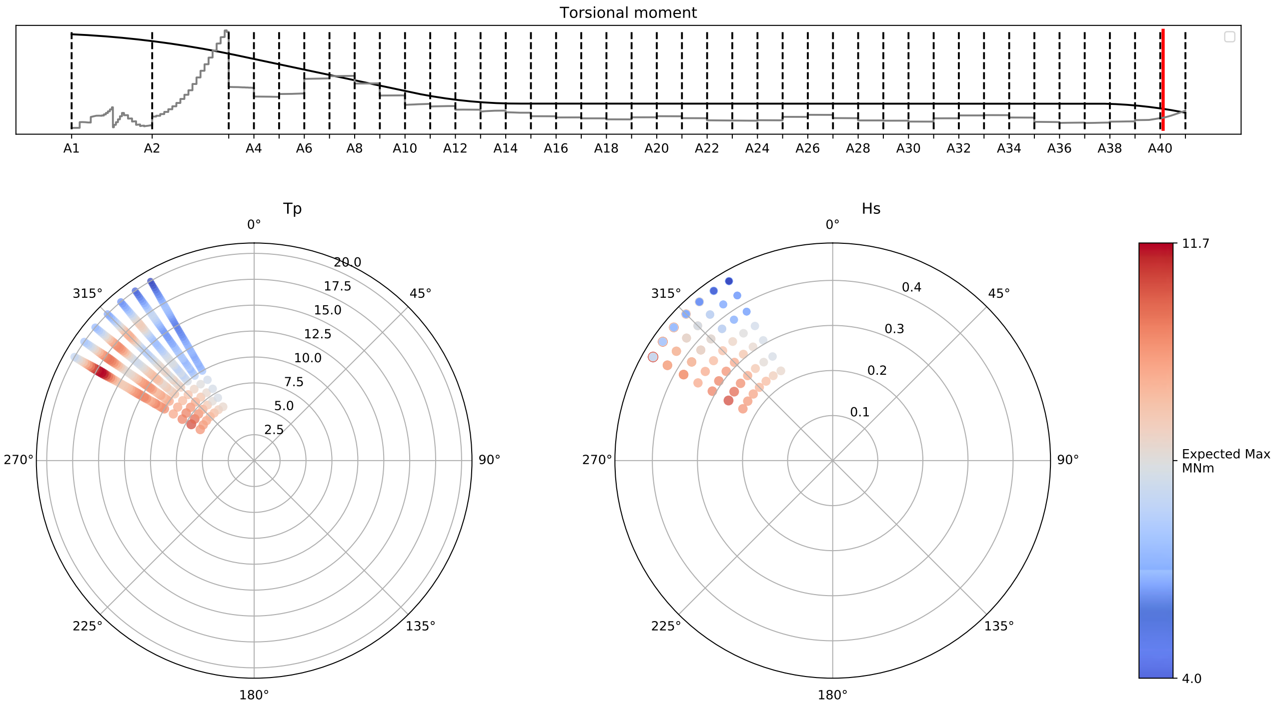
Torsional moment
A1
A2
A4
A6
A8
A10
A12
A14
A16
A18
A20
A22
A24
A26
A28
A30
A32
A34
A36
A38
A40
Tp
Hs
11.7
Expected Max
MNm
4.0

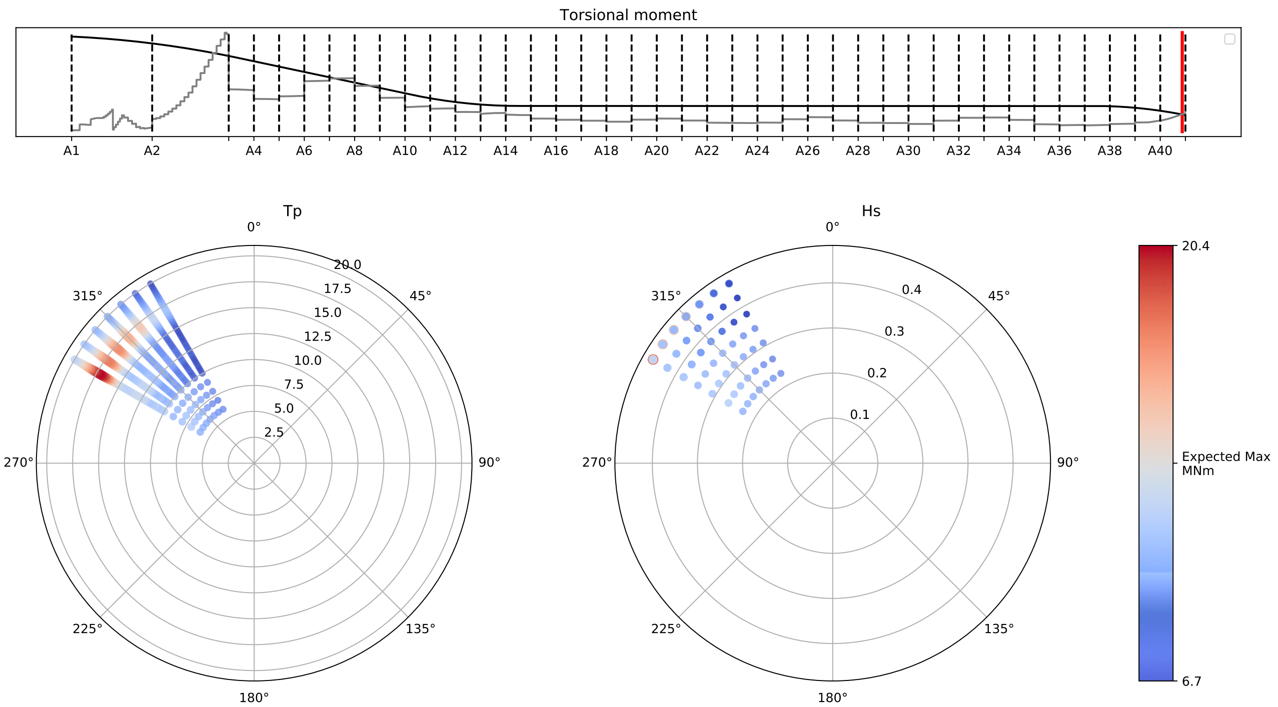
Torsional moment
A1
A2
A4
A6
A8
A10
A12
A14
A16
A18
A20
A22
A24
A26
A28
A30
A32
A34
A36
A38
A40
Tp
Hs
20.4
Expected Max
MNm
6.7

tailor

Concept development, floating bridge
E39 Bjørnafjorden

Appendix G – Enclosure 12

Load combination motions

K12_07_PROD_load_combinations_direct

June 26, 2019

Contents

1 Load groups

1.1 Dynamic wind 1 y

run case	Description
1	From west
2	From east

1.2 Static wind 1y

run case	Description
1	From west
2	From east

1.3 Wave 1 y

run case	Description
1	Hs=1.0, Tp=4.0, dir=75
2	Hs=0.9, Tp=3.7, dir=105
3	Hs=0.9, Tp=3.7, dir=195
4	Hs=1.2, Tp=4.3, dir=315

1.4 Swell 1 y

run case	Description
1	Hs=0.22, Tp=13.44, dir=300
2	Hs=0.22, Tp=17.07, dir=300

1.5 Dynamic wind 100 y

run case	Description
1	From west
2	From east

1.6 Static wind 100 y

run case	Description
1	From west
2	From east

1.7 Wave 100 y

run case	Description
1	Hs=2.1, Tp=5.5, dir=75
2	Hs=2.1, Tp=5.5, dir=105
3	Hs=1.4, Tp=4.6, dir=195
4	Hs=2.0, Tp=5.2, dir=315

1.8 Swell 100 y

run case	Description
1	Hs=0.34, Tp=13.44, dir=300
2	Hs=0.34, Tp=17.07, dir=300

2 Load combinations

2.1 1 year

2.1.1 Load group info

load group	load_factor	return_period	system	restype	use_envelope
Dynamic wind 1 y	1.12	1	orcaflex	timeseries	False
Static wind 1y	1.12	1	numpy	static	False
Wave 1 y	1.12	1	orcaflex	timeseries	False
Swell 1 y	1.12	1	orcaflex	timeseries	False

2.1.2 Combination info

	Case 1	Case 2	Case 3	Case 4	Case 5	Case 6
Dynamic wind 1 y	2	2	1	1	1	1
Static wind 1y	2	2	1	1	1	1
Wave 1 y	1	2	3	4	3	4
Swell 1 y			1	1	2	2

2.2 100 year

2.2.1 Load group info

load group	load_factor	return_period	system	restype	use_envelope
Dynamic wind 100 y	1.6	100	orcaflex	timeseries	False
Static wind 100 y	1.6	100	numpy	static	False
Wave 100 y	1.6	100	orcaflex	timeseries	False
Swell 100 y	1.6	100	orcaflex	timeseries	False

2.2.2 Combination info

	Case 1	Case 2	Case 3	Case 4	Case 5	Case 6
Dynamic wind 100 y	2	2	1	1	1	1
Static wind 100 y	2	2	1	1	1	1
Wave 100 y	1	2	3	4	3	4
Swell 100 y			1	1	2	2

3 Section types

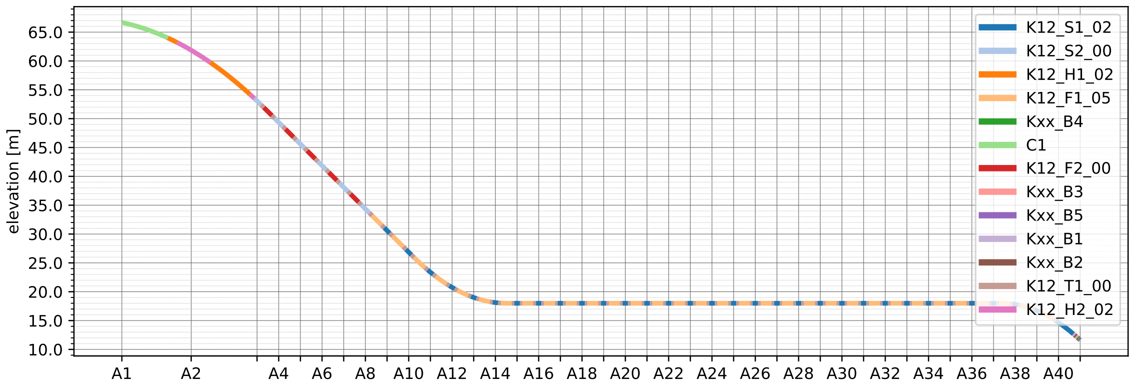

4 Results per load group (characteristic values)

4.1 Vertical displacement

4.1.1 Dynamic wind 1 y

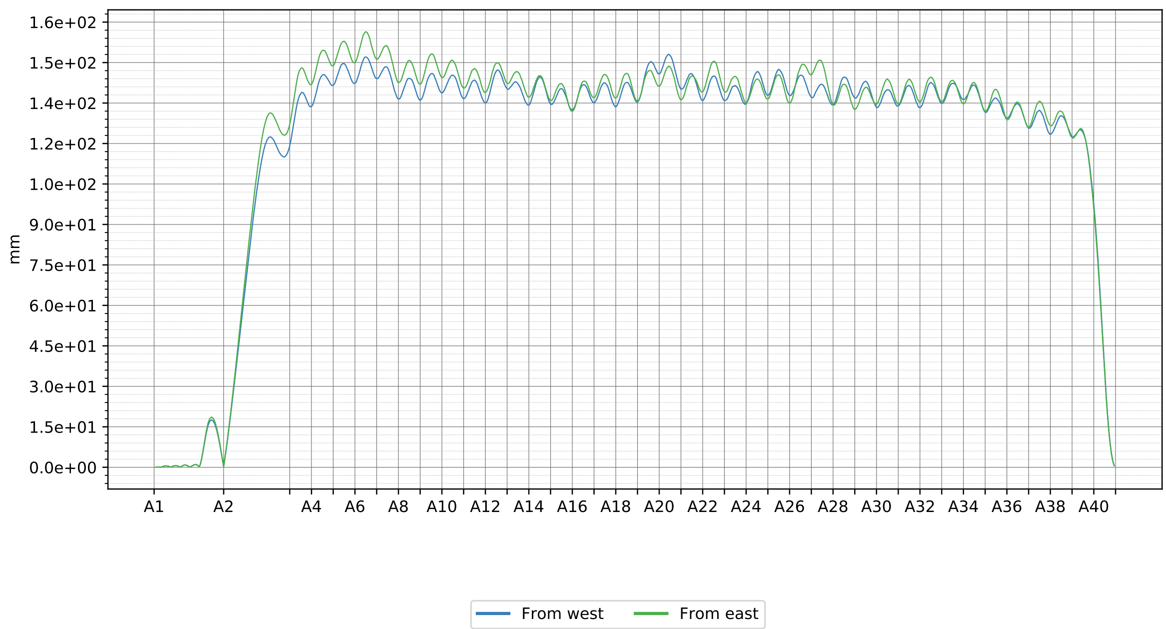

tailor

4.1.2 Static wind 1y

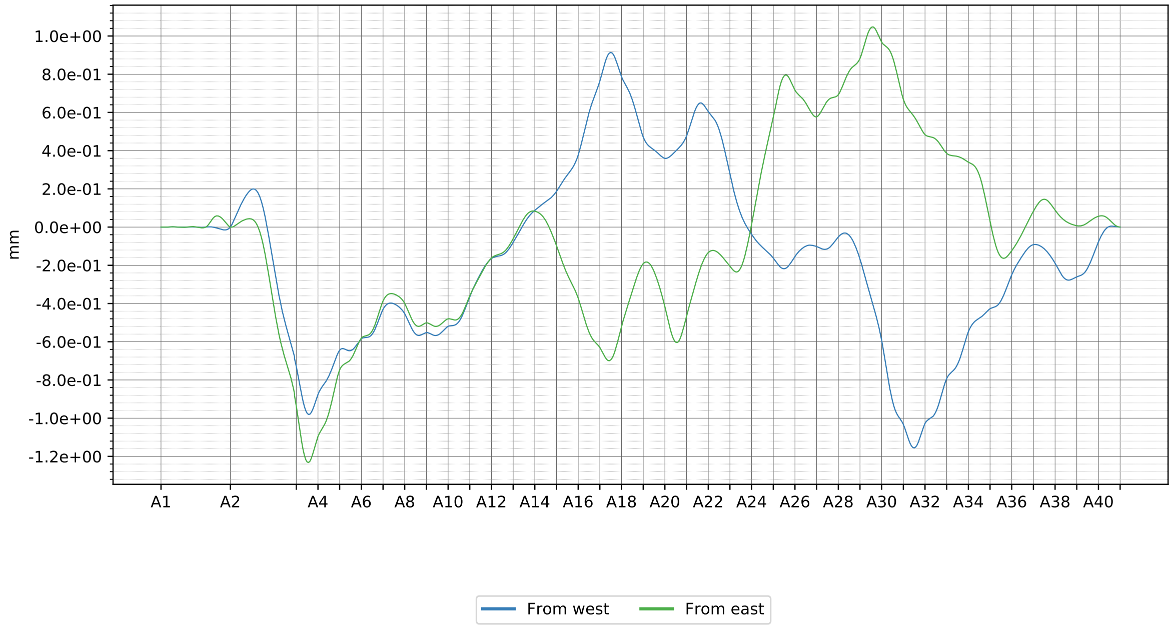

4.1.3 Wave 1 y

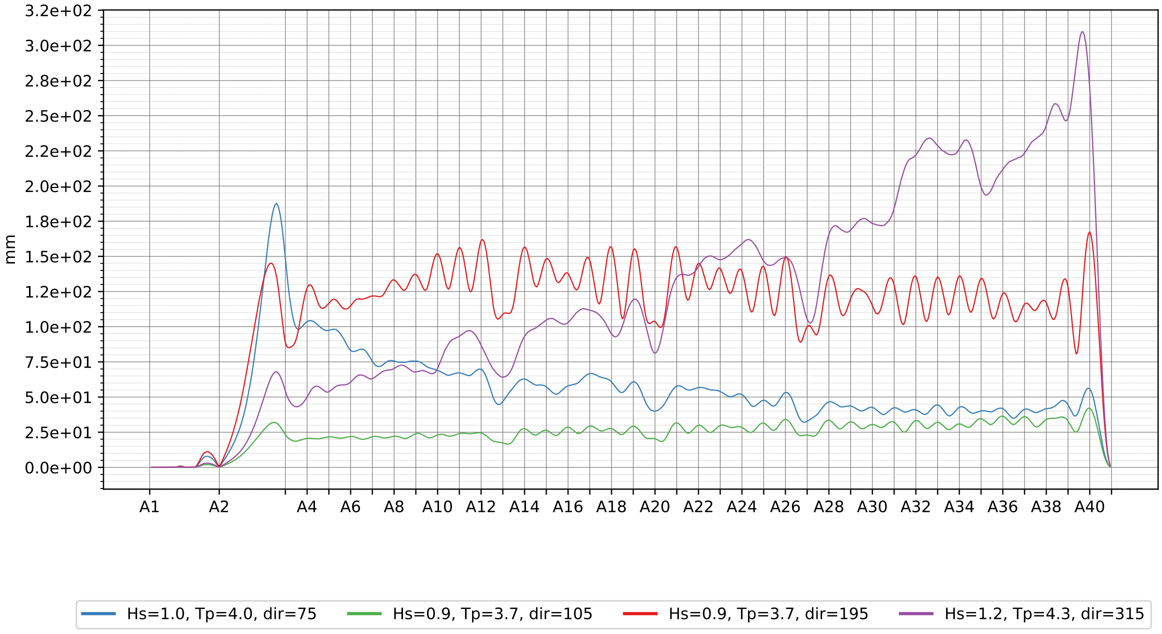

4.1.4 Swell 1 y

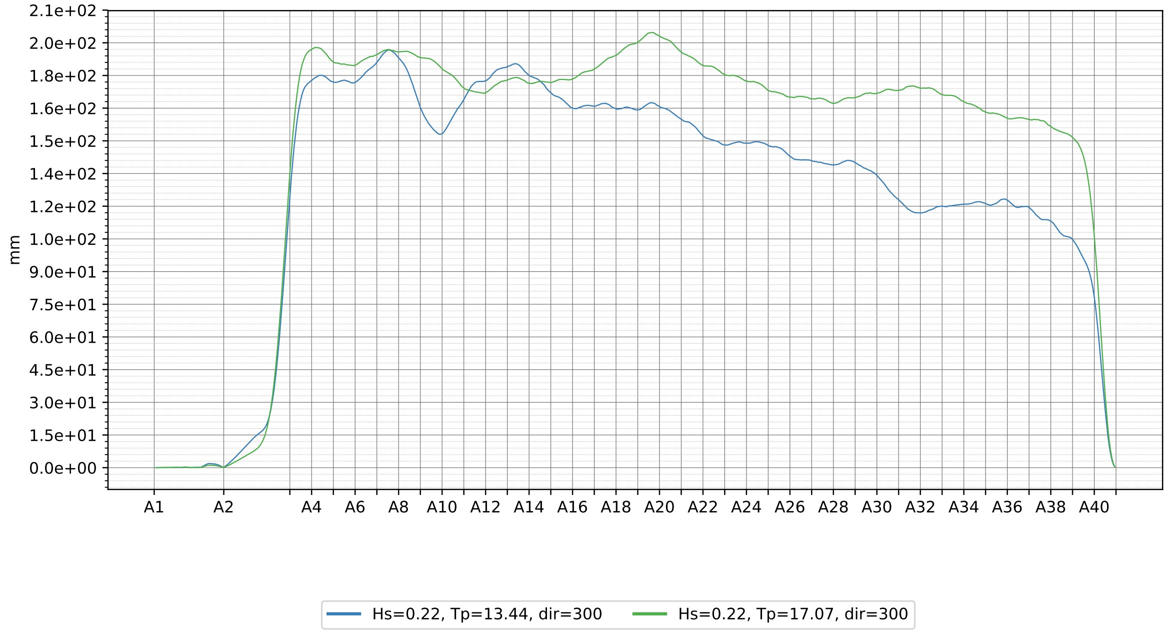

4.1.5 Dynamic wind 100 y

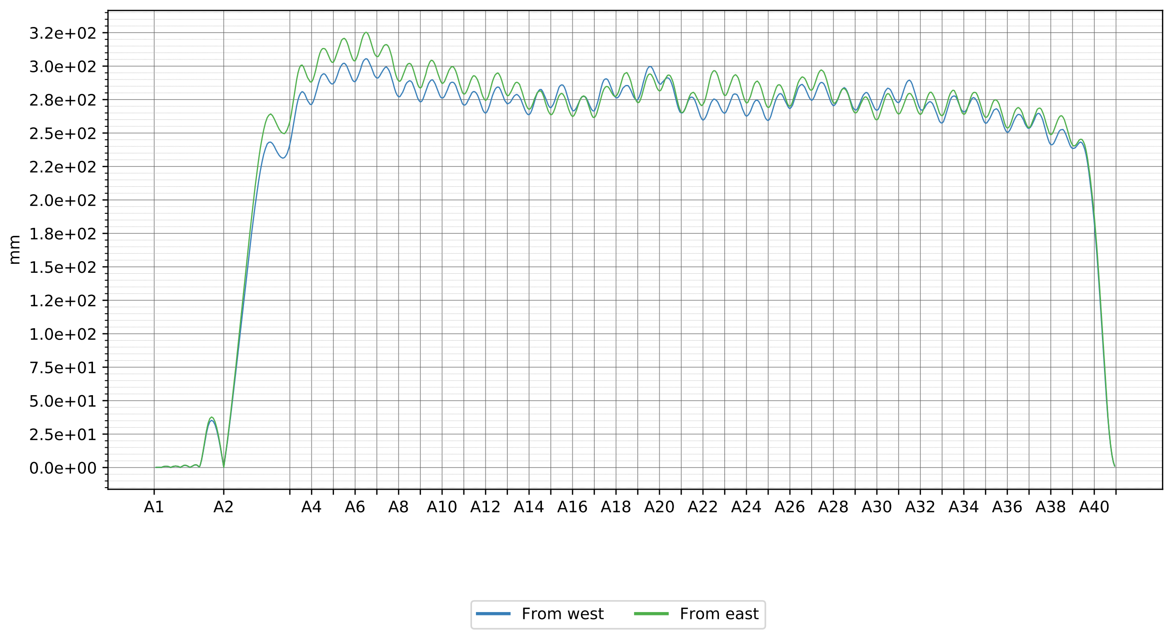

4.1.6 Static wind 100 y

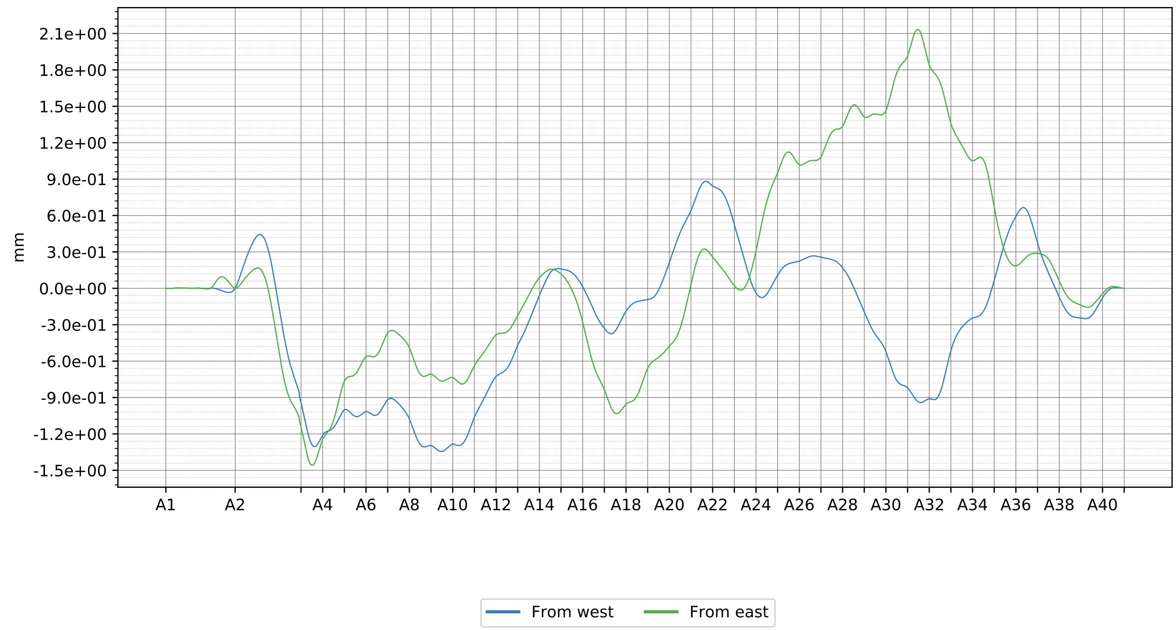

4.1.7 Wave 100 y

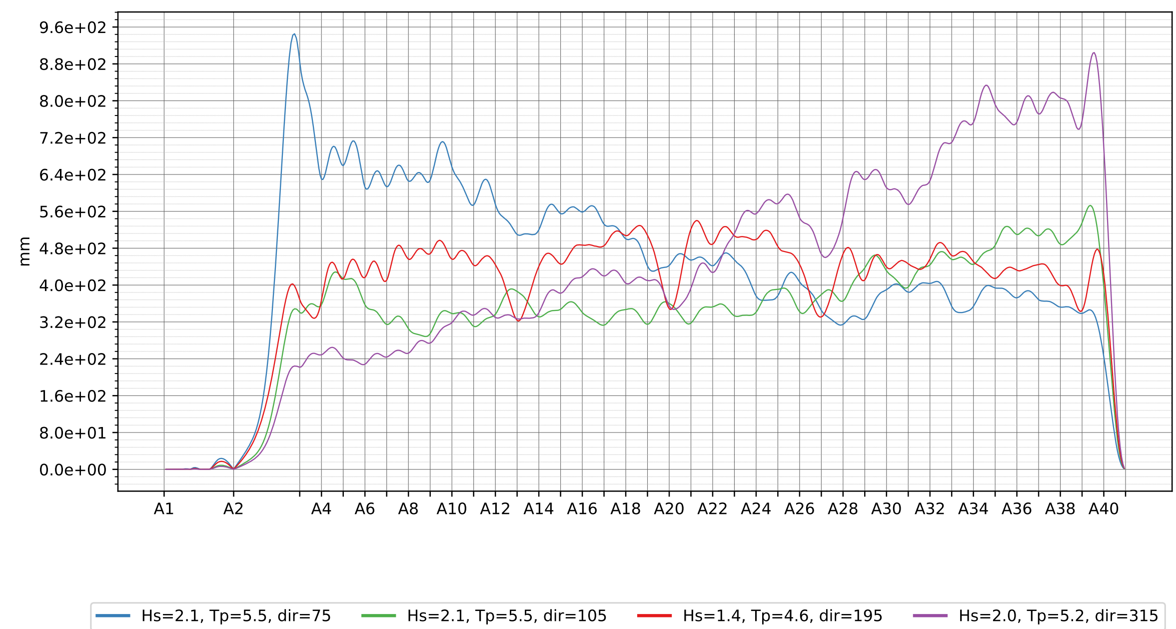

4.1.8 Swell 100 y

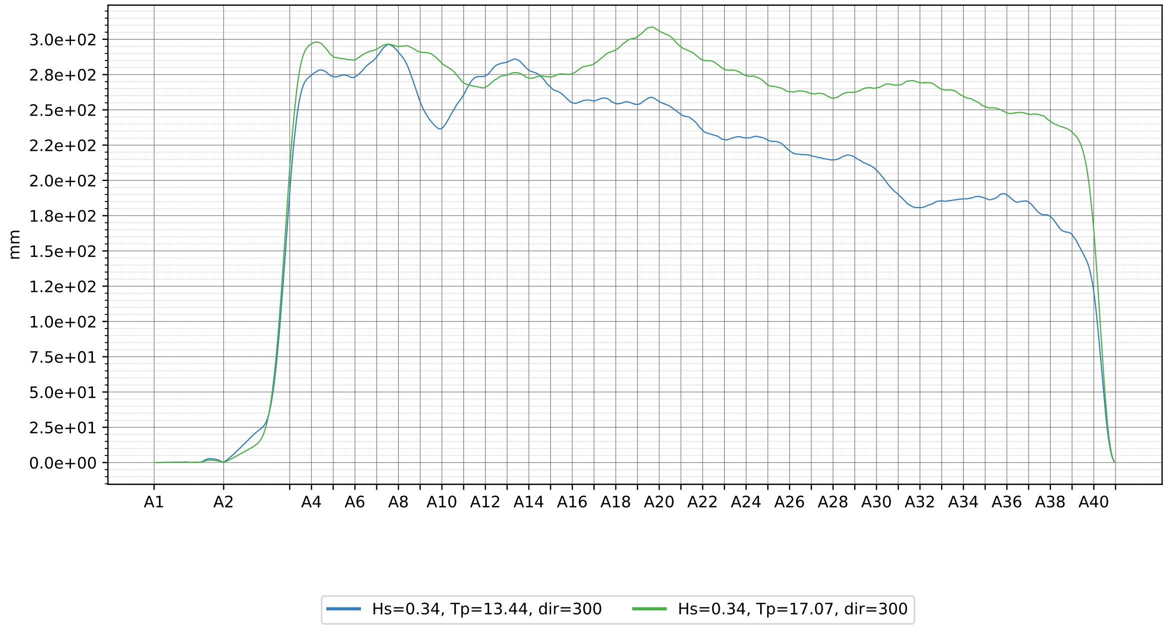

4.2 Transverse displacement

4.2.1 Dynamic wind 1 y

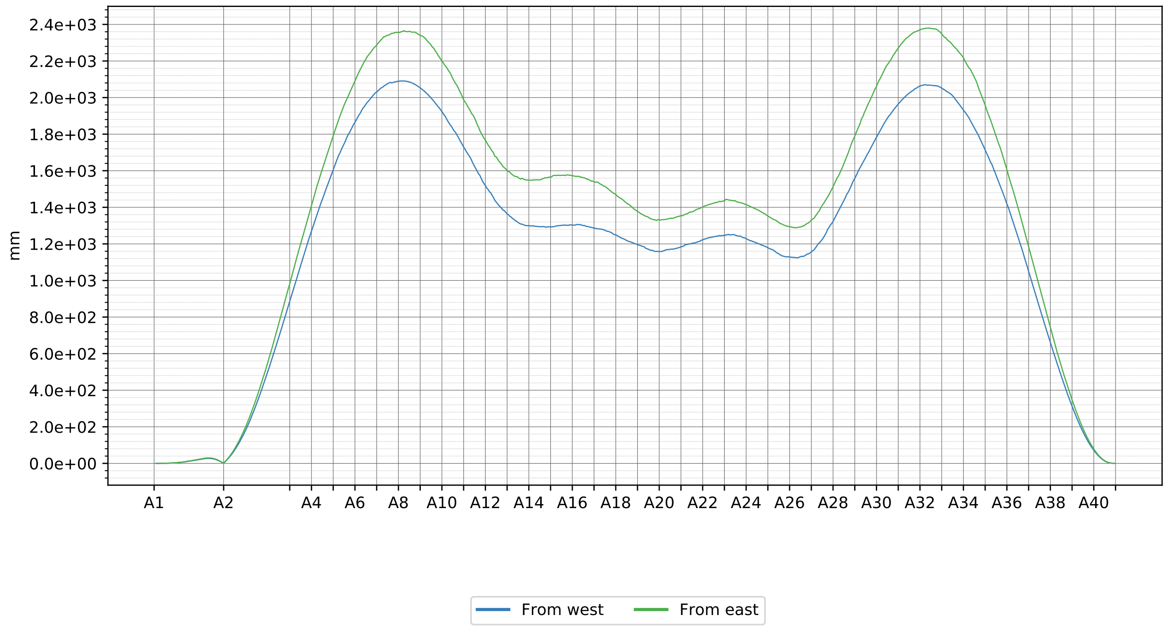

4.2.2 Static wind 1y

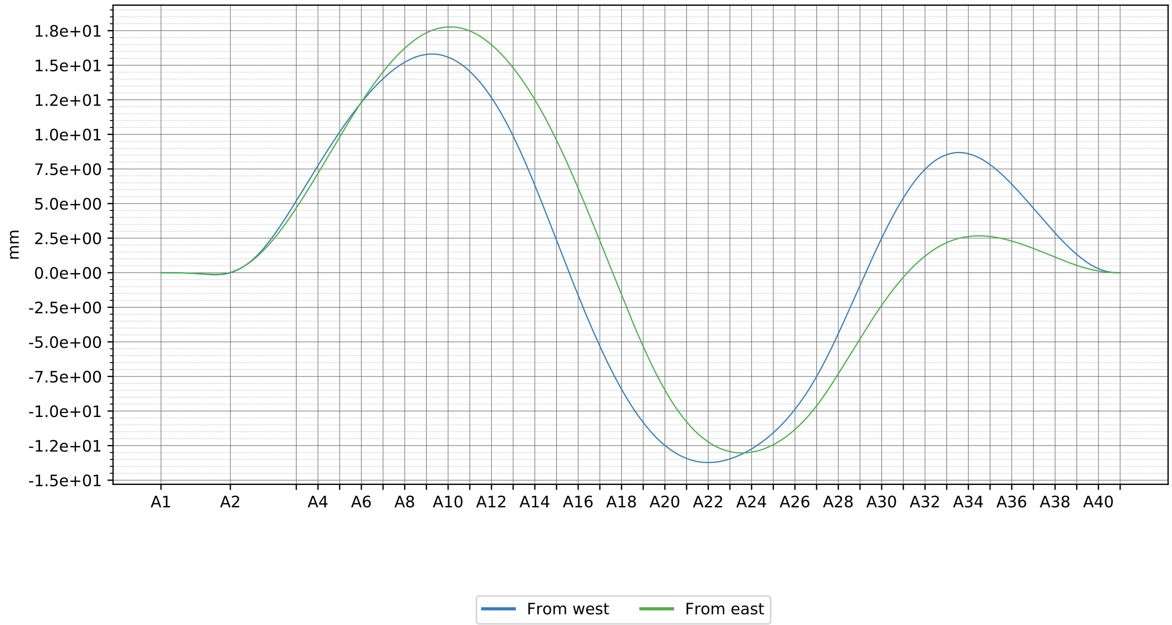

4.2.3 Wave 1 y

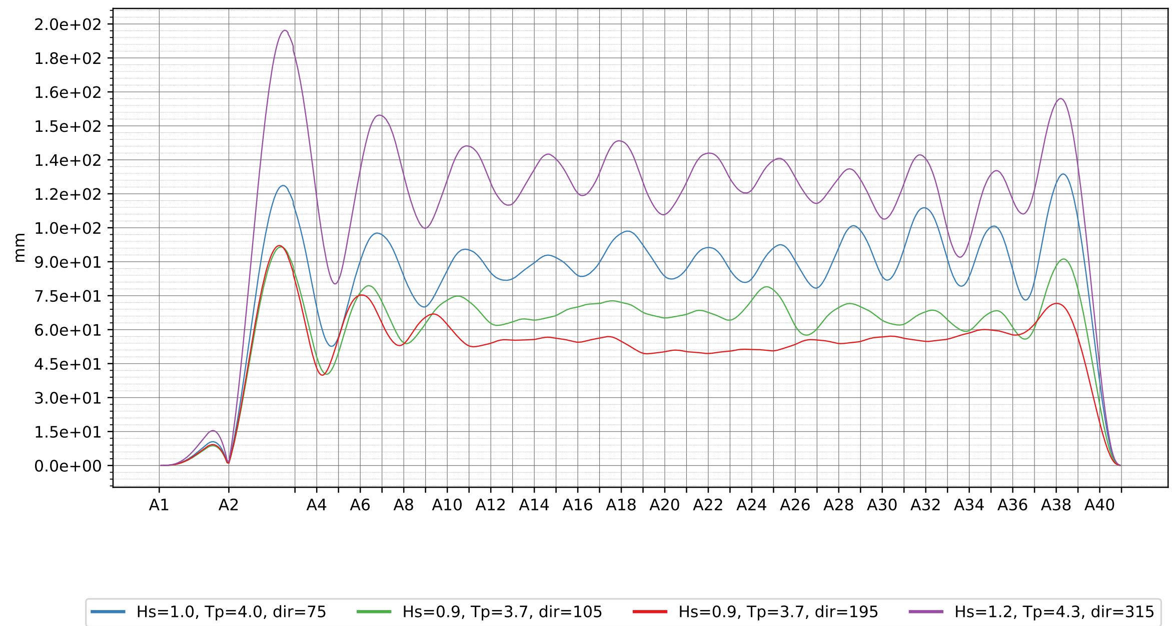

4.2.4 Swell 1 y

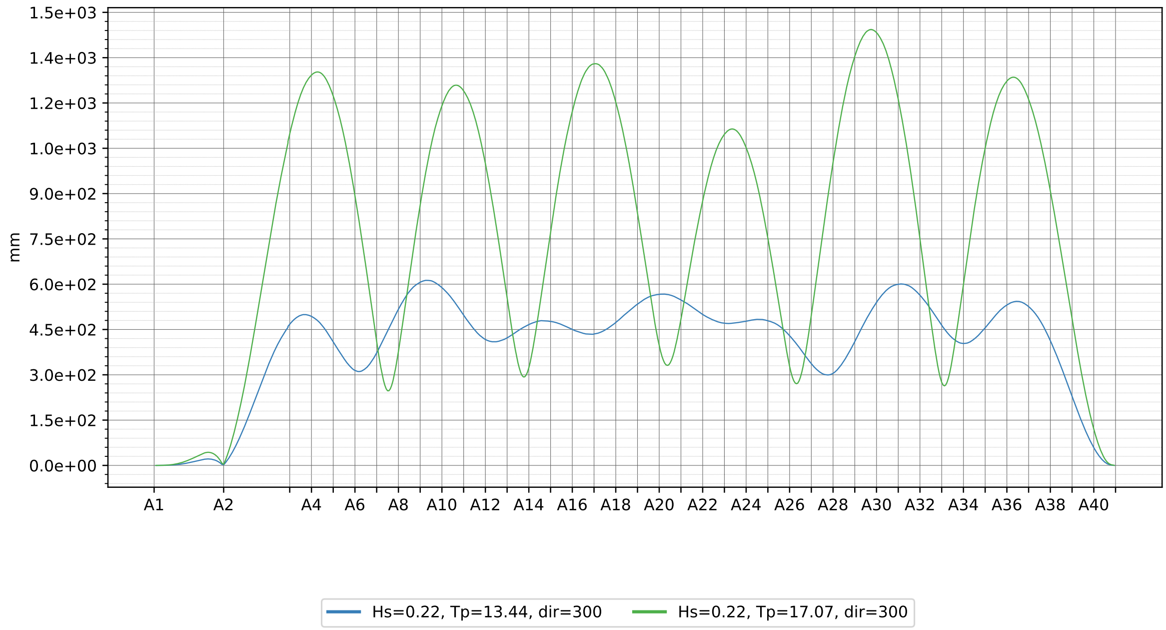

4.2.5 Dynamic wind 100 y

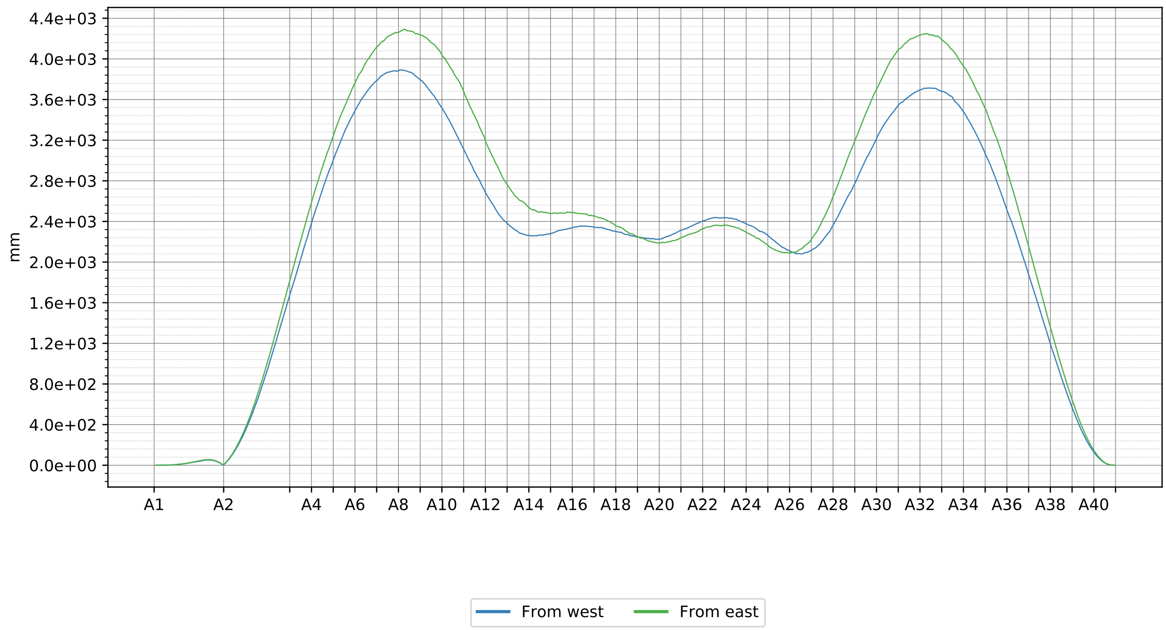

4.2.6 Static wind 100 y

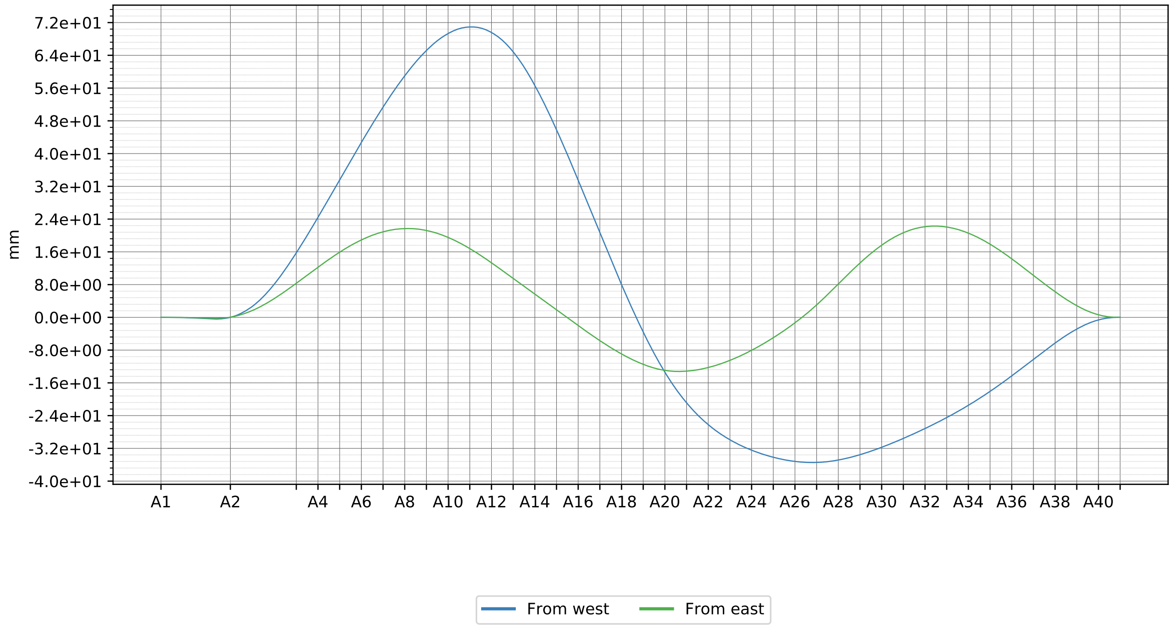

4.2.7 Wave 100 y

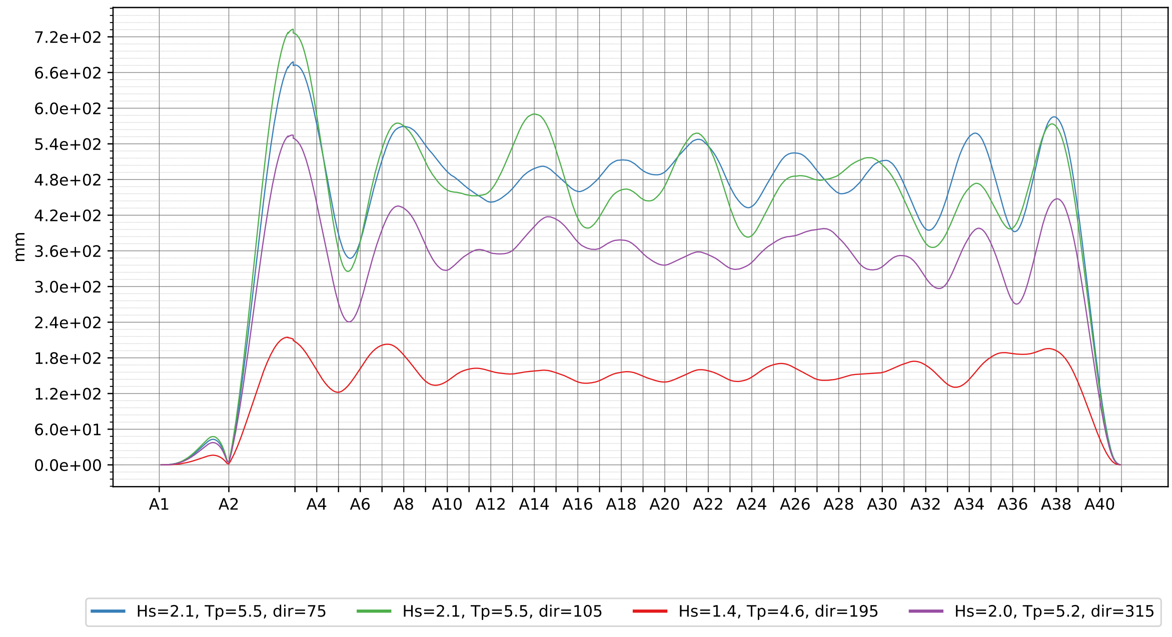

4.2.8 Swell 100 y

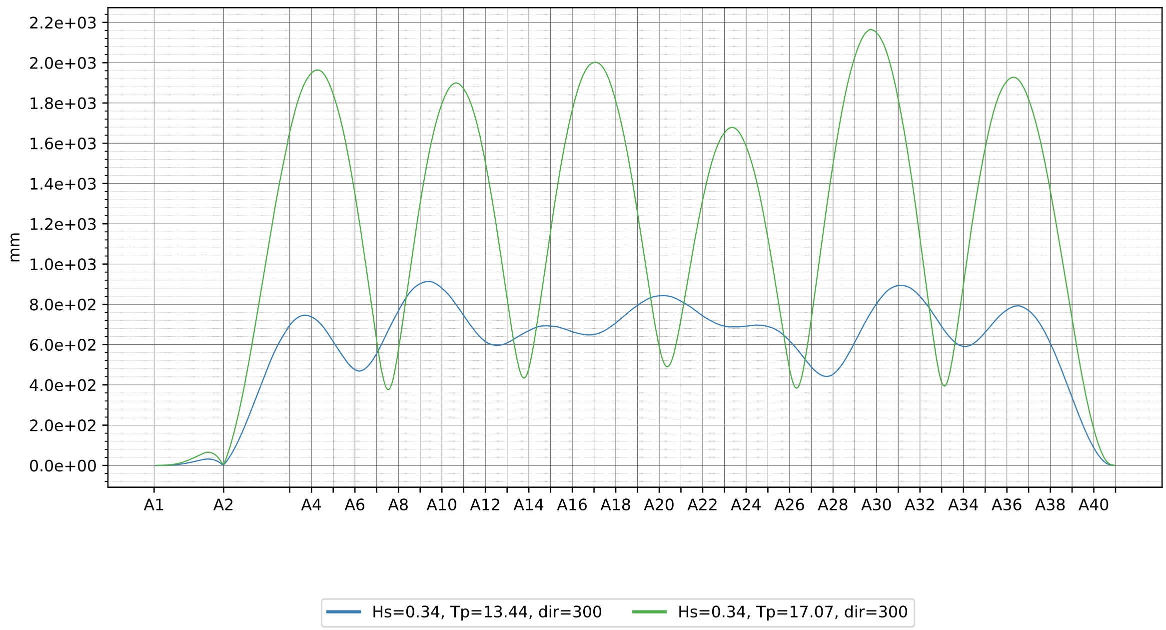

4.3 Longitudinal displacement

4.3.1 Dynamic wind 1 y

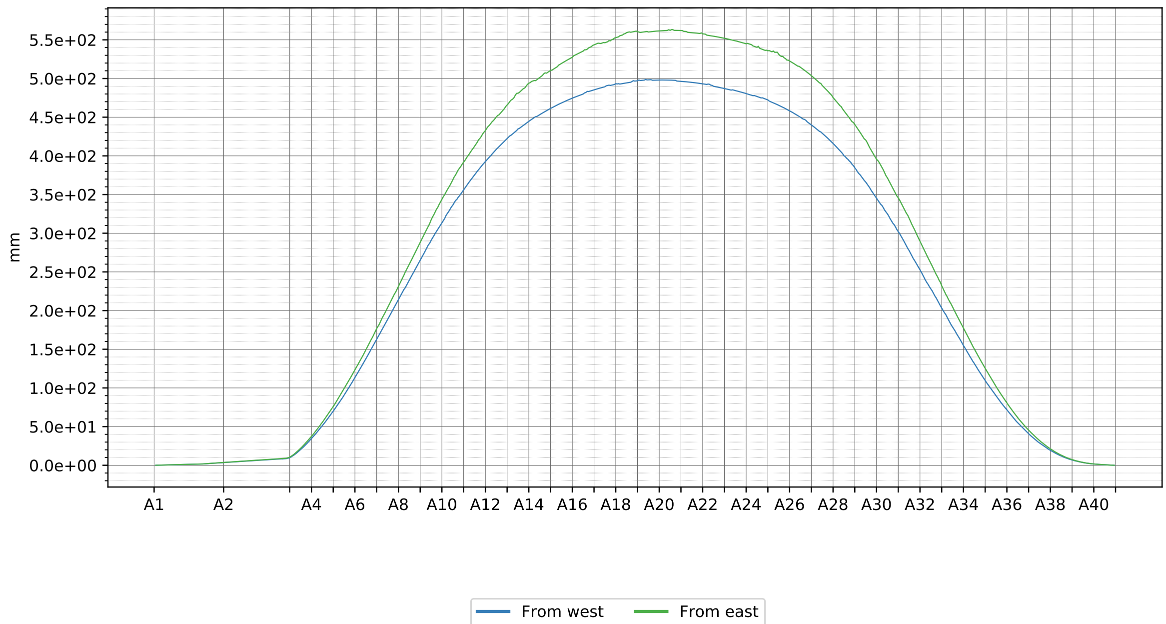

4.3.2 Static wind 1y

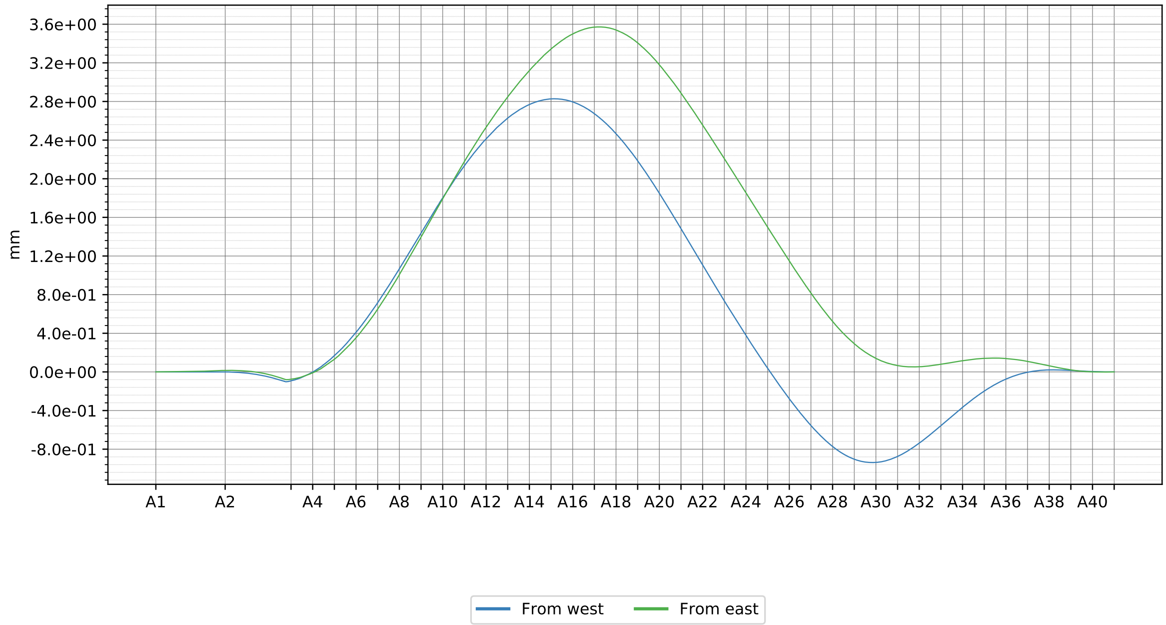

4.3.3 Wave 1 y

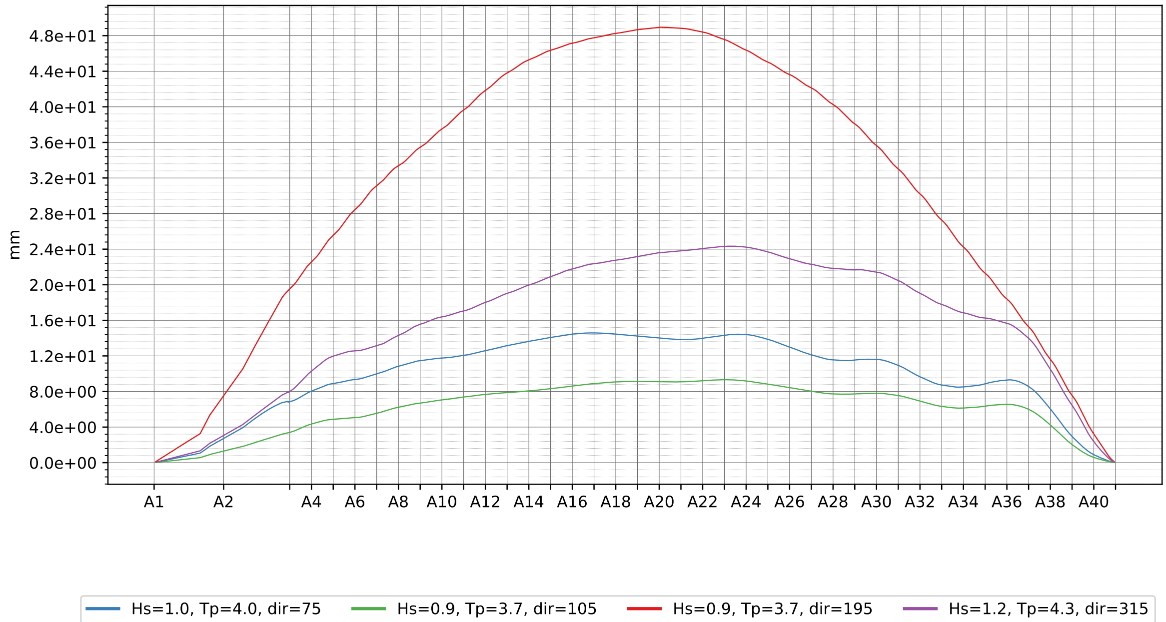

4.3.4 Swell 1 y

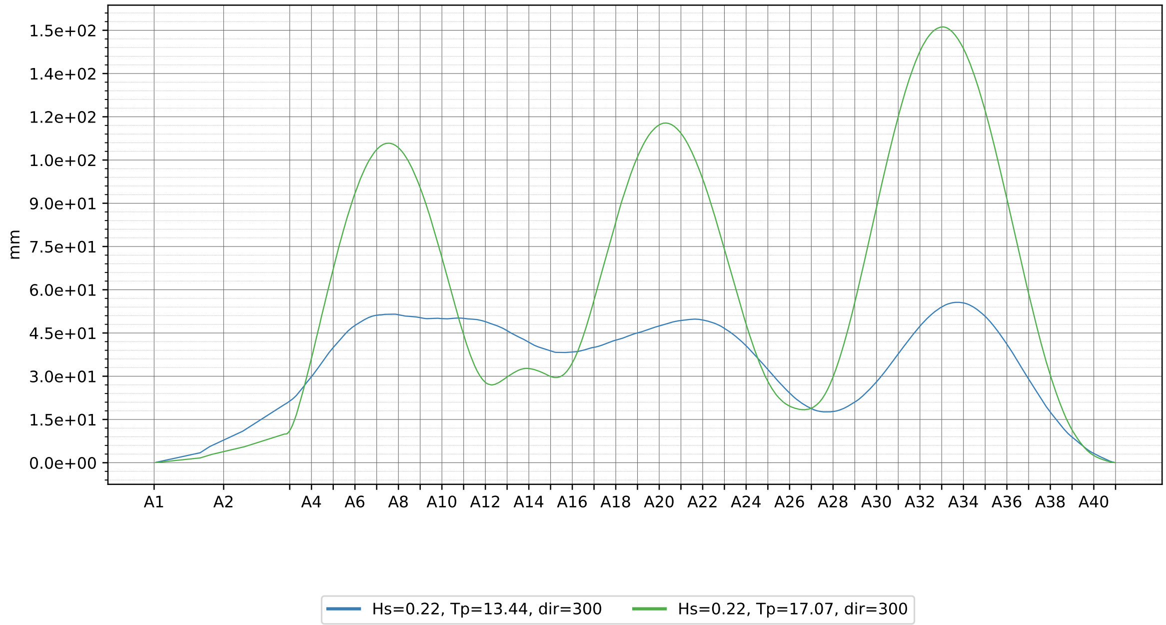

4.3.5 Dynamic wind 100 y

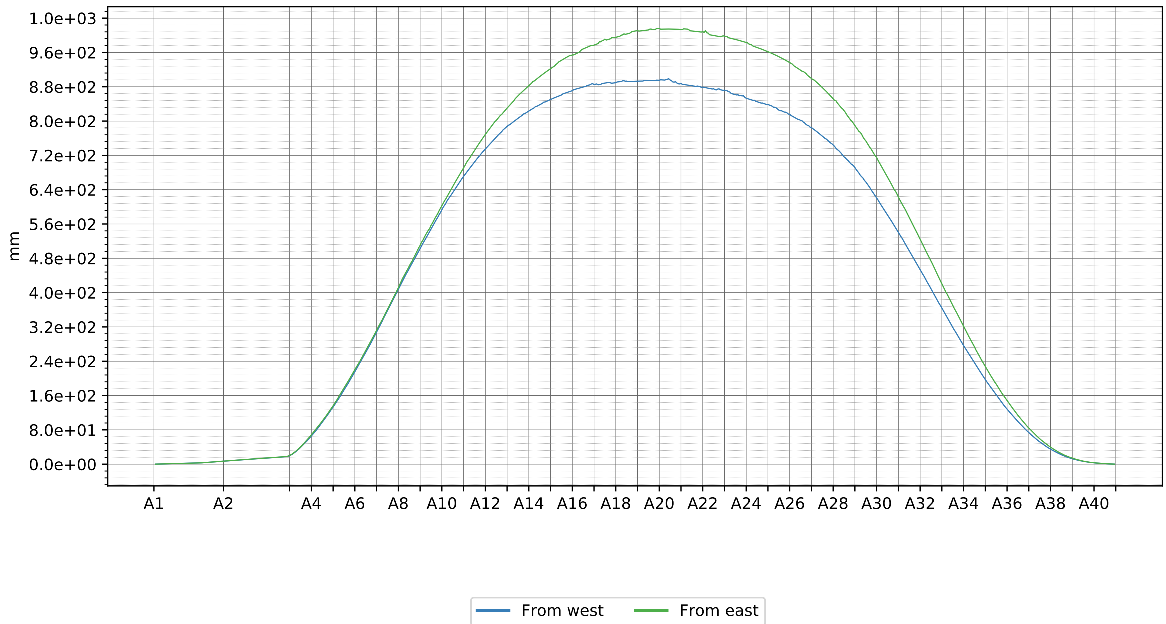

4.3.6 Static wind 100 y

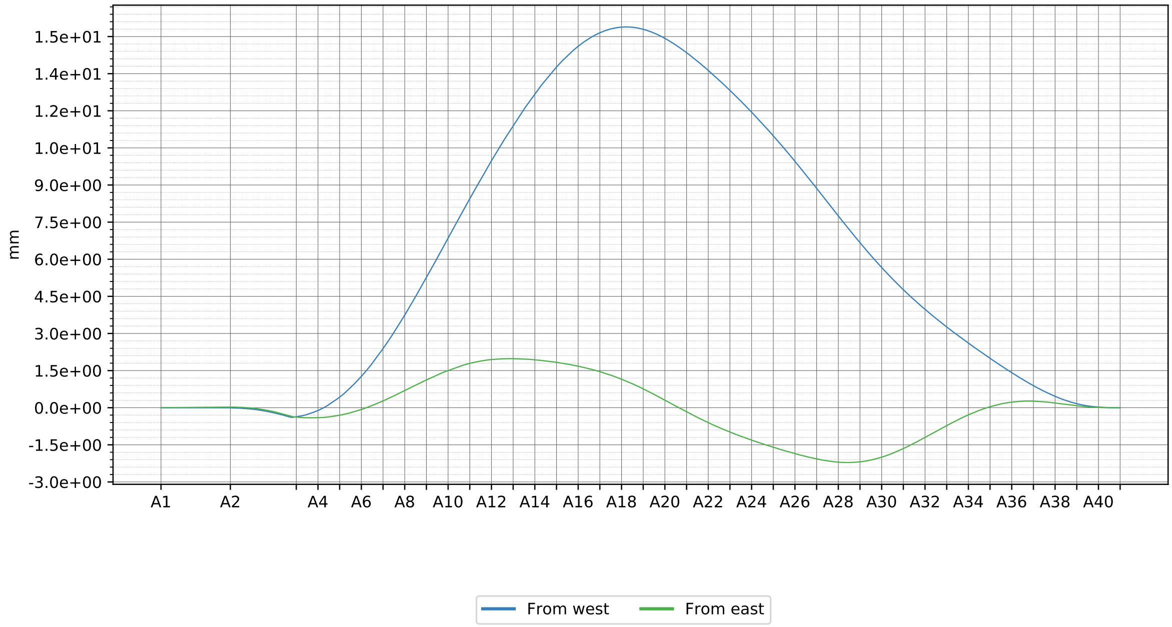

4.3.7 Wave 100 y

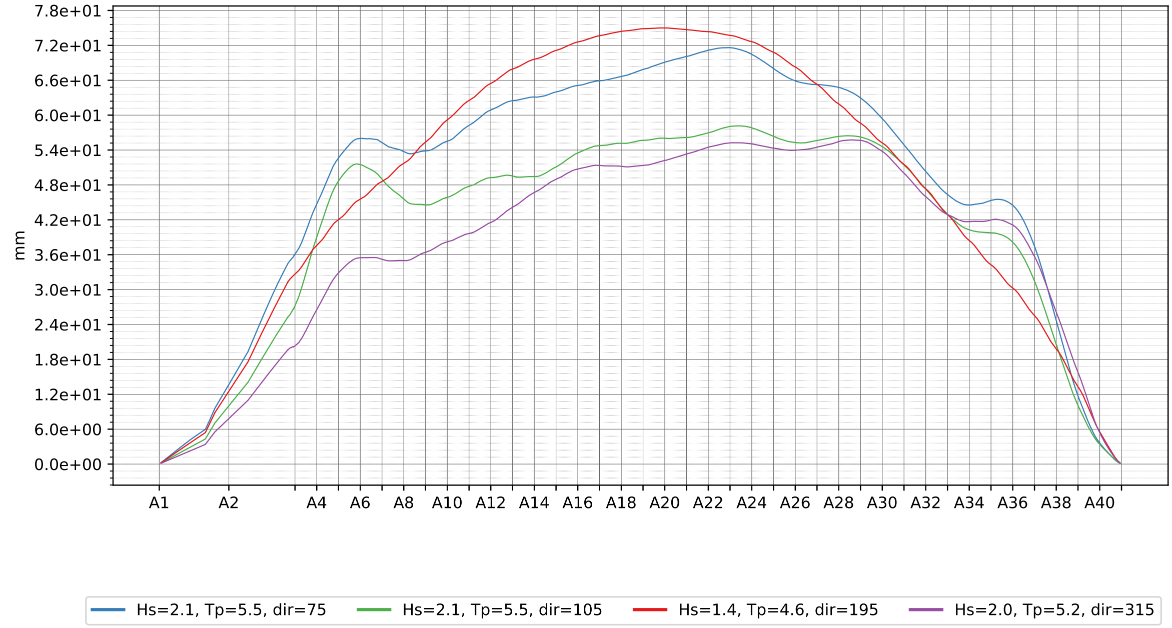

4.3.8 Swell 100 y

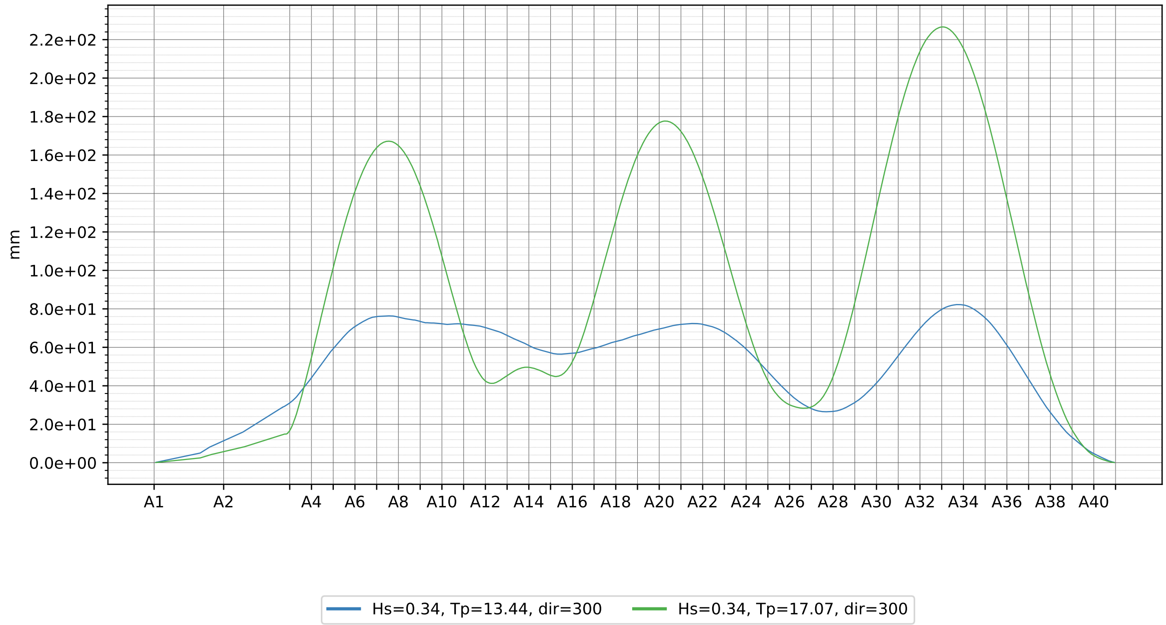

4.4 Global Longitudinal displacement

4.4.1 Dynamic wind 1 y

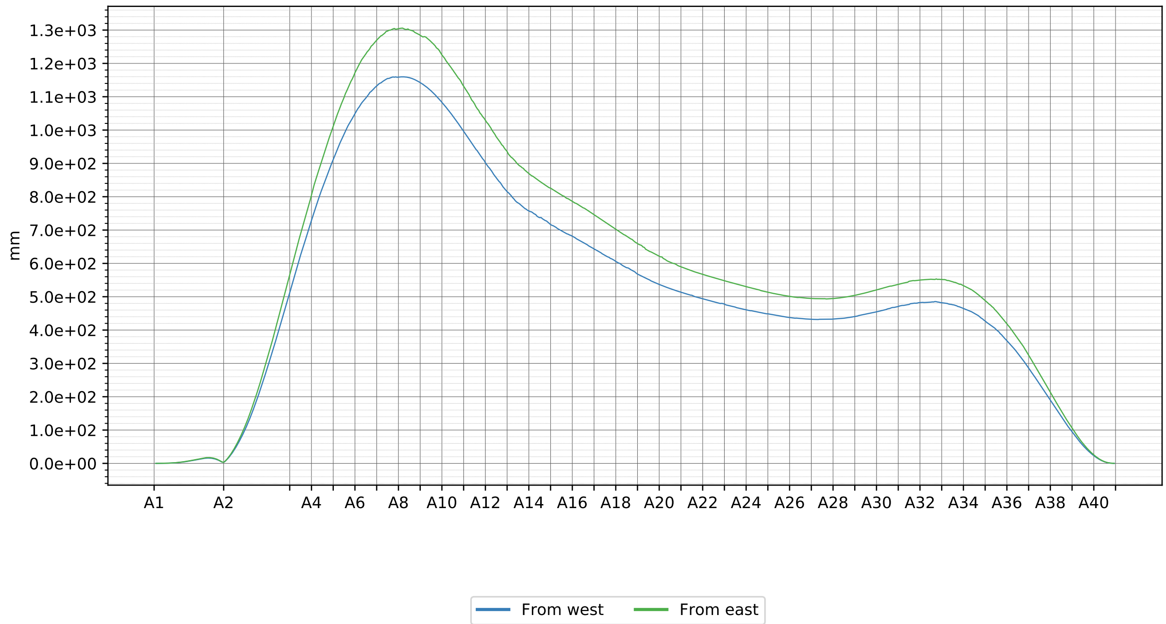

4.4.2 Static wind 1y

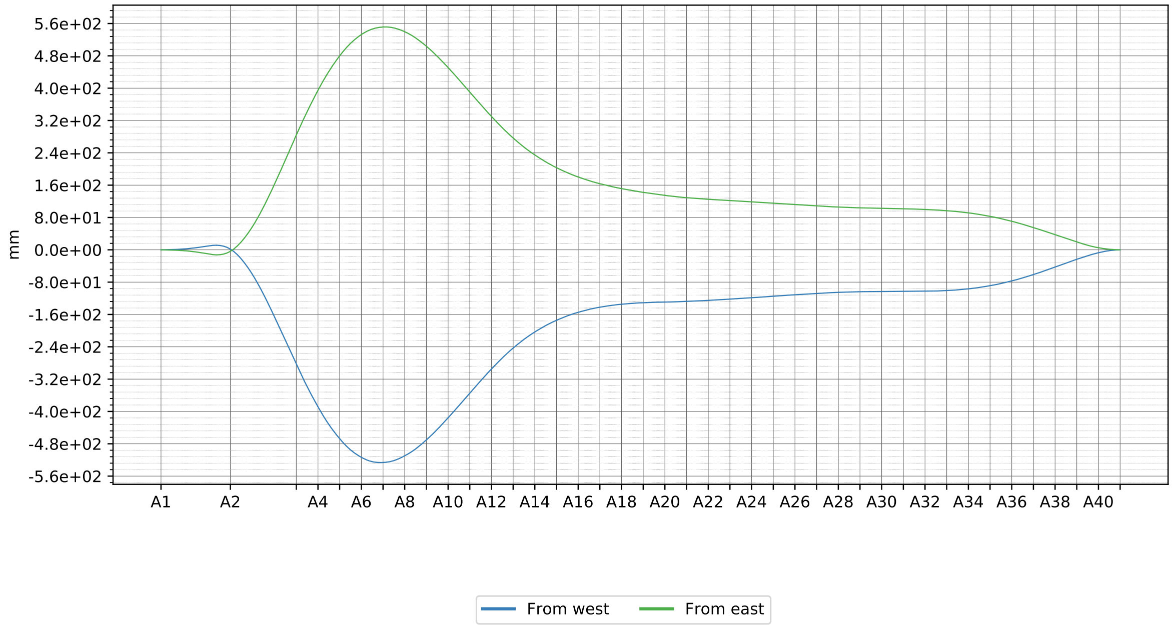

4.4.3 Wave 1 y

4.4.4 Swell 1 y

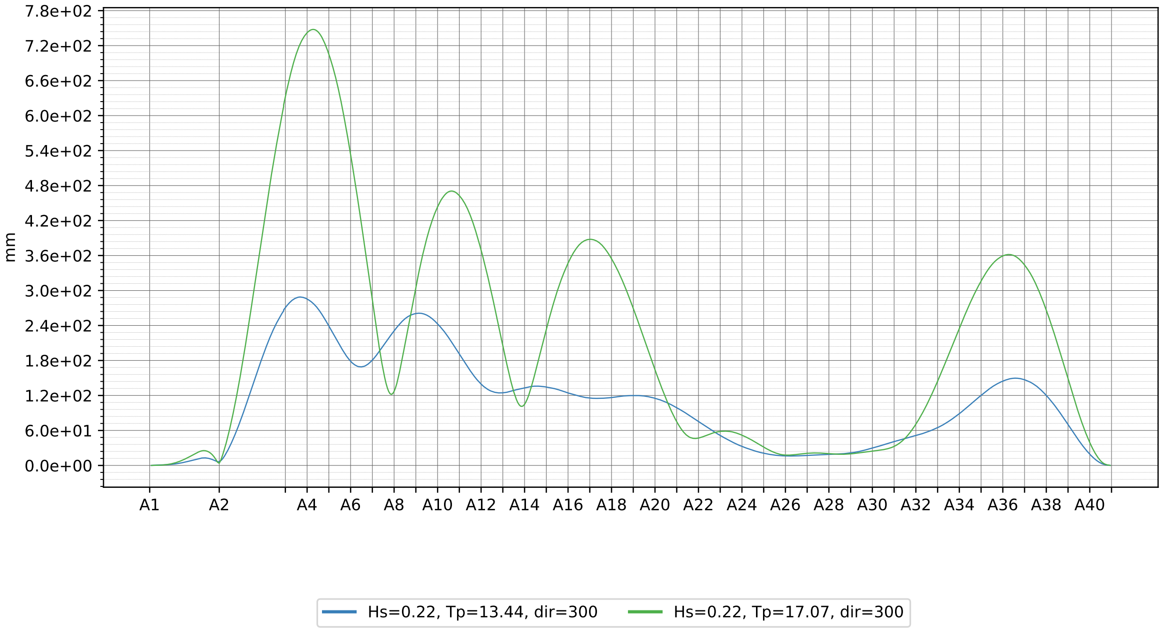

4.4.5 Dynamic wind 100 y

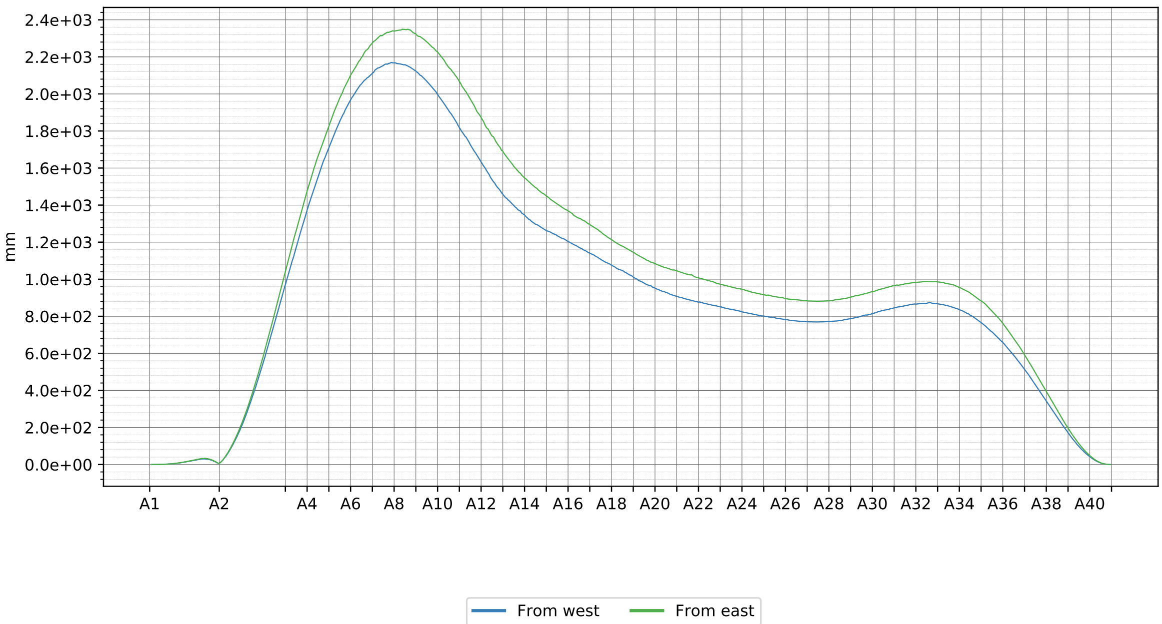

4.4.6 Static wind 100 y

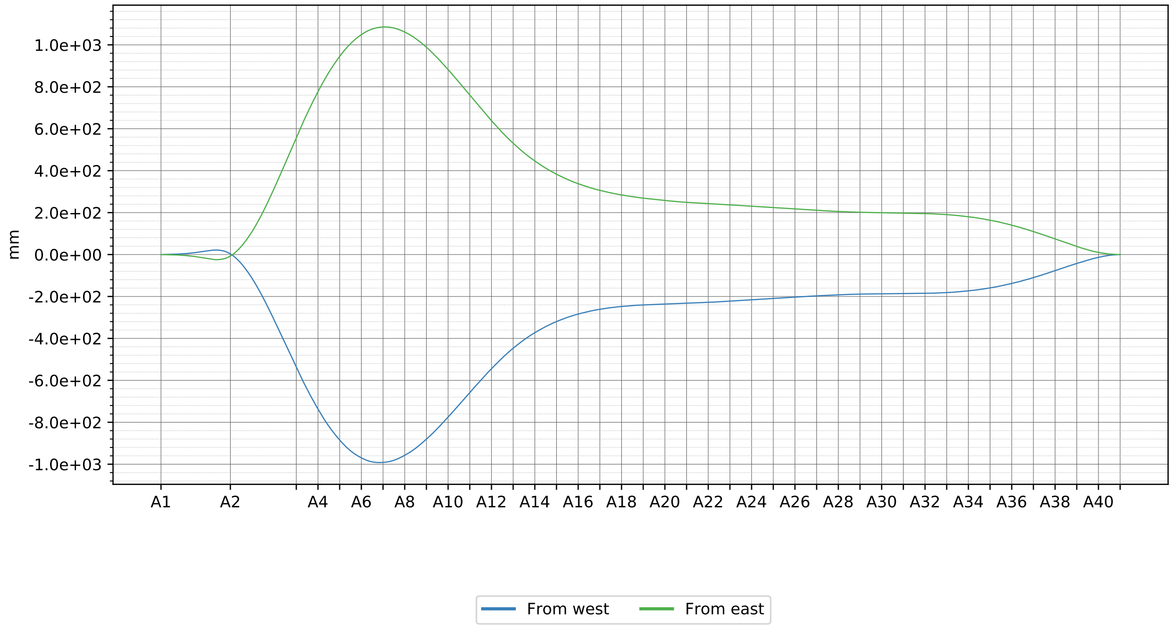

4.4.7 Wave 100 y

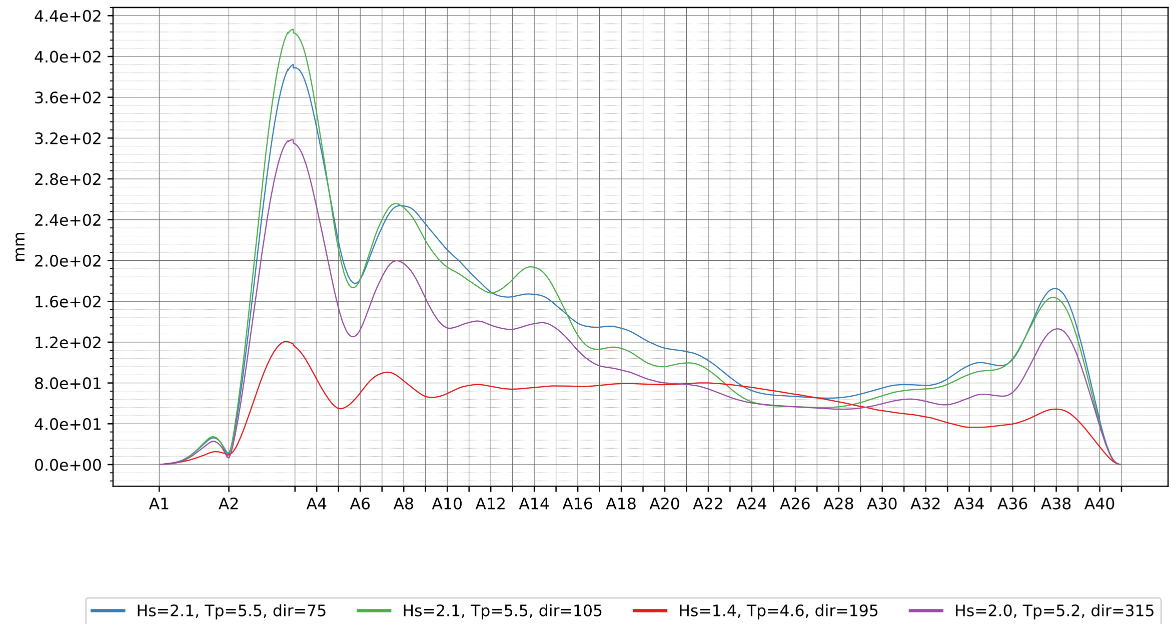

4.4.8 Swell 100 y

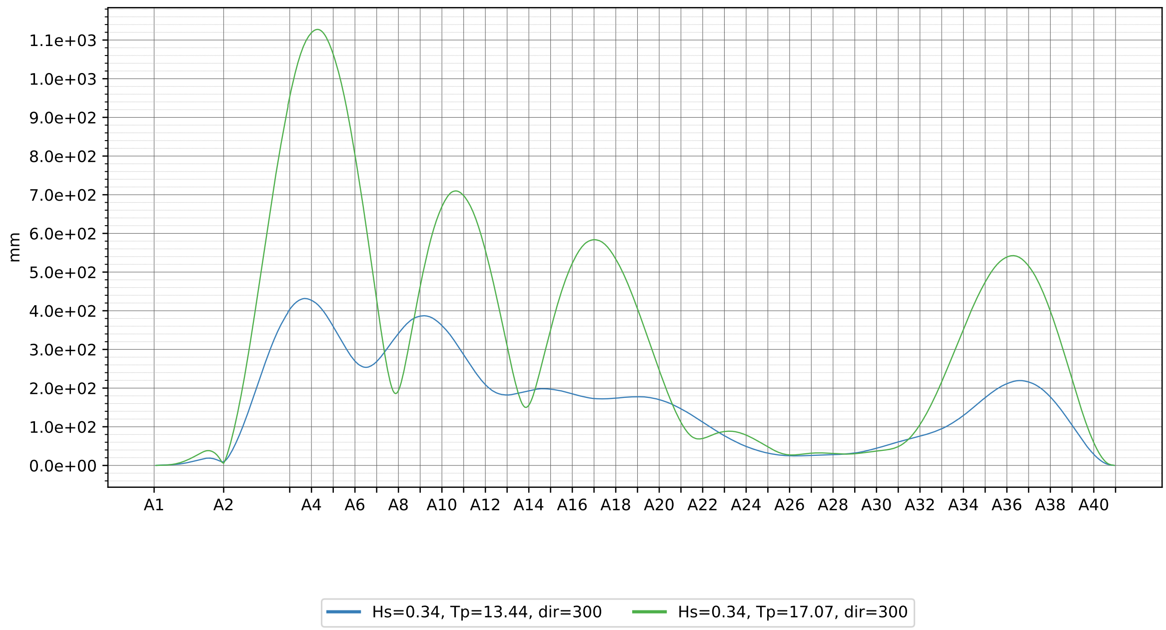

4.5 Global Transverse displacement

4.5.1 Dynamic wind 1 y

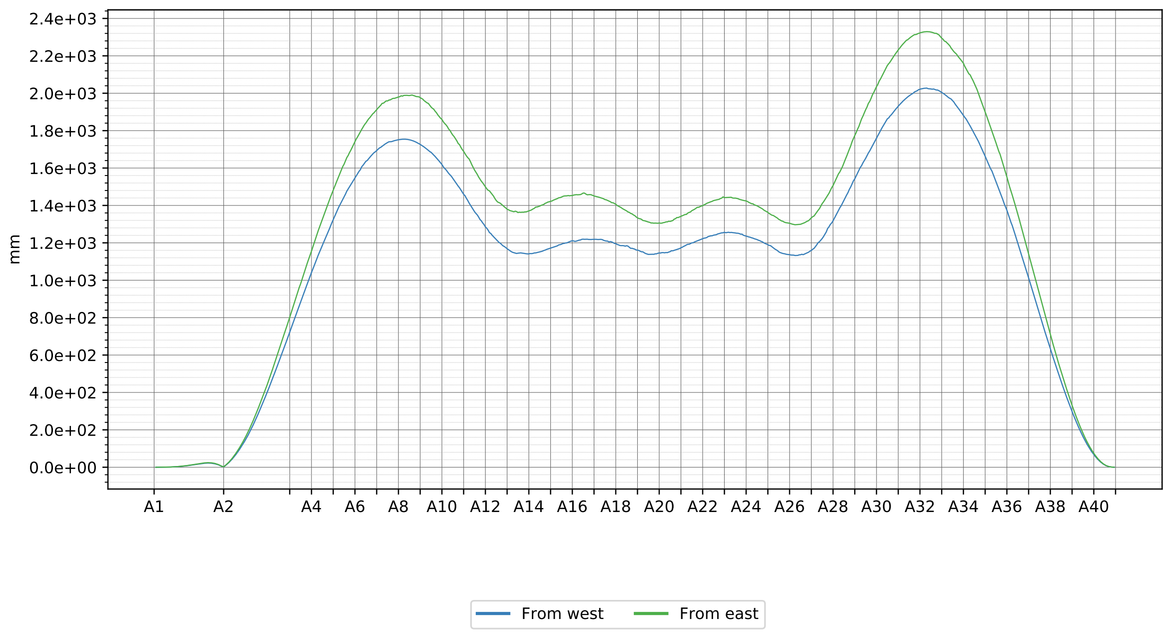

4.5.2 Static wind 1y

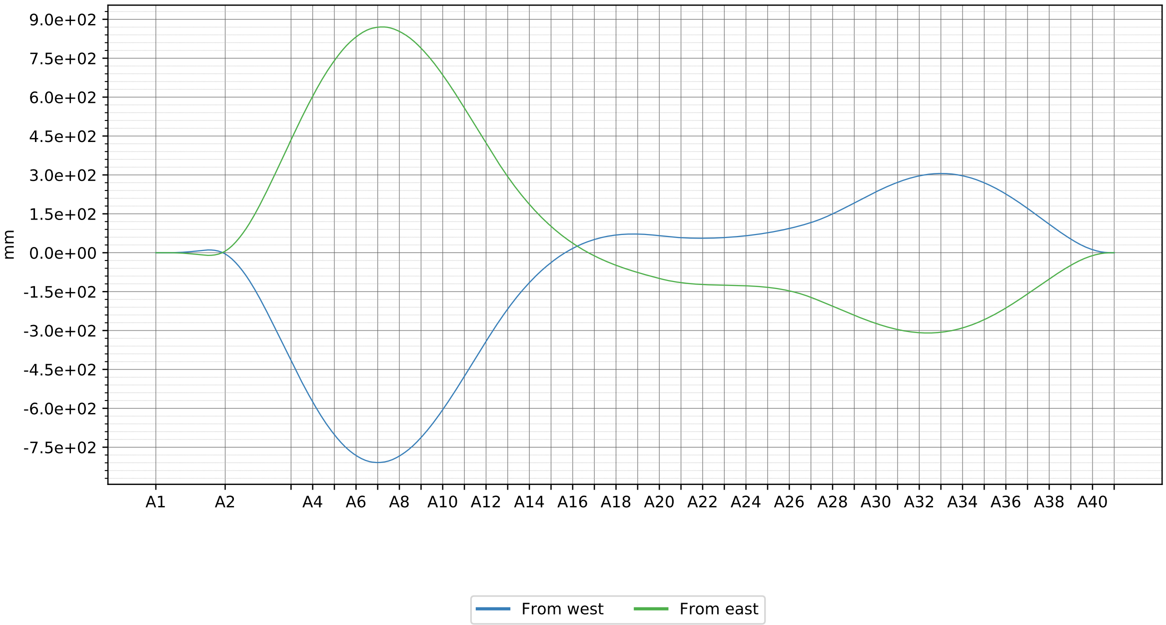

4.5.3 Wave 1 y

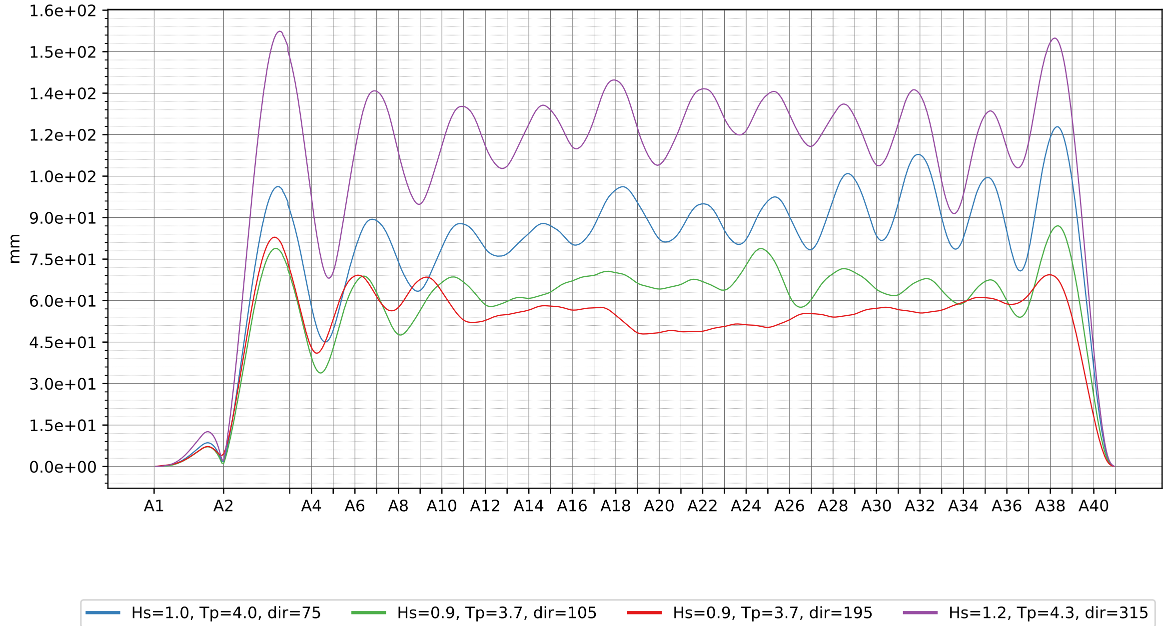

4.5.4 Swell 1 y

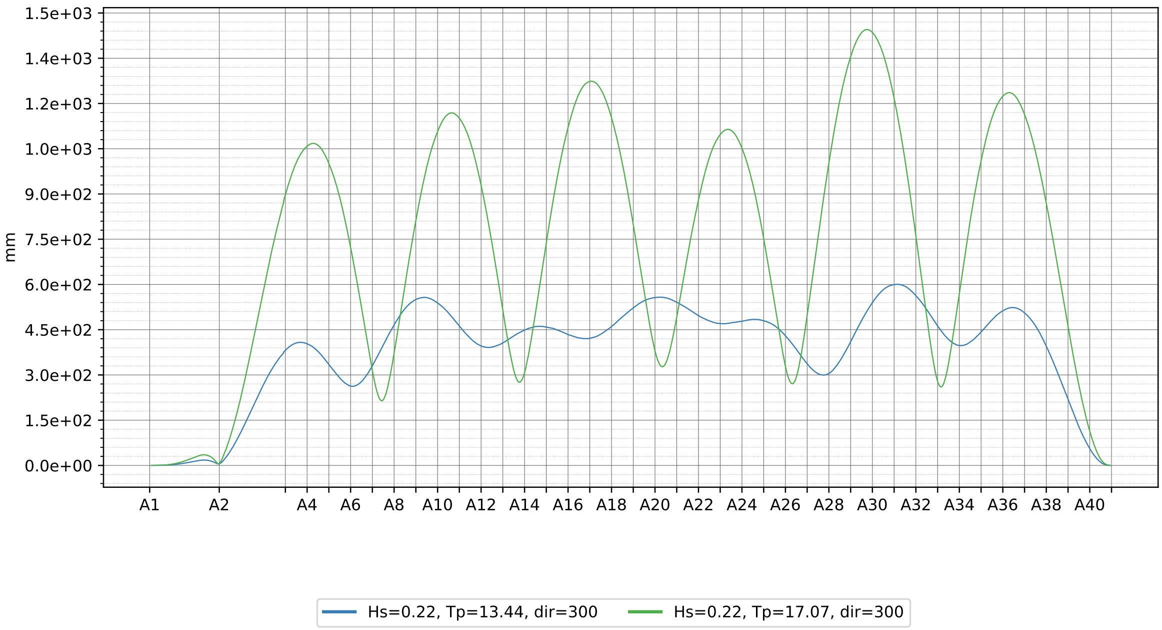

4.5.5 Dynamic wind 100 y

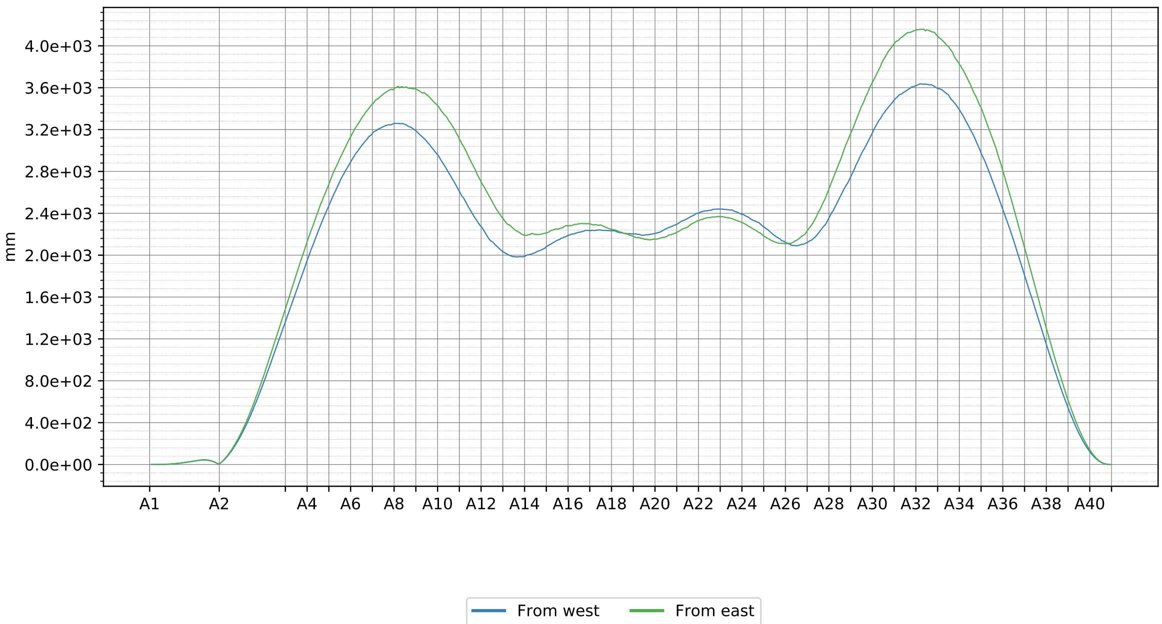

4.5.6 Static wind 100 y

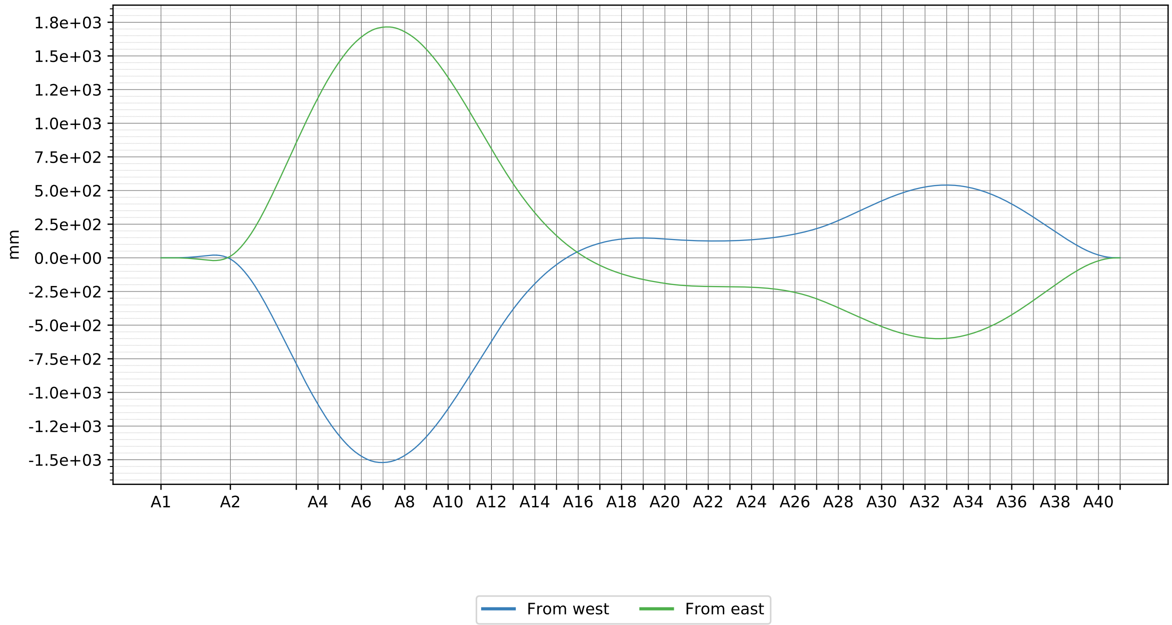

4.5.7 Wave 100 y

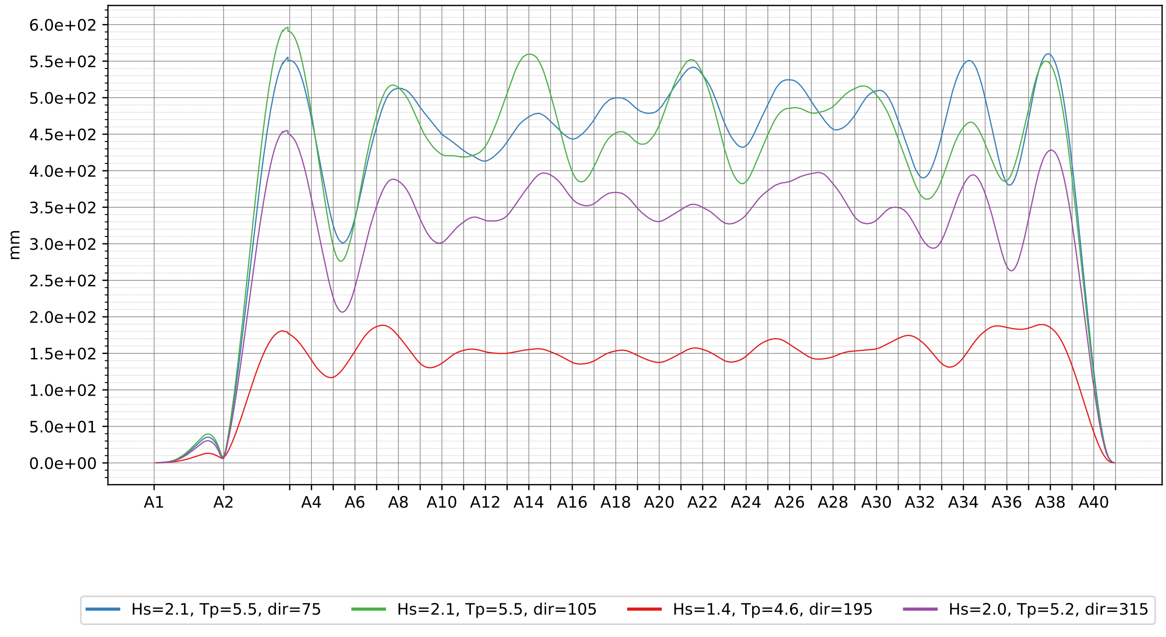

4.5.8 Swell 100 y

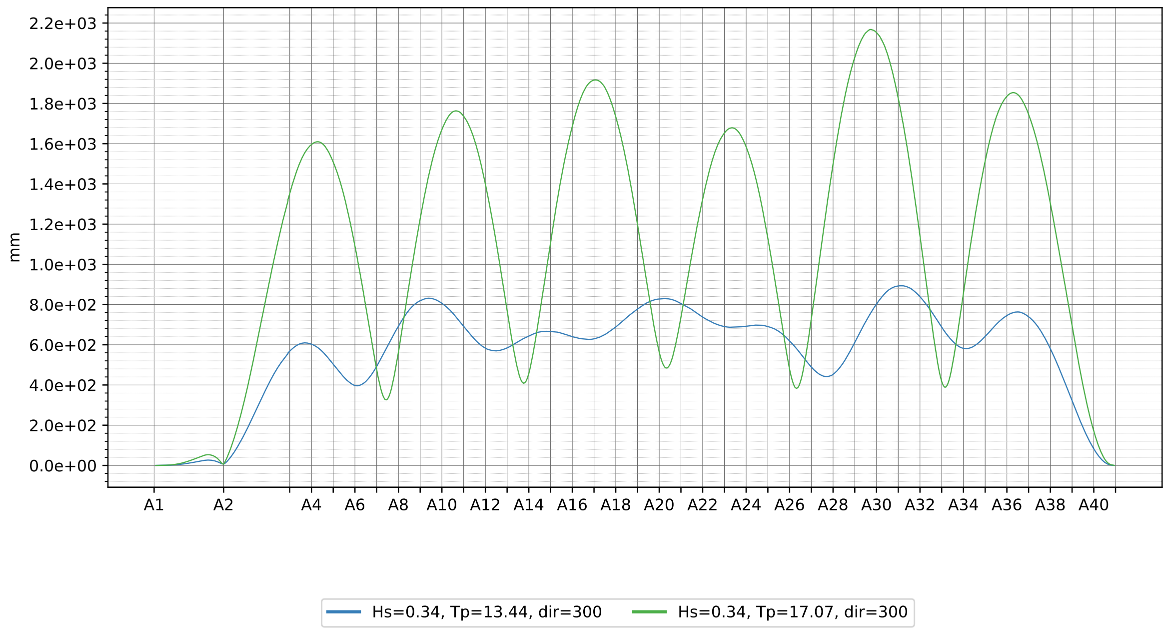

4.6 Global Vertical displacement

4.6.1 Dynamic wind 1 y

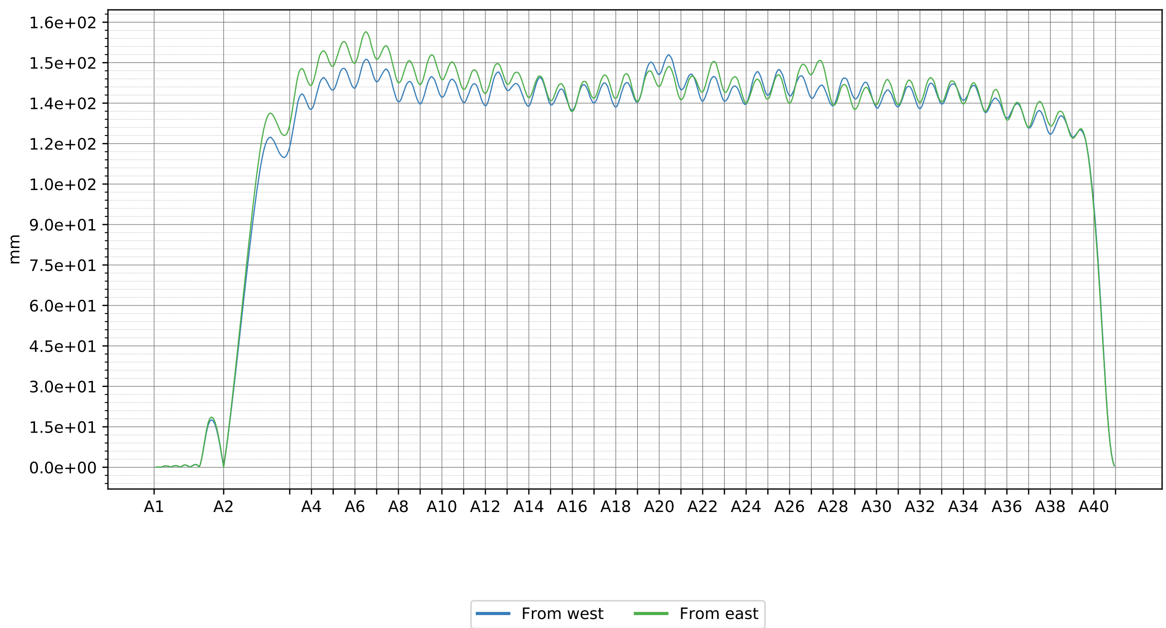

4.6.2 Static wind 1y

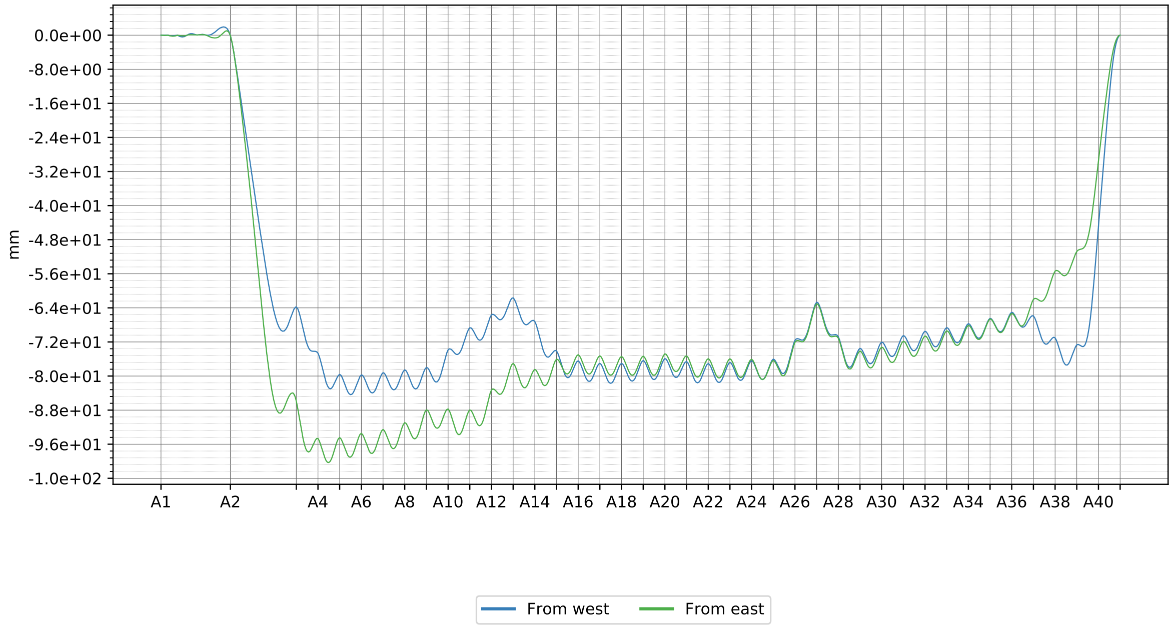

4.6.3 Wave 1 y

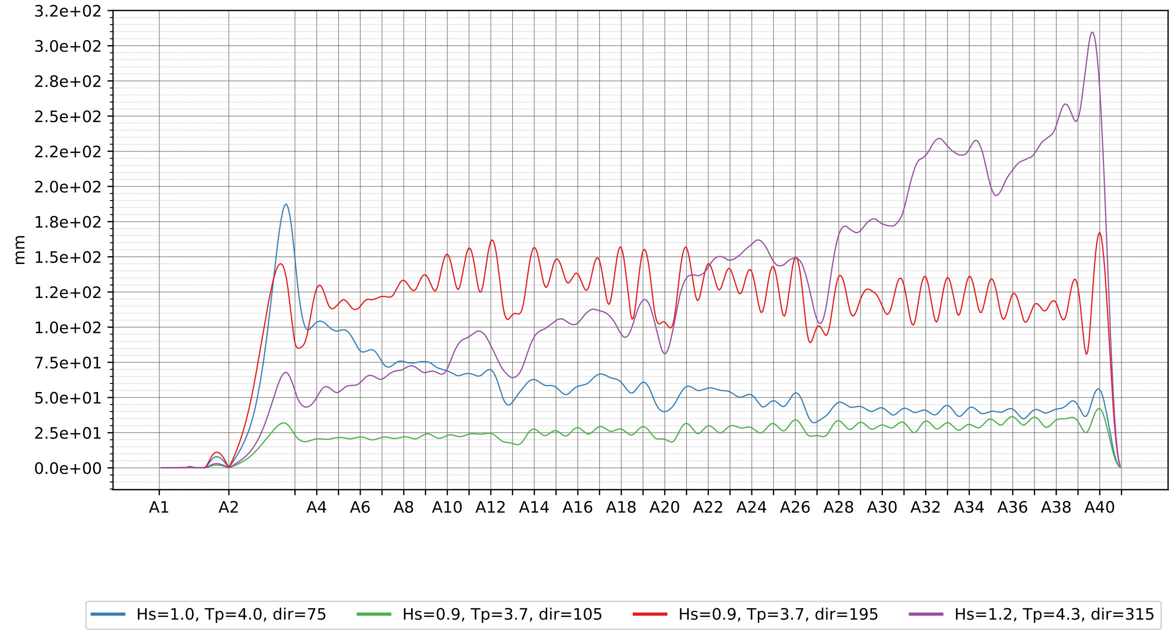

4.6.4 Swell 1 y

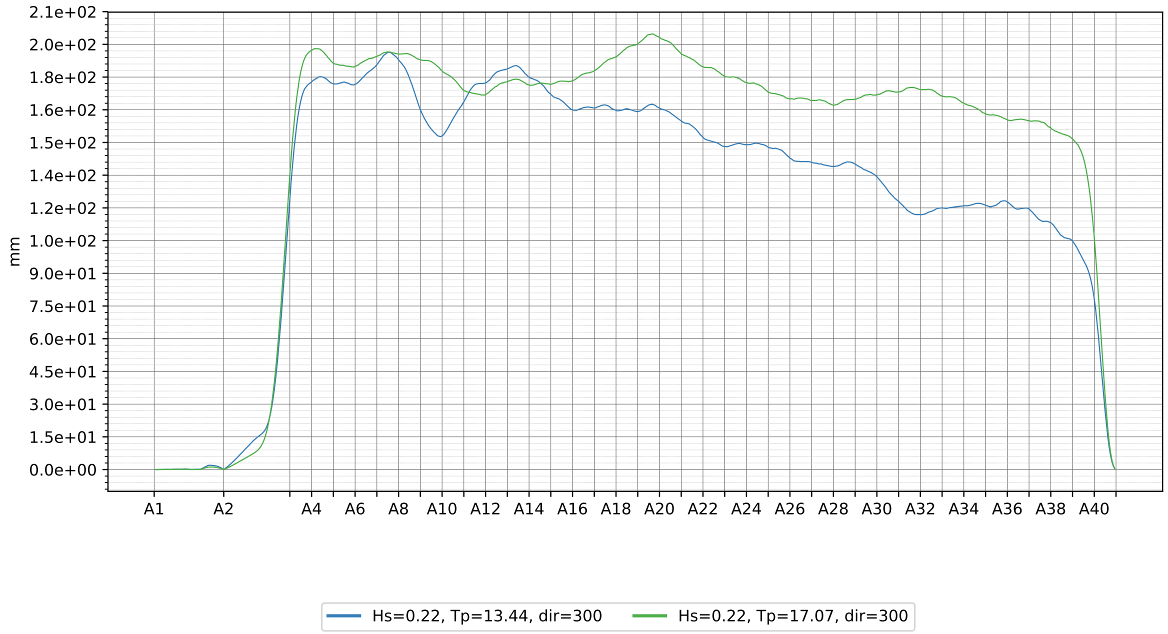

4.6.5 Dynamic wind 100 y

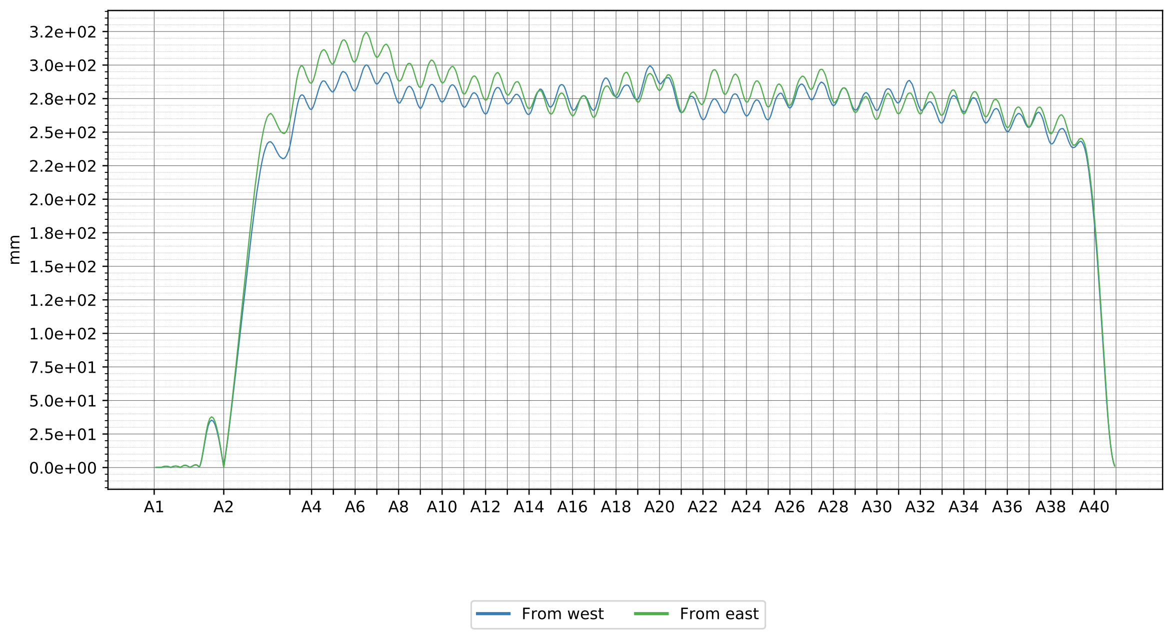

4.6.6 Static wind 100 y

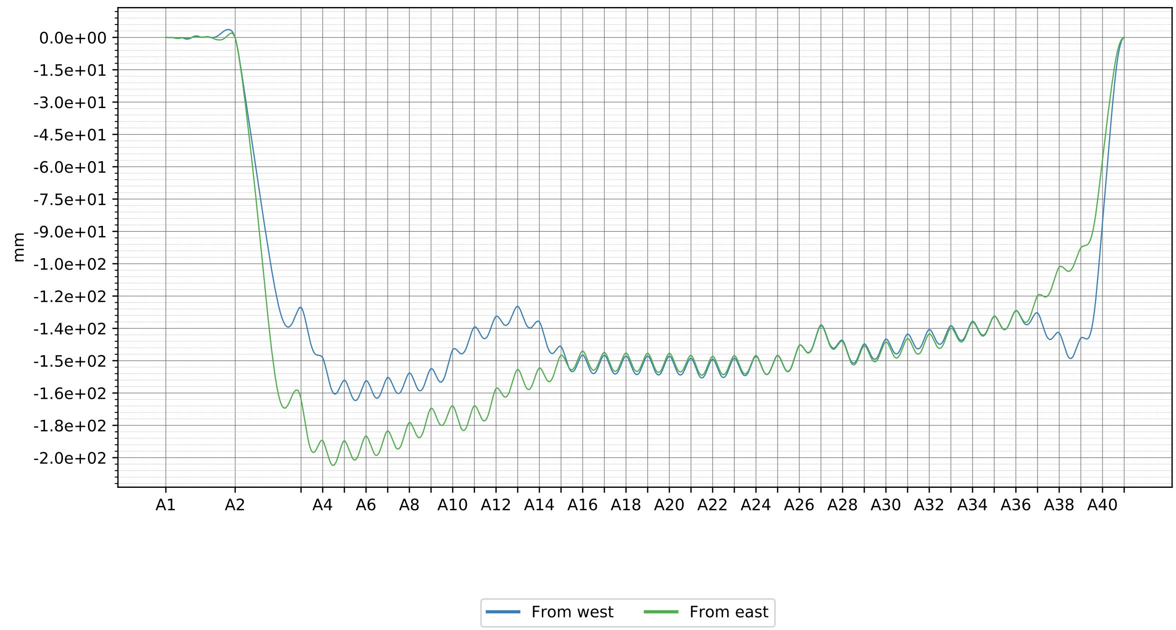

4.6.7 Wave 100 y

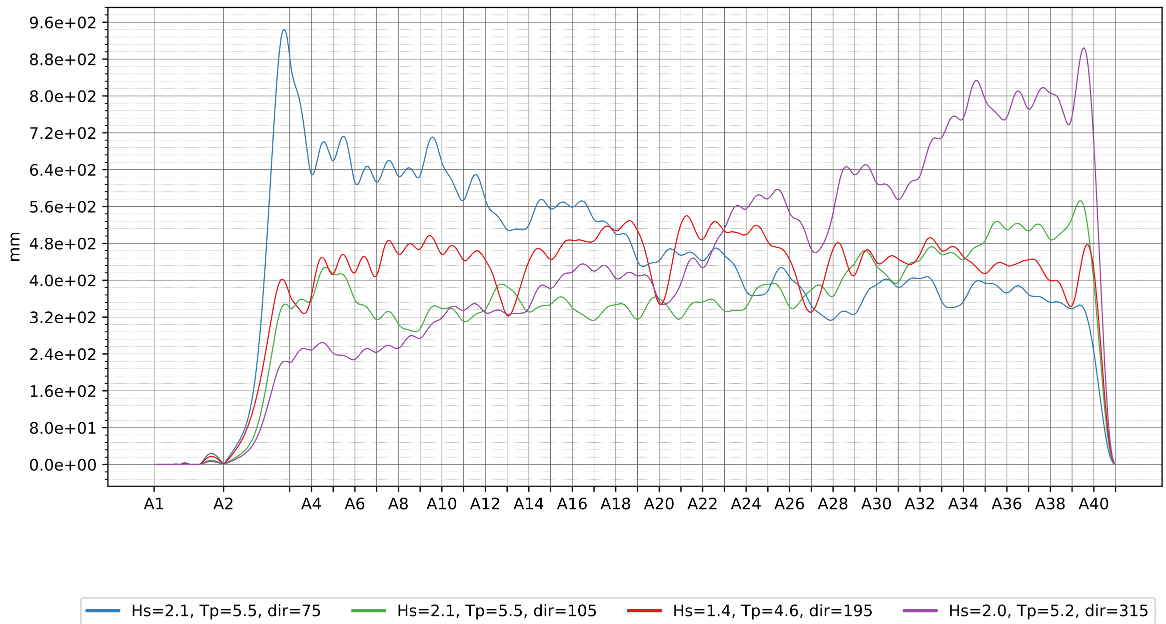

4.6.8 Swell 100 y

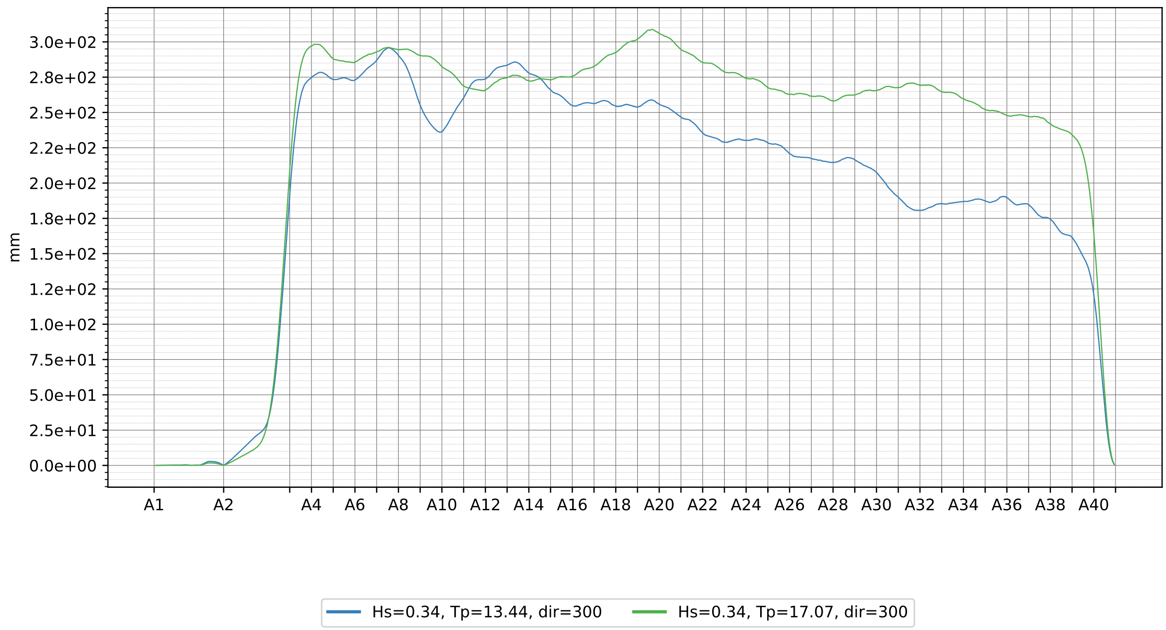

4.7 Rotation about vertical axis

4.7.1 Dynamic wind 1 y

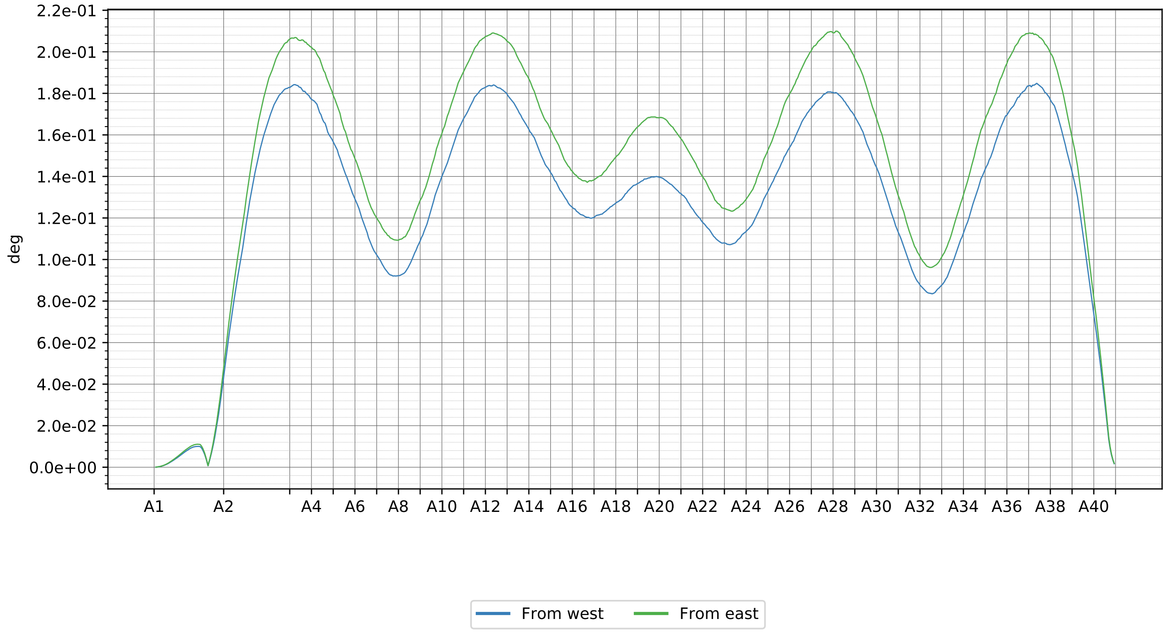

4.7.2 Static wind 1y

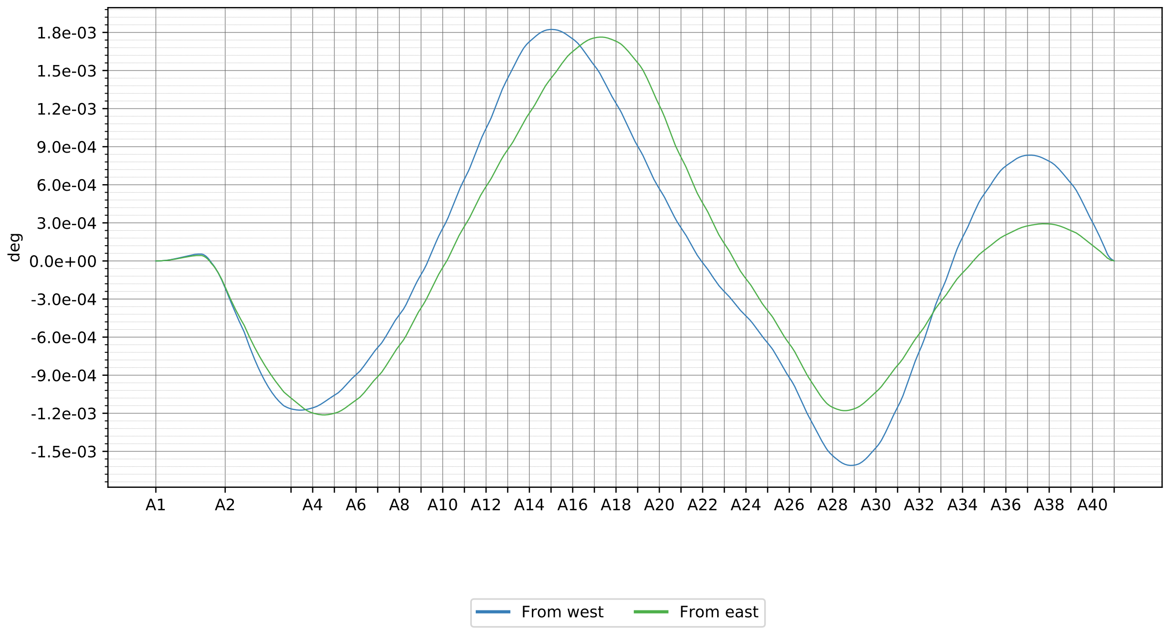

4.7.3 Wave 1 y

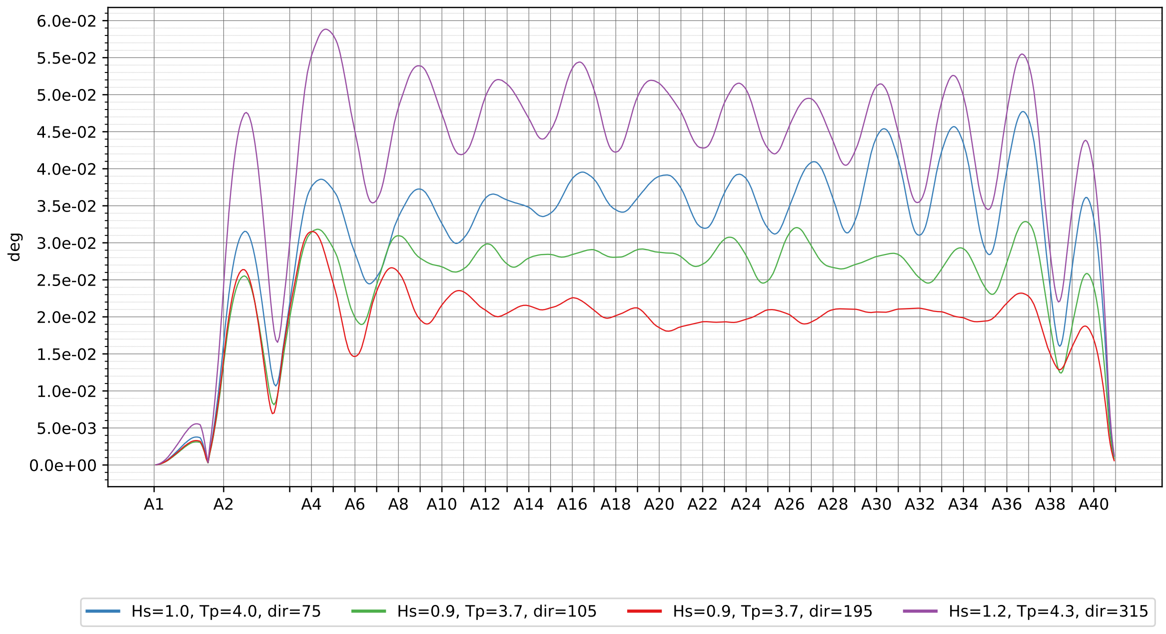

4.7.4 Swell 1 y

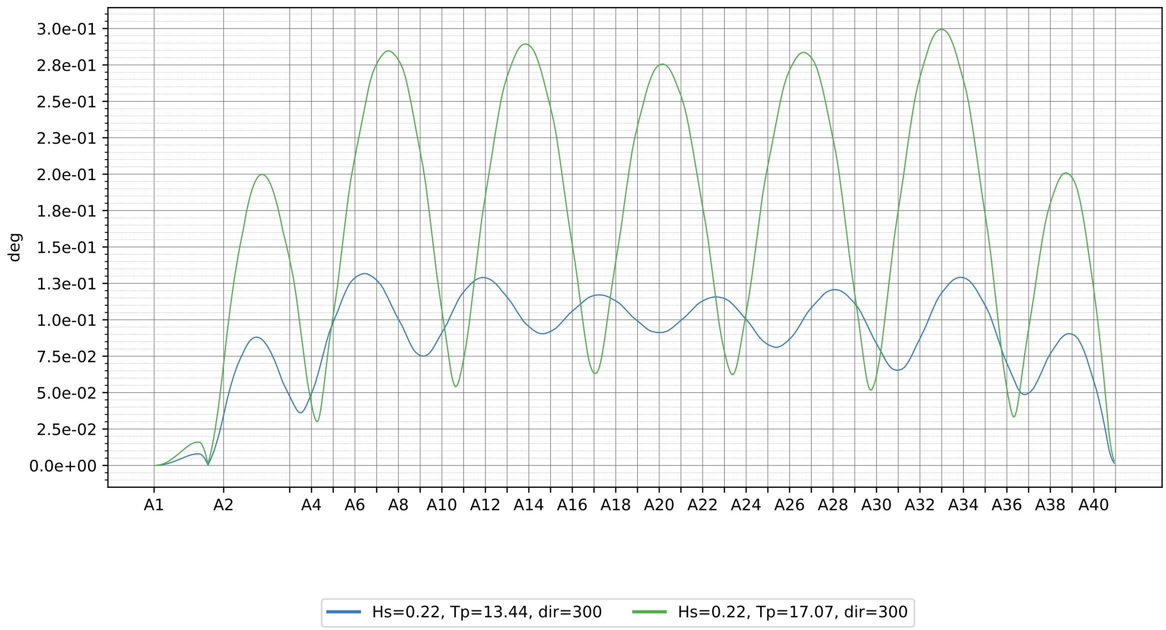

4.7.5 Dynamic wind 100 y

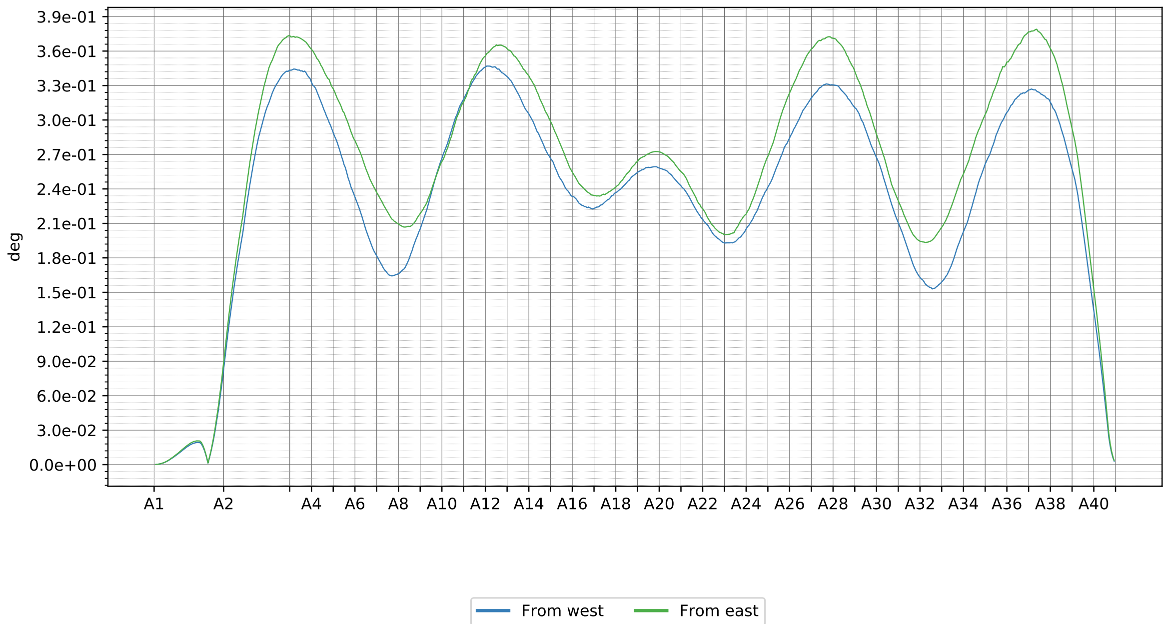

4.7.6 Static wind 100 y

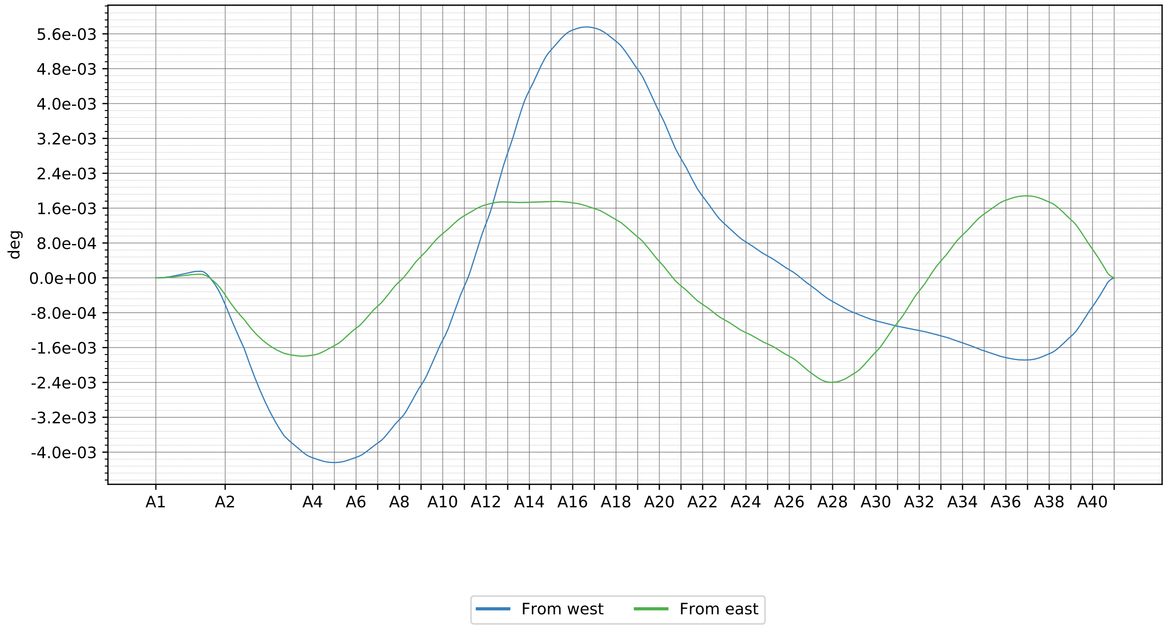

4.7.7 Wave 100 y

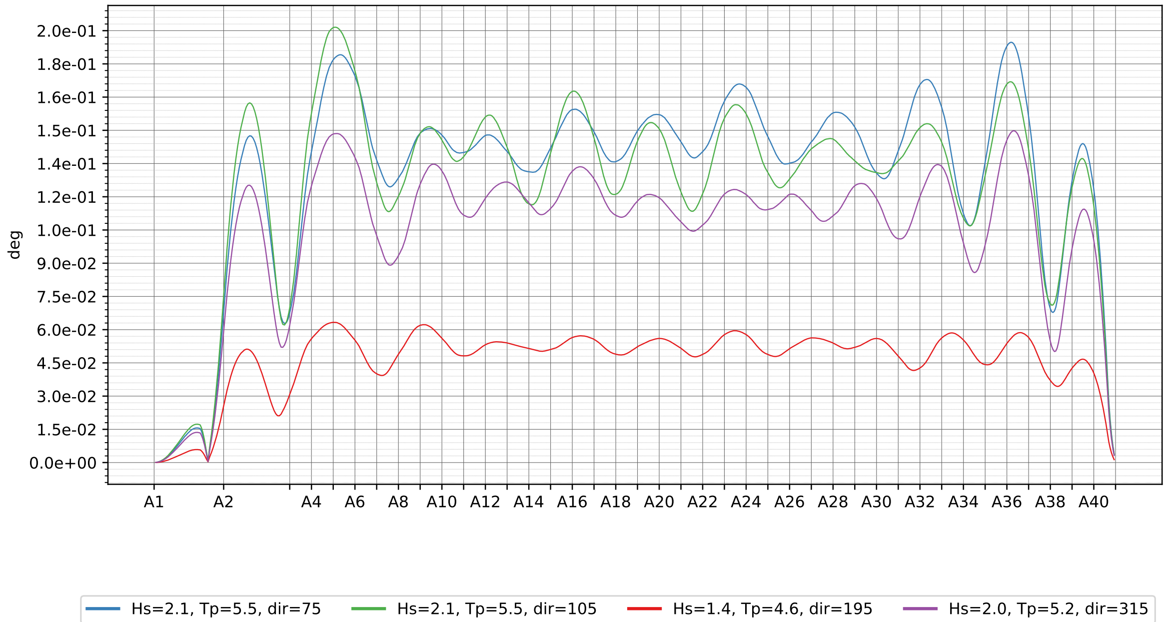

4.7.8 Swell 100 y

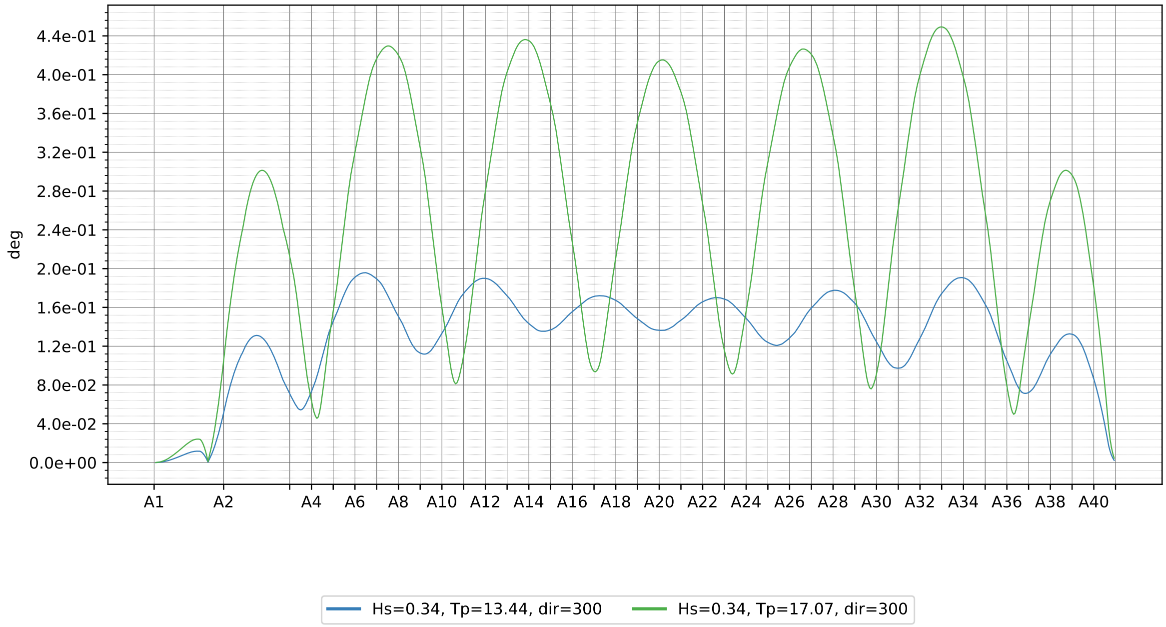

4.8 Rotation about transverse axis

4.8.1 Dynamic wind 1 y

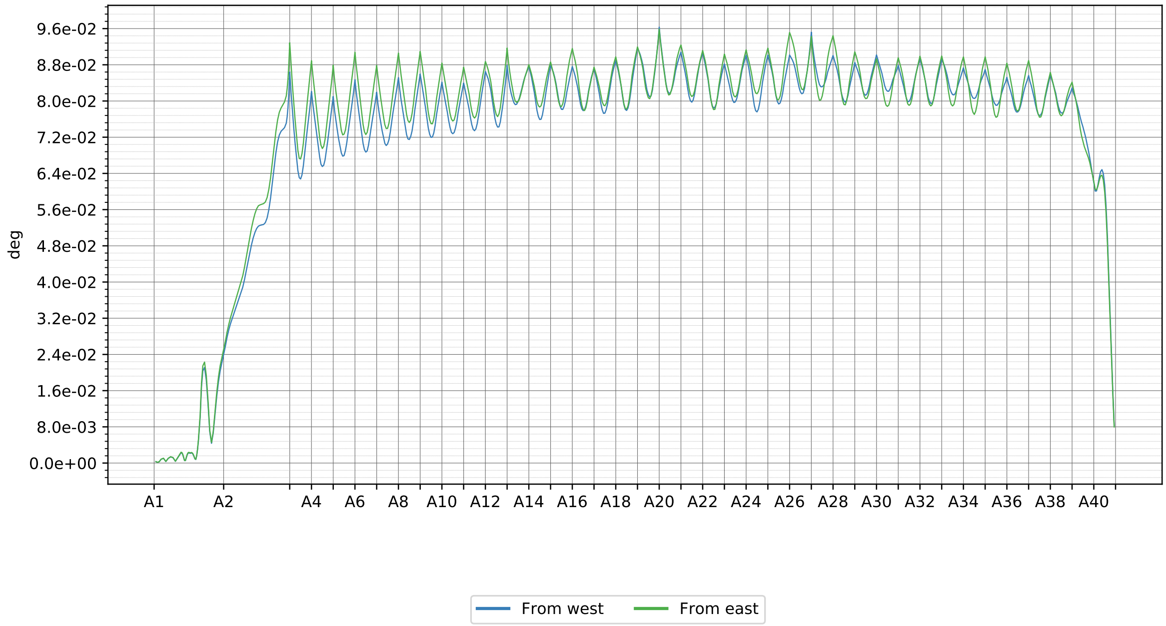

4.8.2 Static wind 1y

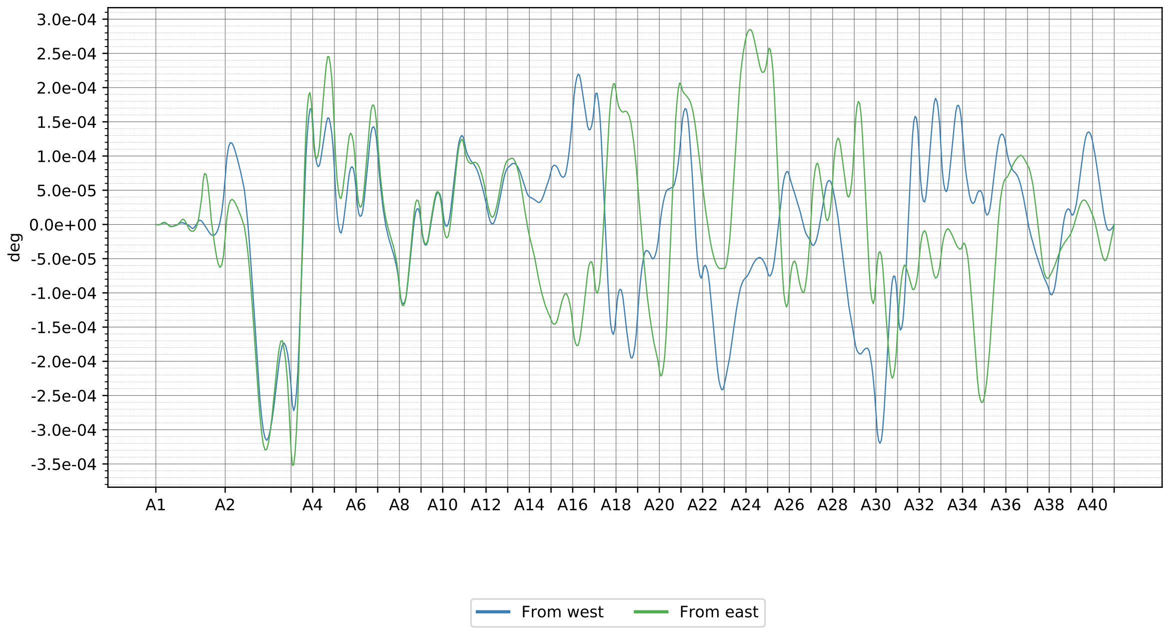

4.8.3 Wave 1 y

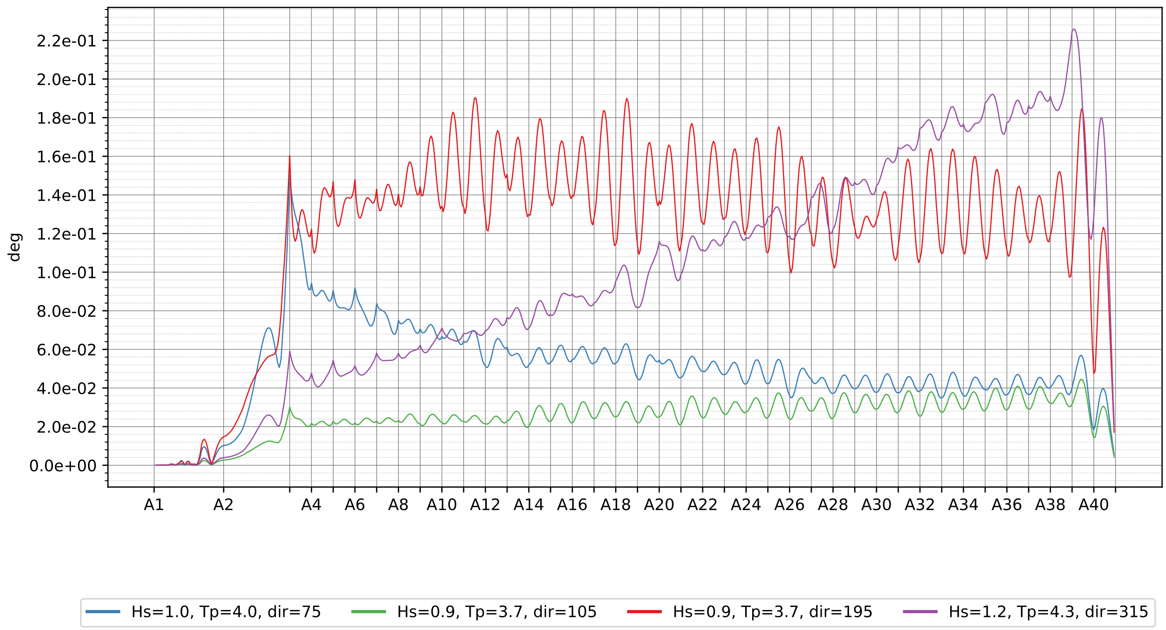

4.8.4 Swell 1 y

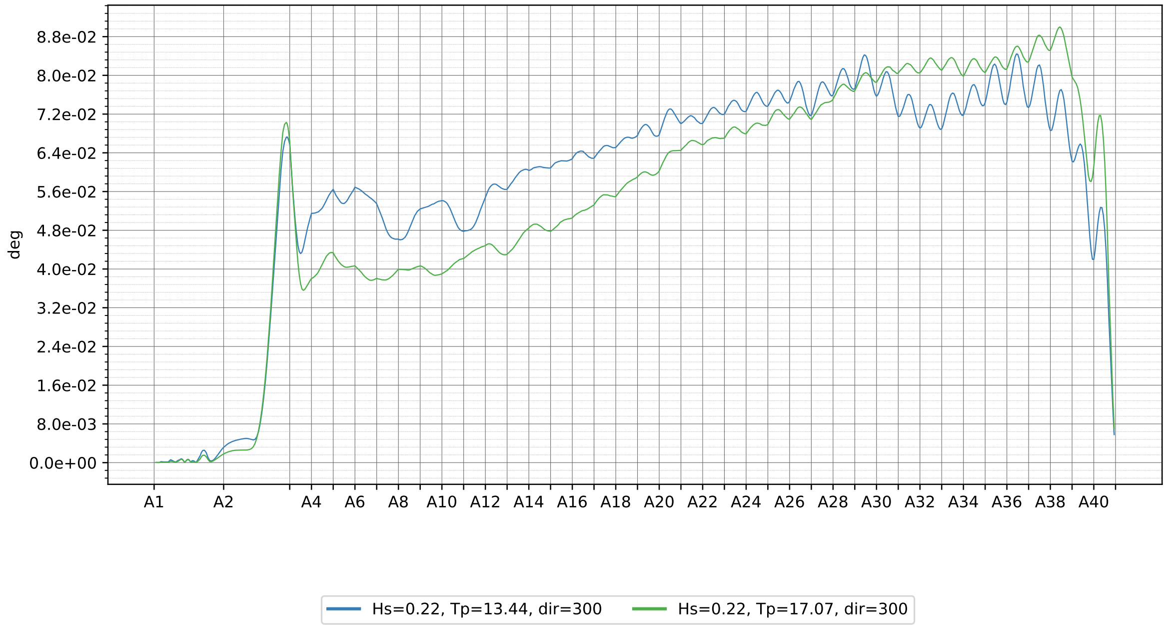

4.8.5 Dynamic wind 100 y

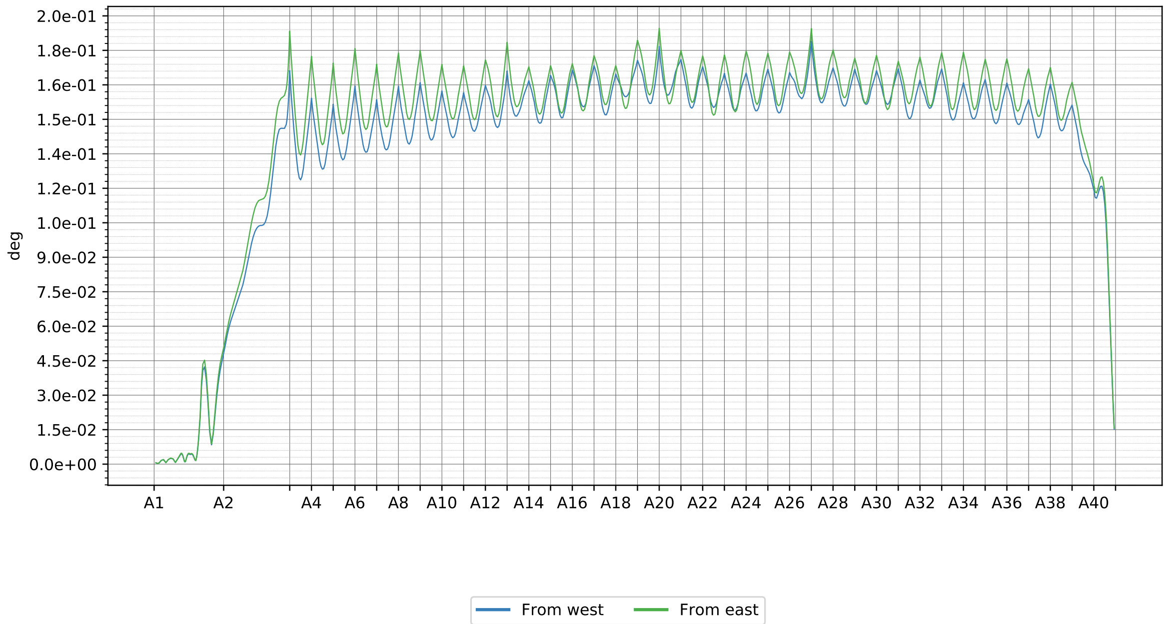

4.8.6 Static wind 100 y

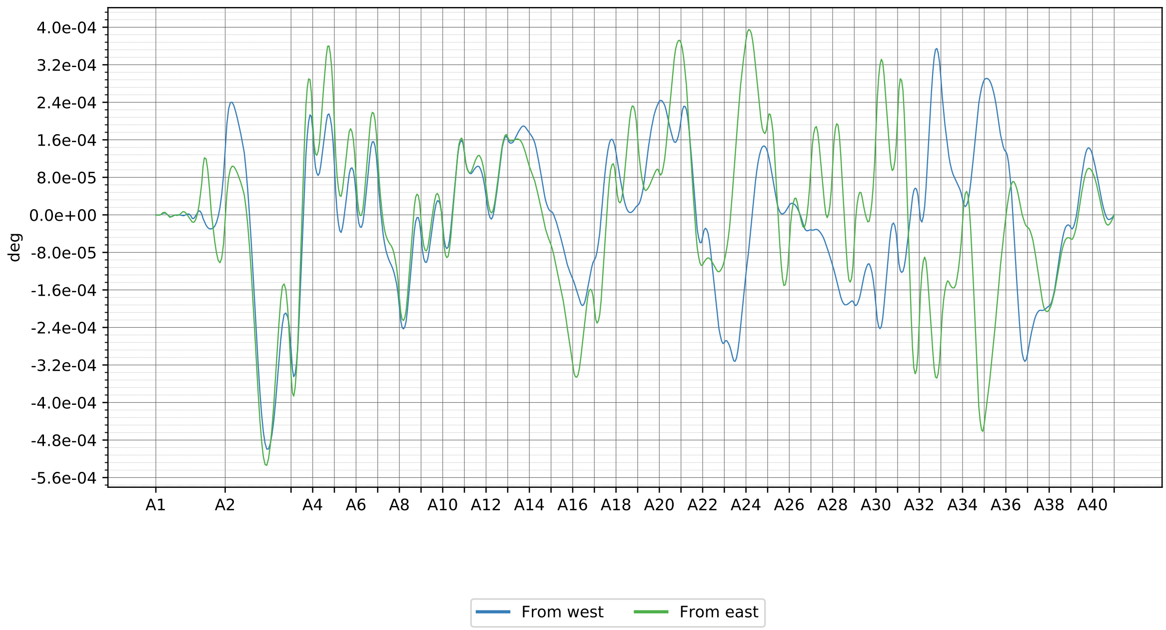

4.8.7 Wave 100 y

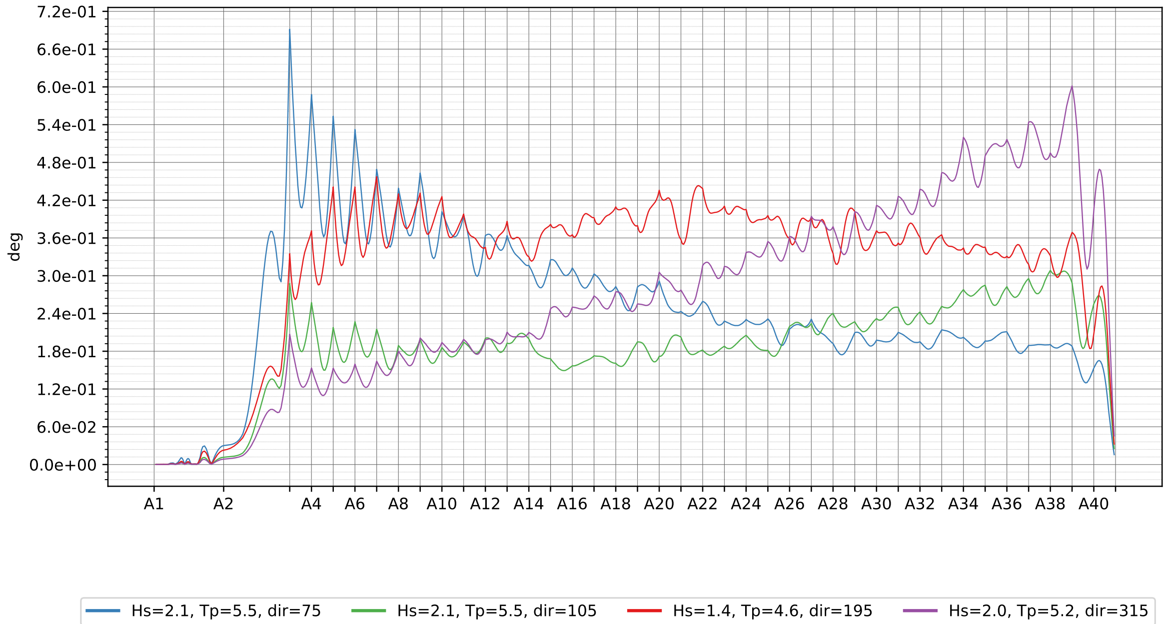

4.8.8 Swell 100 y

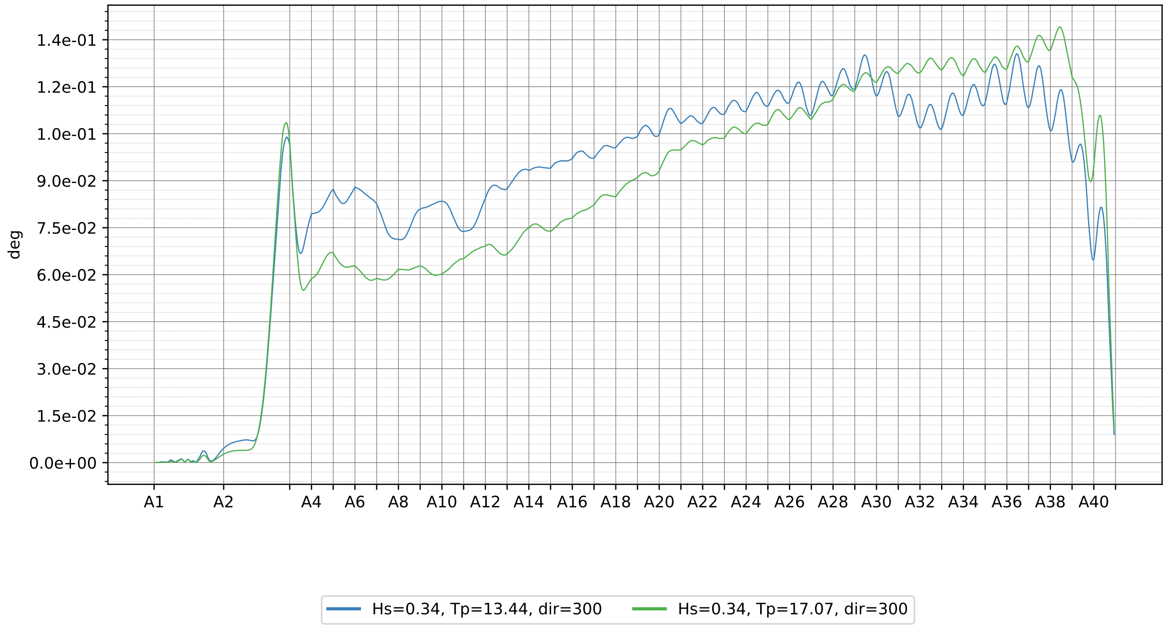

4.9 Rotation about bridge axis

4.9.1 Dynamic wind 1 y

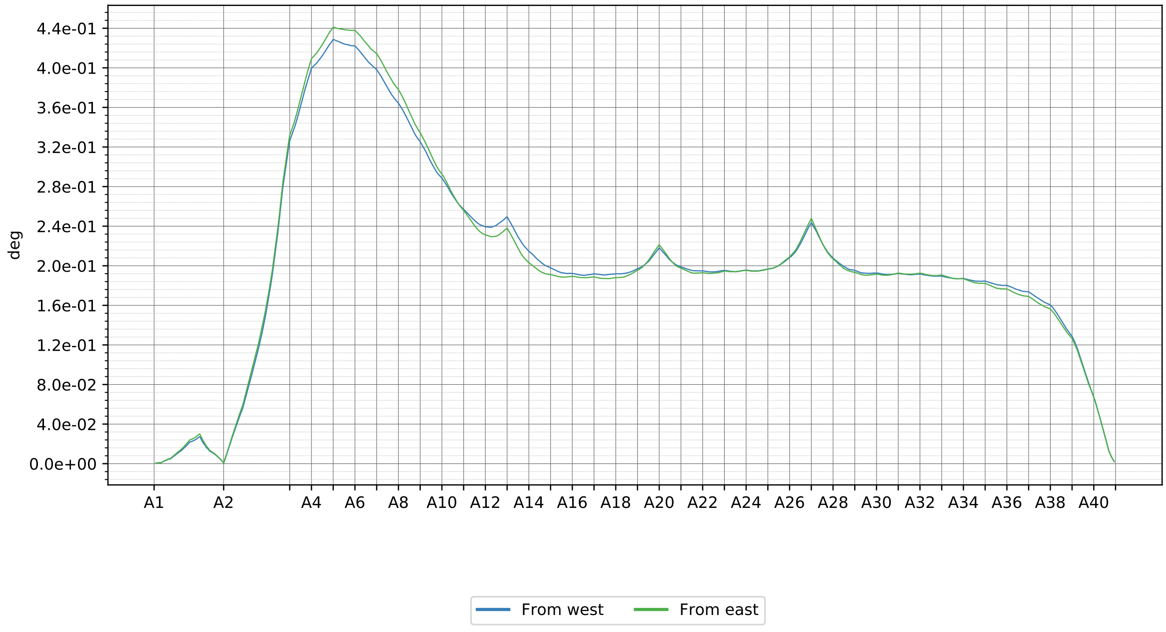

4.9.2 Static wind 1y

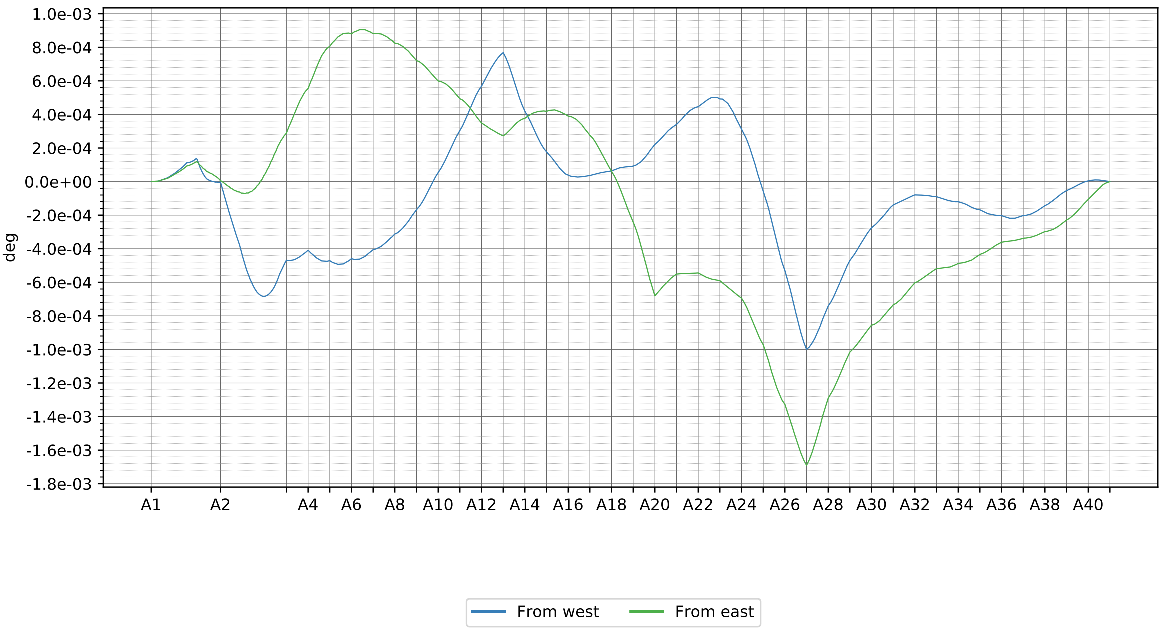

4.9.3 Wave 1 y

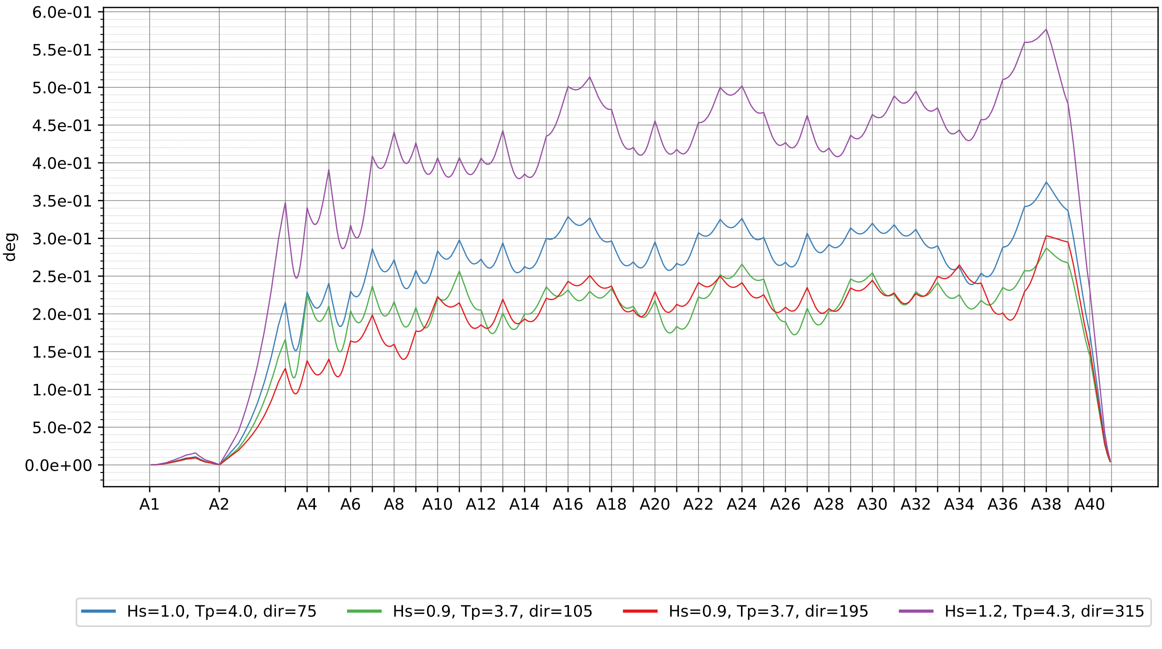

4.9.4 Swell 1 y

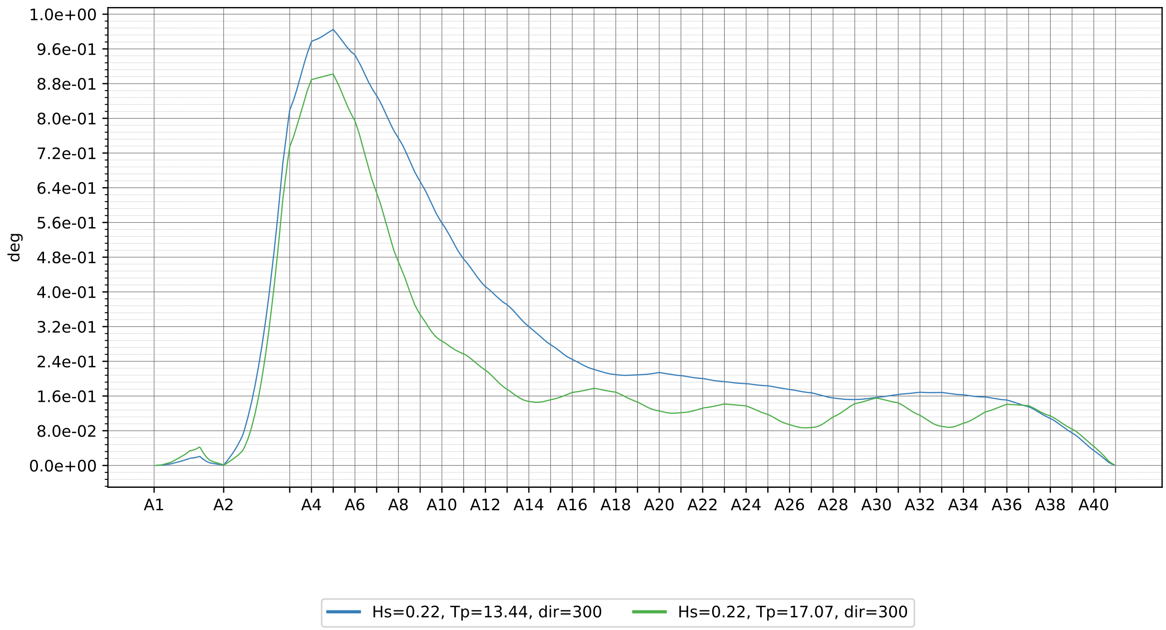

4.9.5 Dynamic wind 100 y

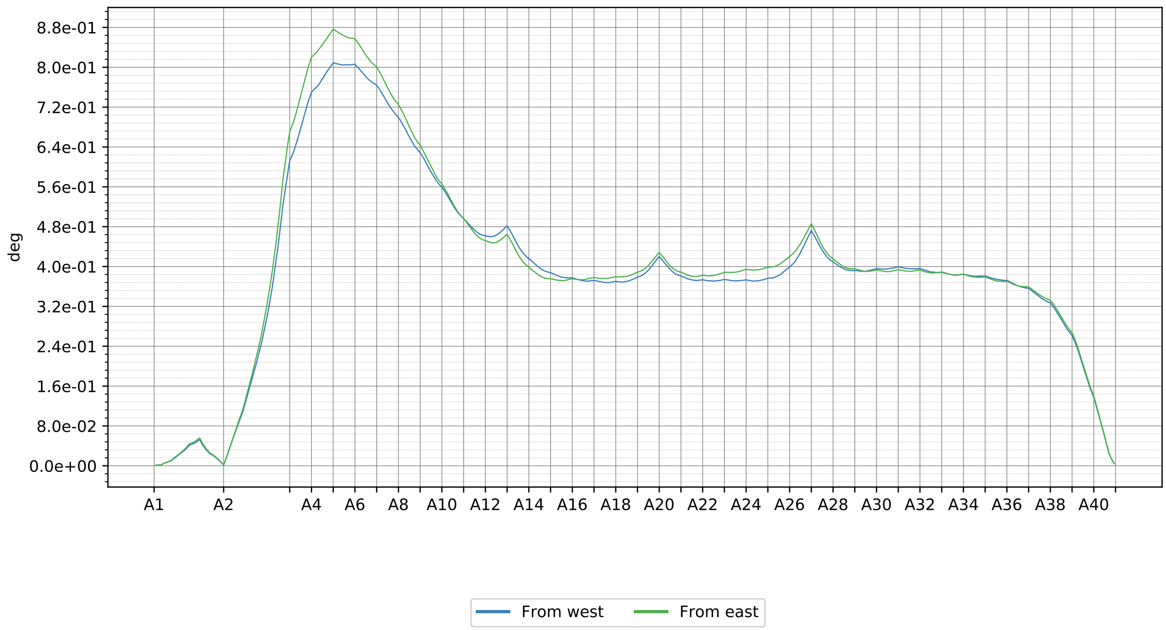

4.9.6 Static wind 100 y

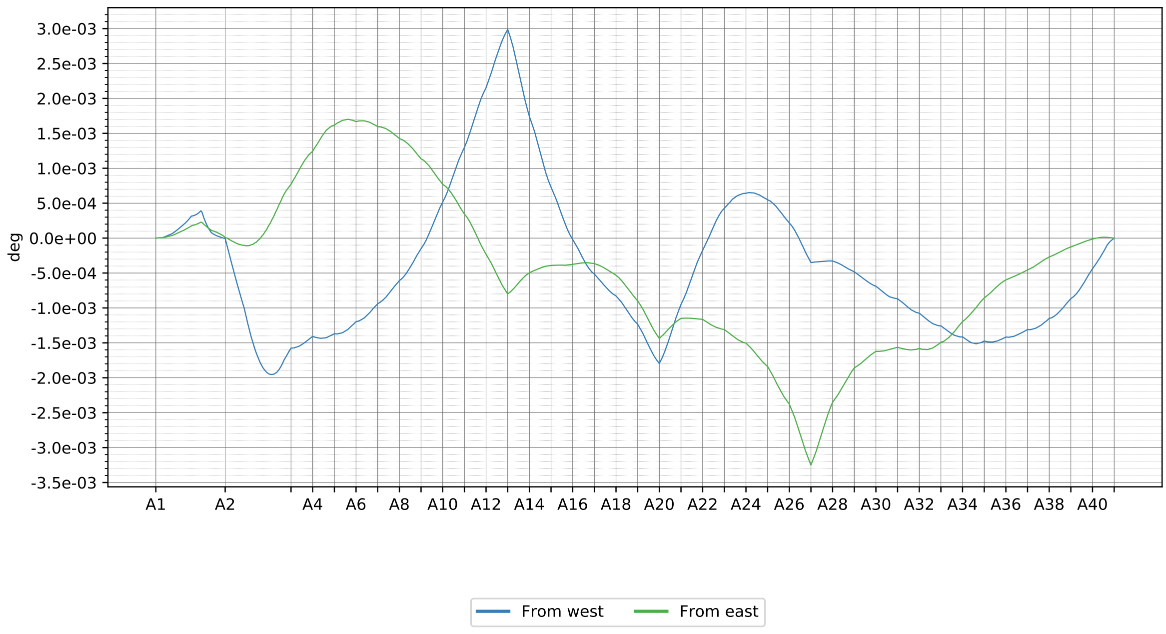

4.9.7 Wave 100 y

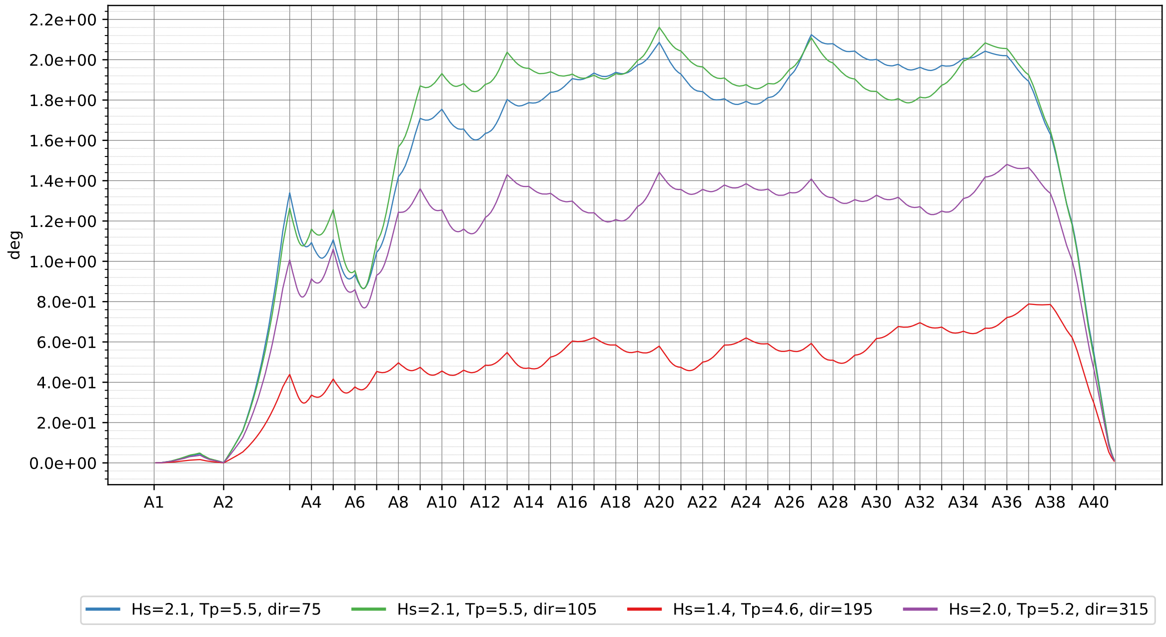

4.9.8 Swell 100 y

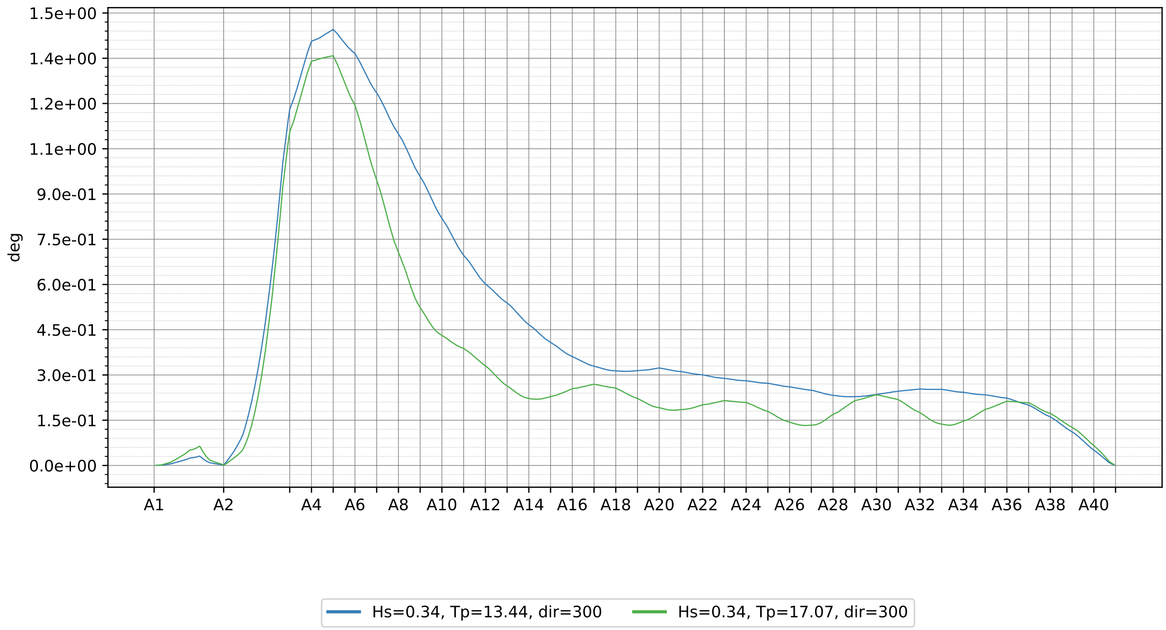

4.10 Global Transverse acceleration

4.10.1 Dynamic wind 1 y

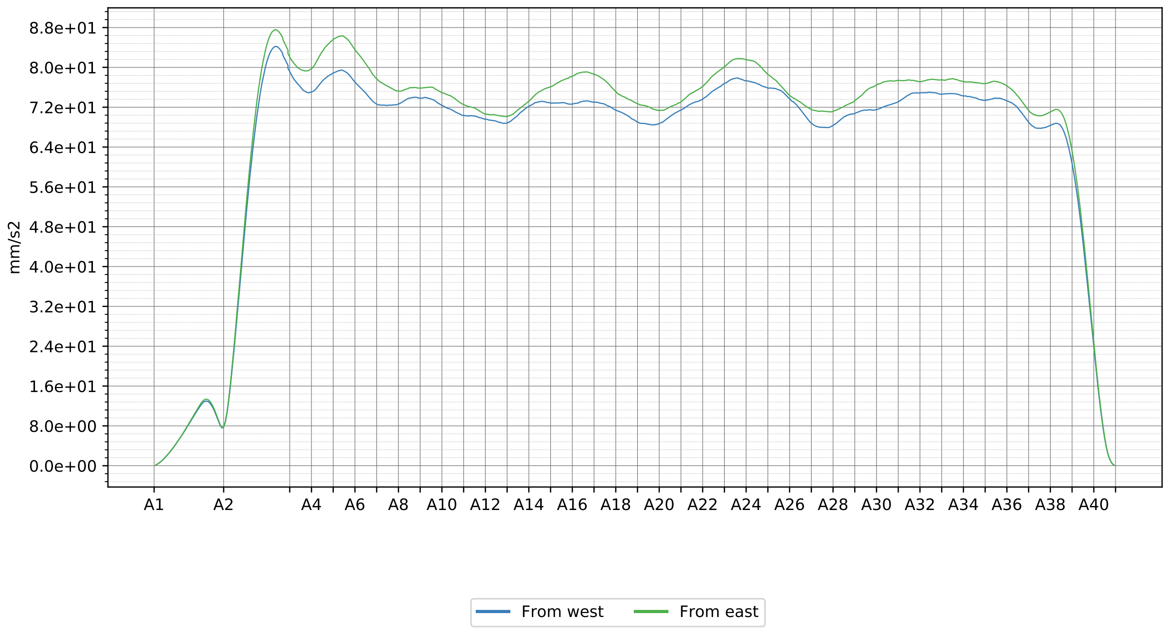

4.10.2 Static wind 1y

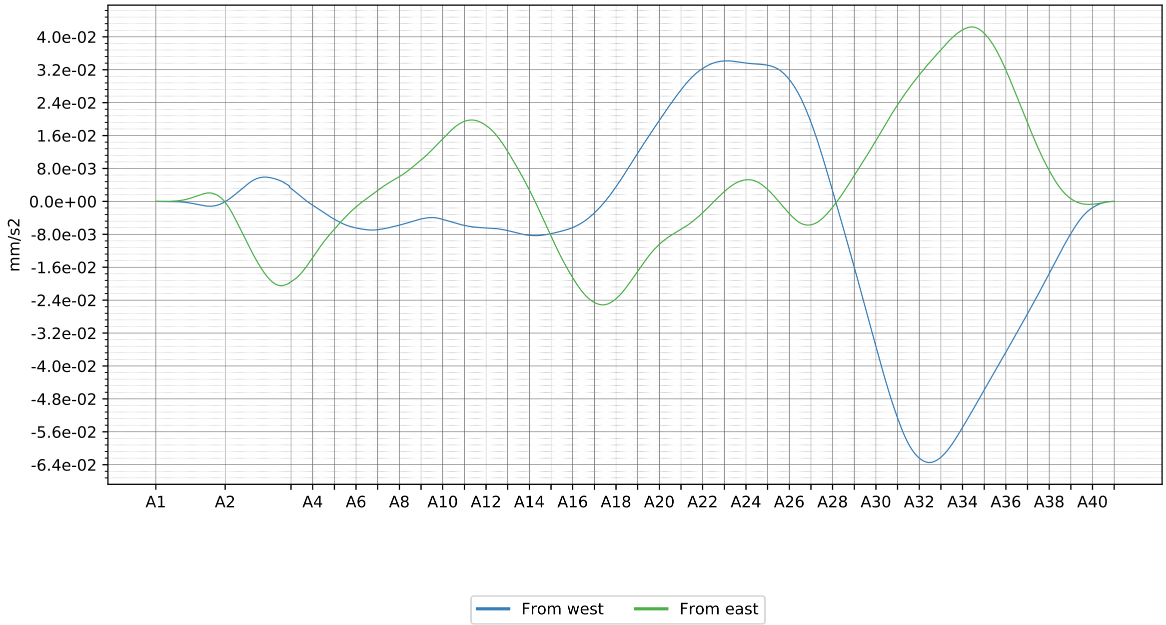

4.10.3 Wave 1 y

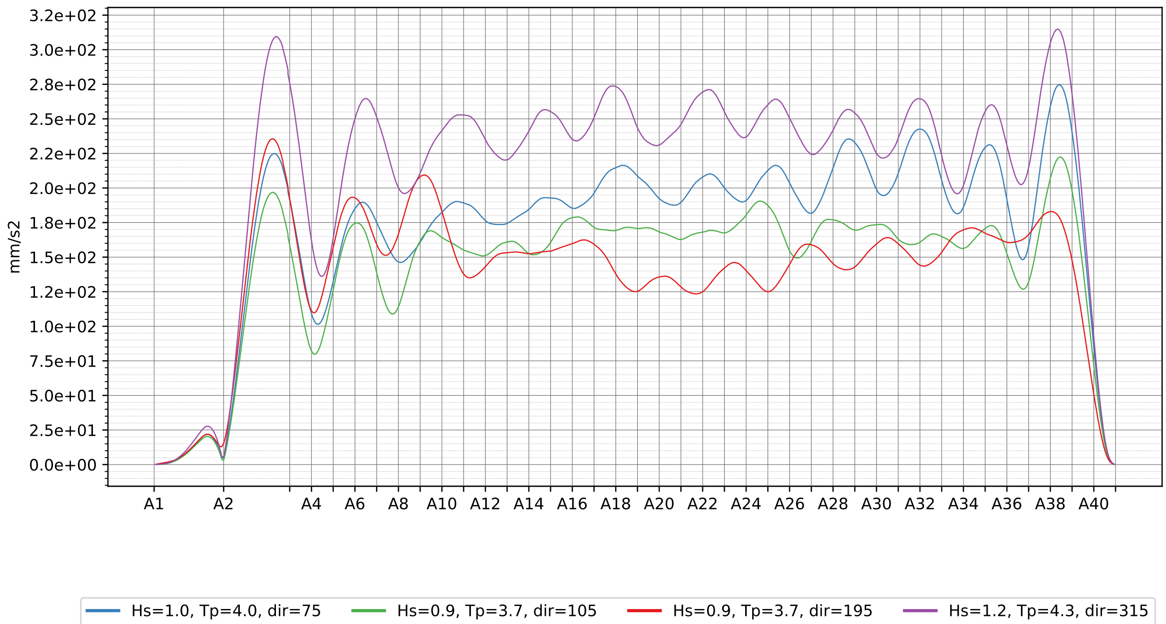

4.10.4 Swell 1 y

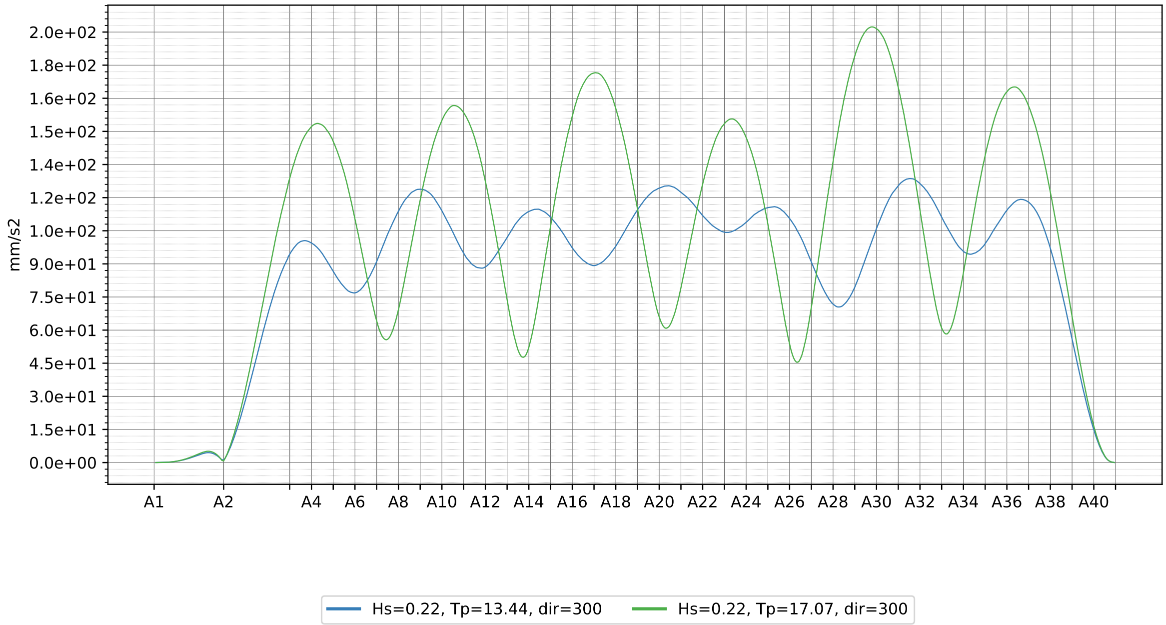

4.10.5 Dynamic wind 100 y

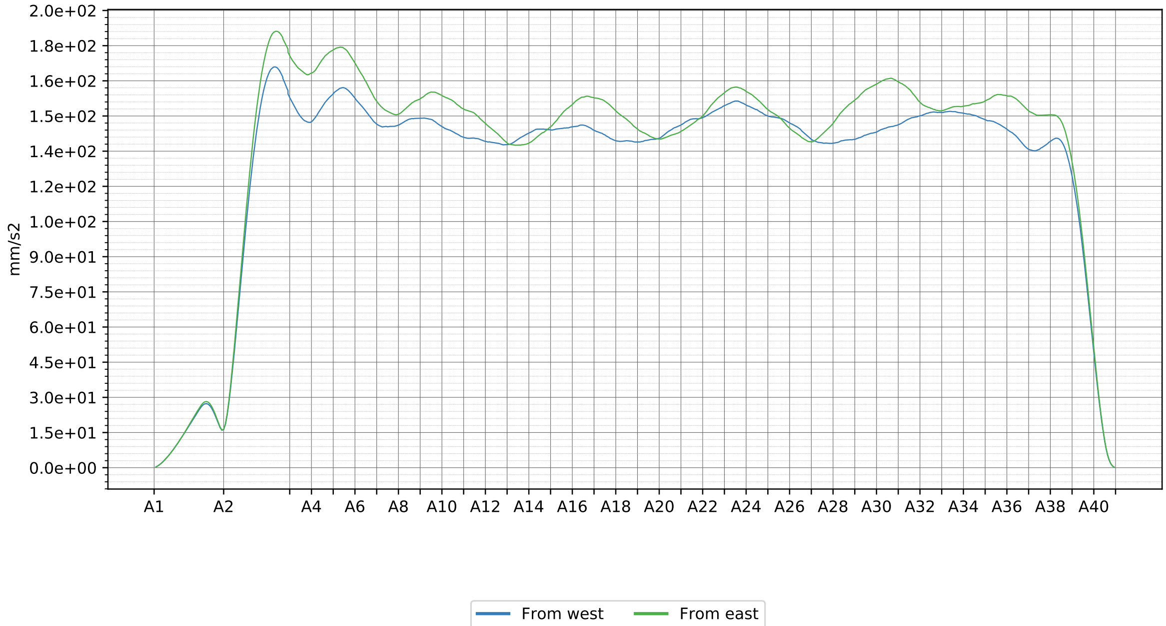

4.10.6 Static wind 100 y

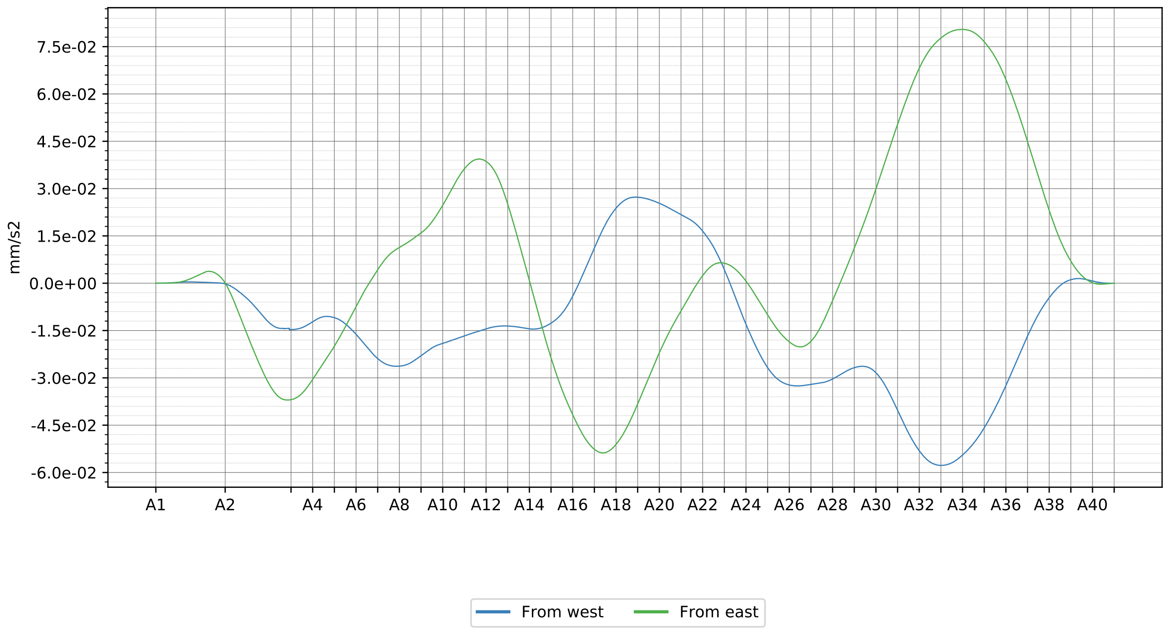

4.10.7 Wave 100 y

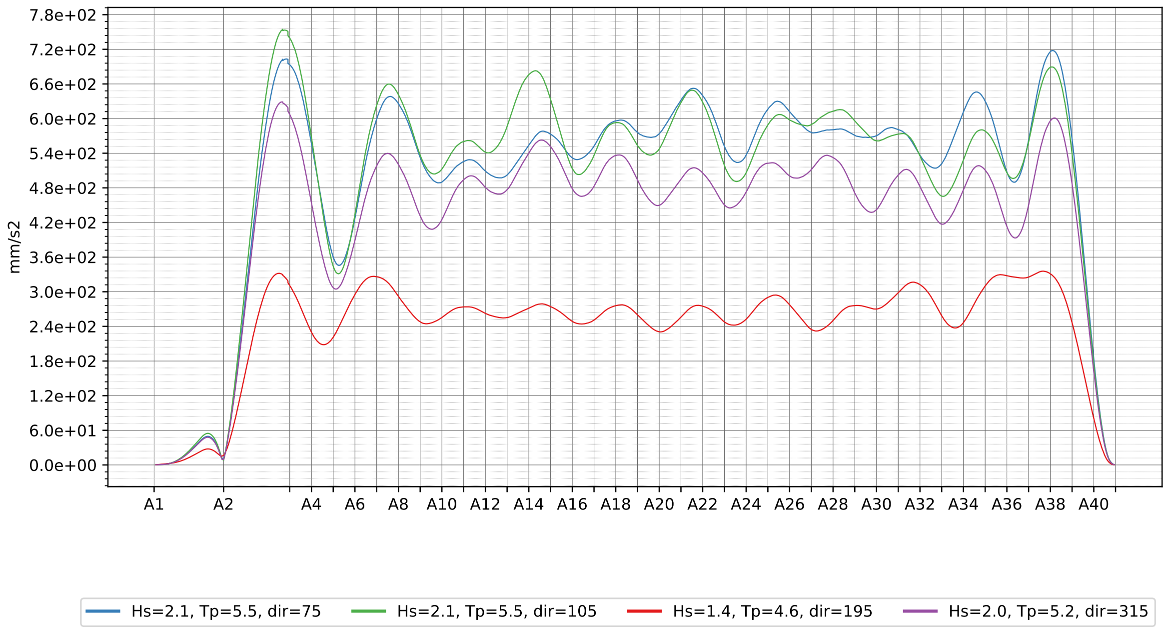

4.10.8 Swell 100 y

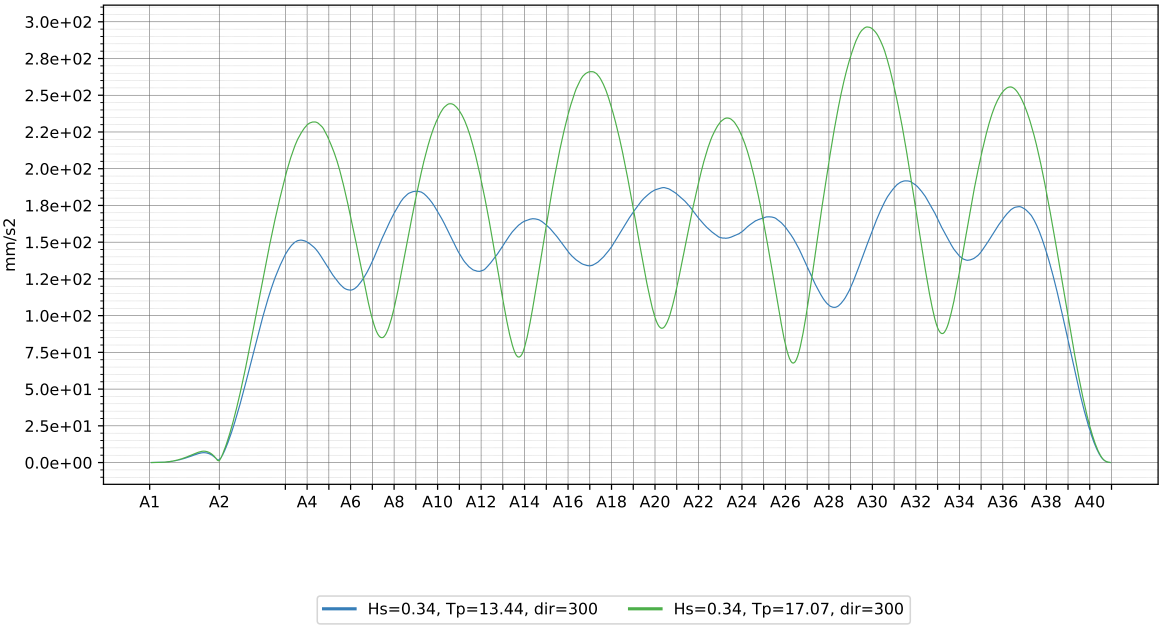

4.11 Global Vertical acceleration

4.11.1 Dynamic wind 1 y

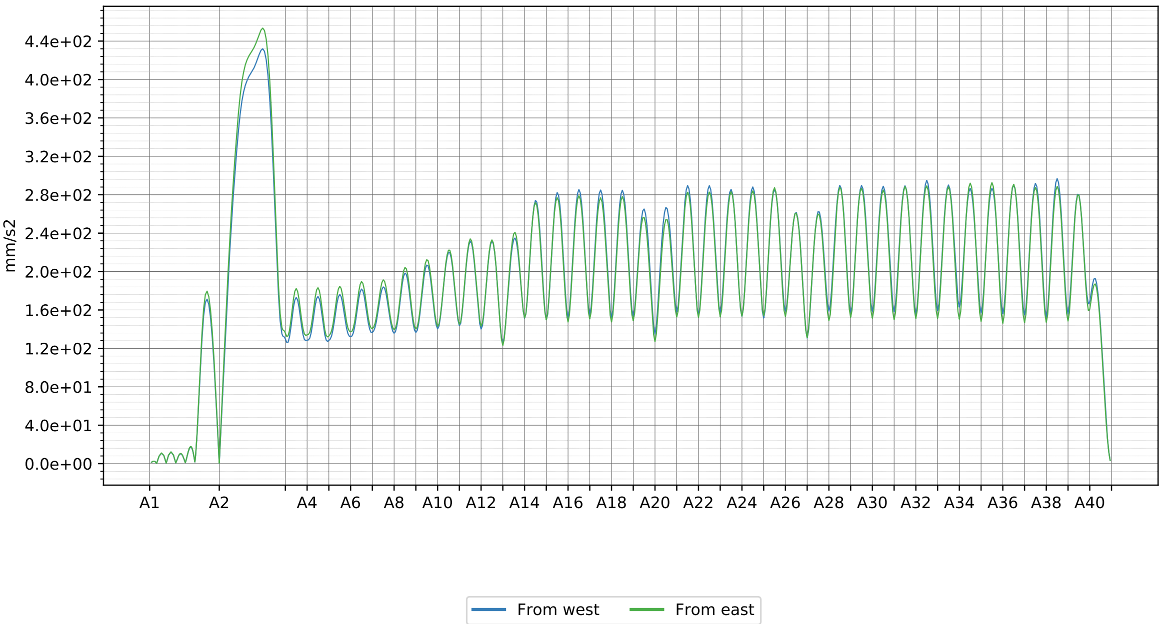

4.11.2 Static wind 1y

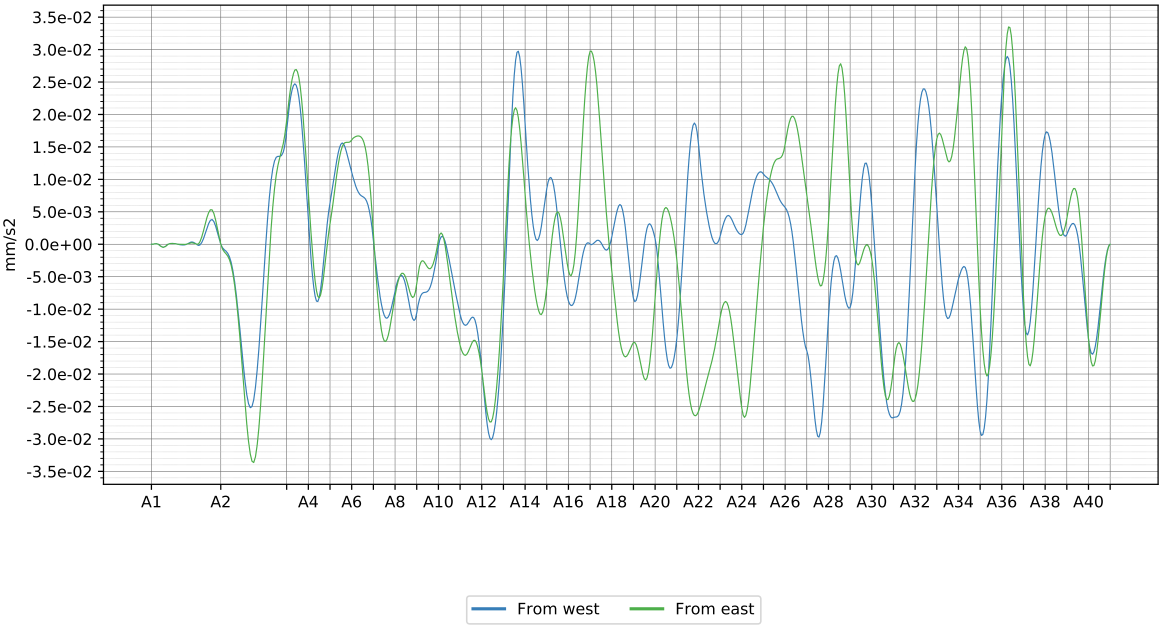

4.11.3 Wave 1 y

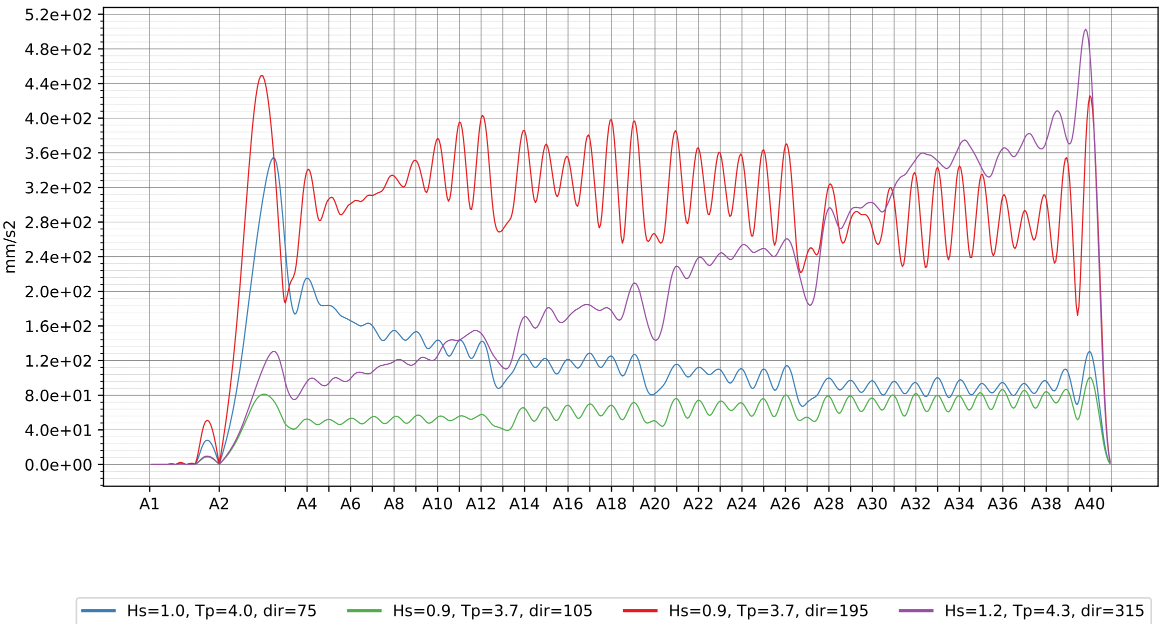

4.11.4 Swell 1 y

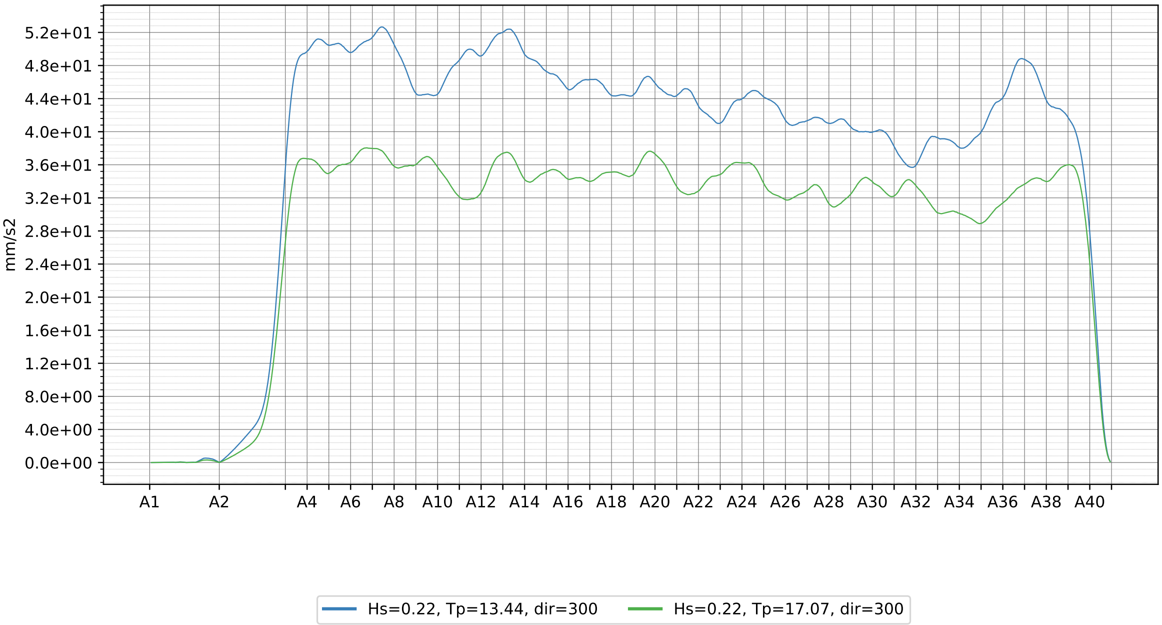

4.11.5 Dynamic wind 100 y

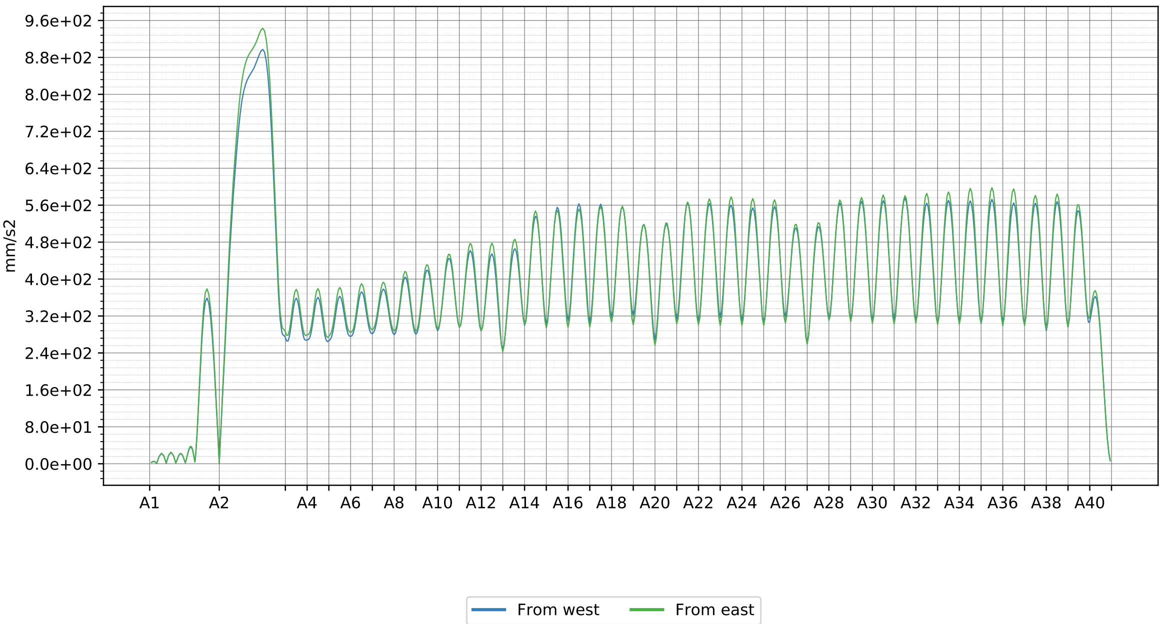

4.11.6 Static wind 100 y

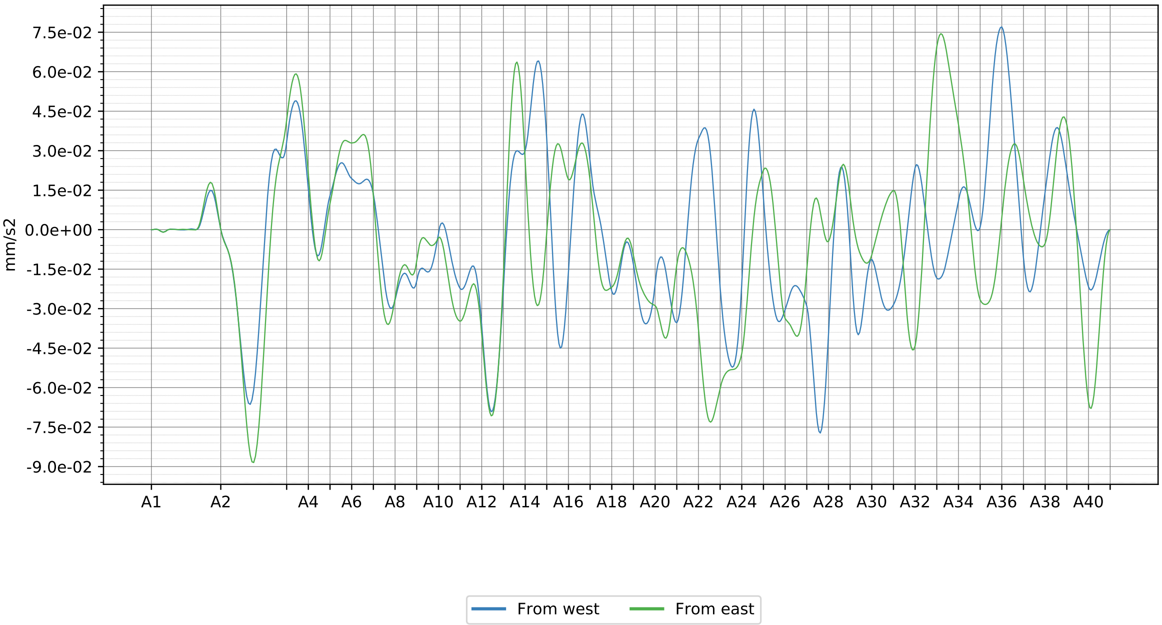

4.11.7 Wave 100 y

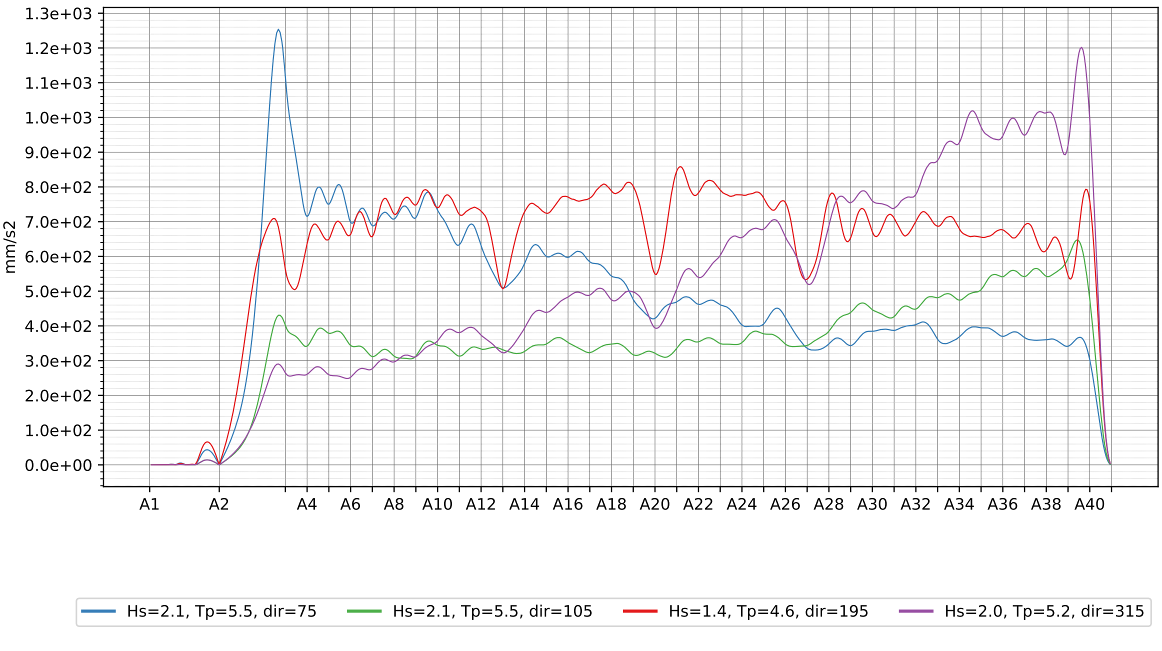

tailor

4.11.8 Swell 100 y

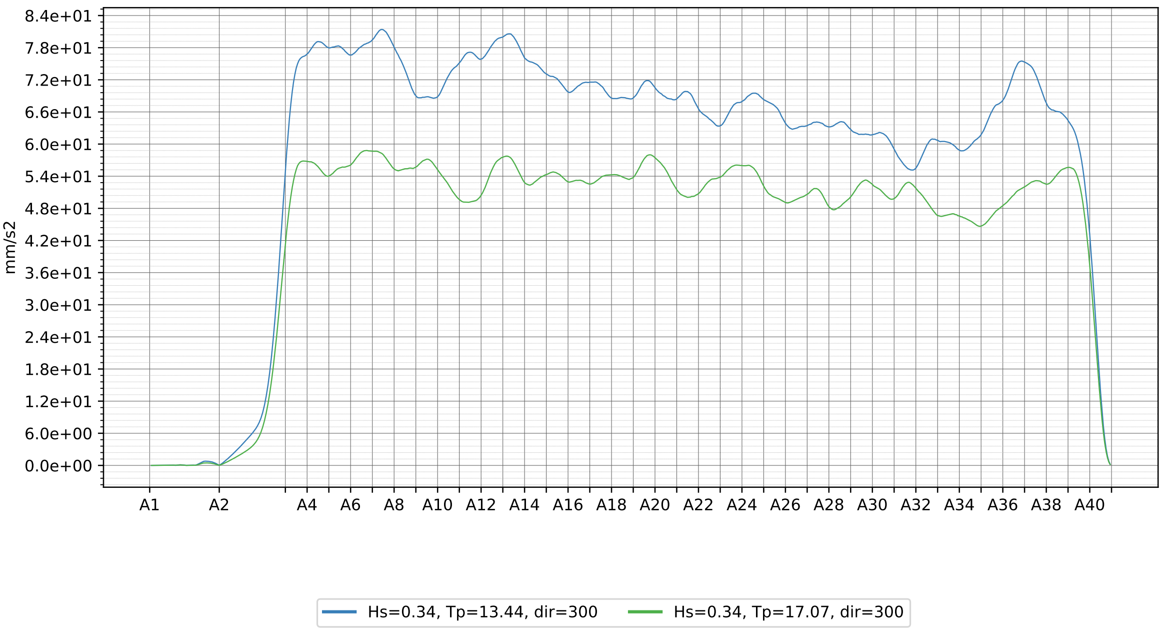

5 Combined results (excl. load factors)

5.1 1 year

5.1.1 Vertical displacement

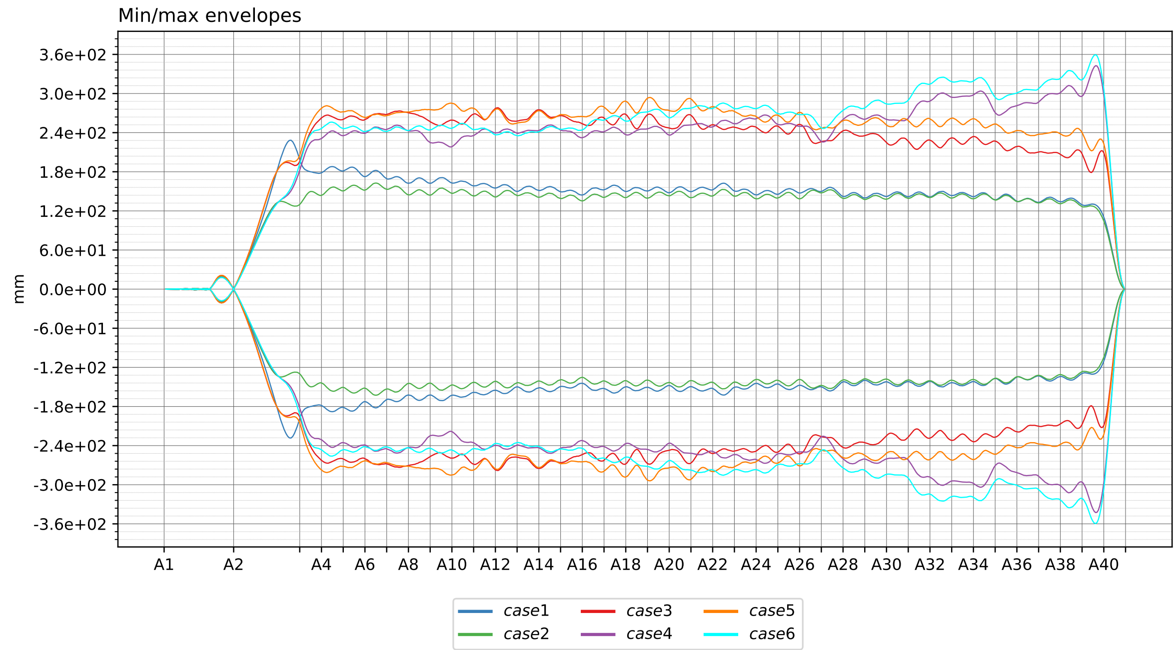

5.1.2 Transverse displacement

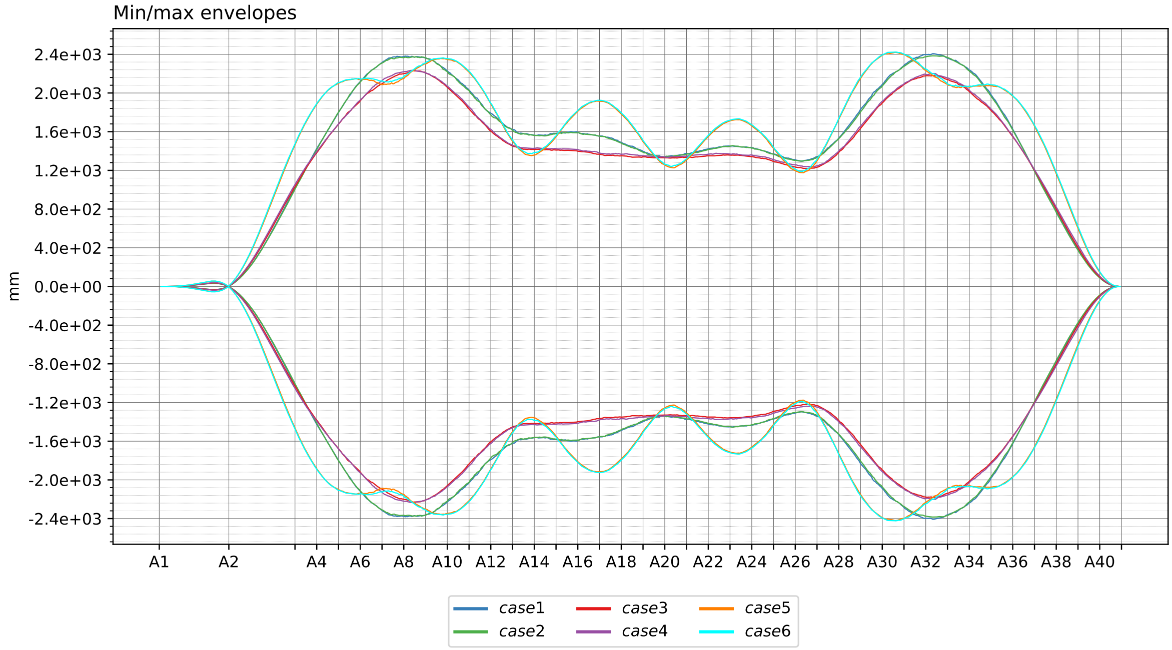

5.1.3 Longitudinal displacement

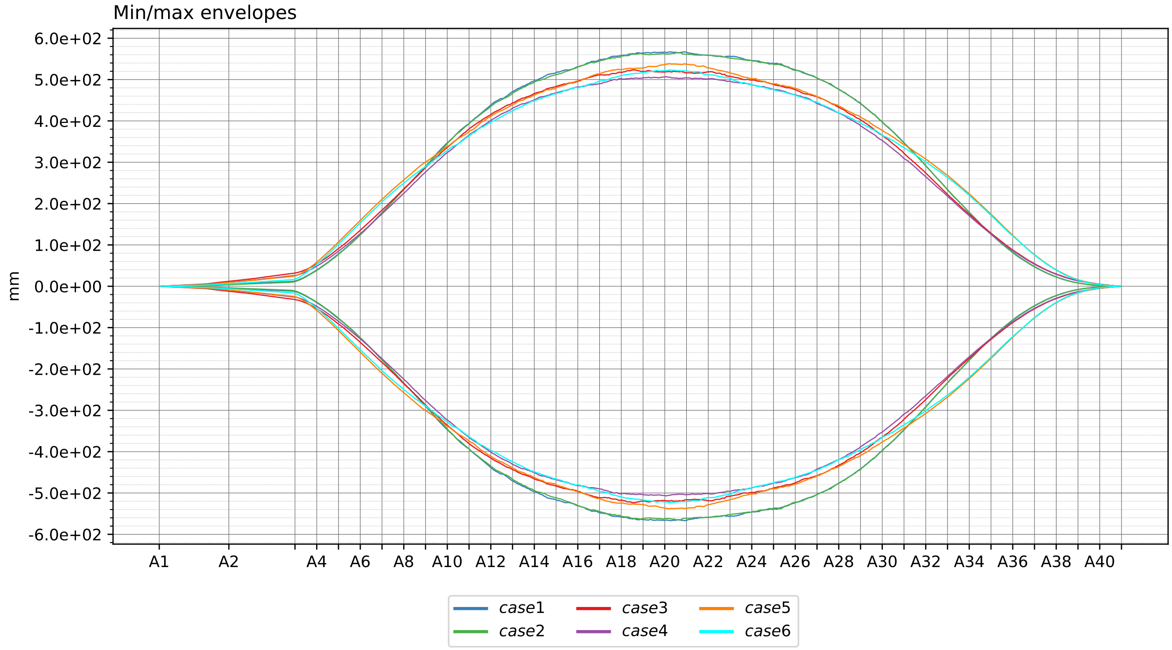

5.1.4 Global Longitudinal displacement

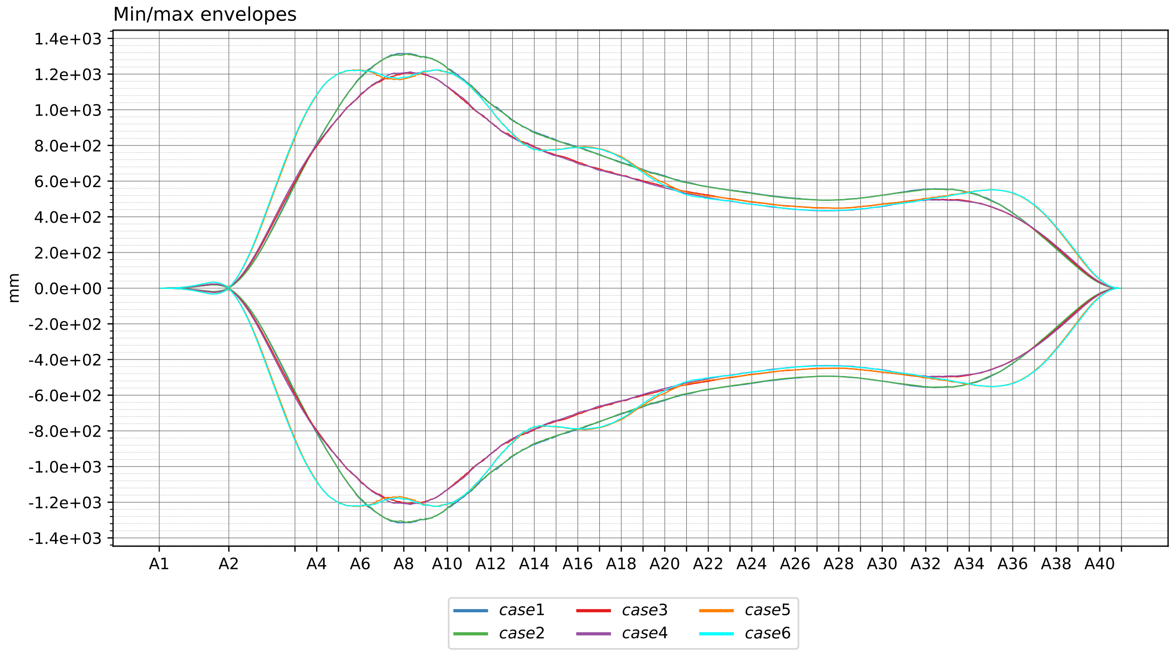

5.1.5 Global Transverse displacement

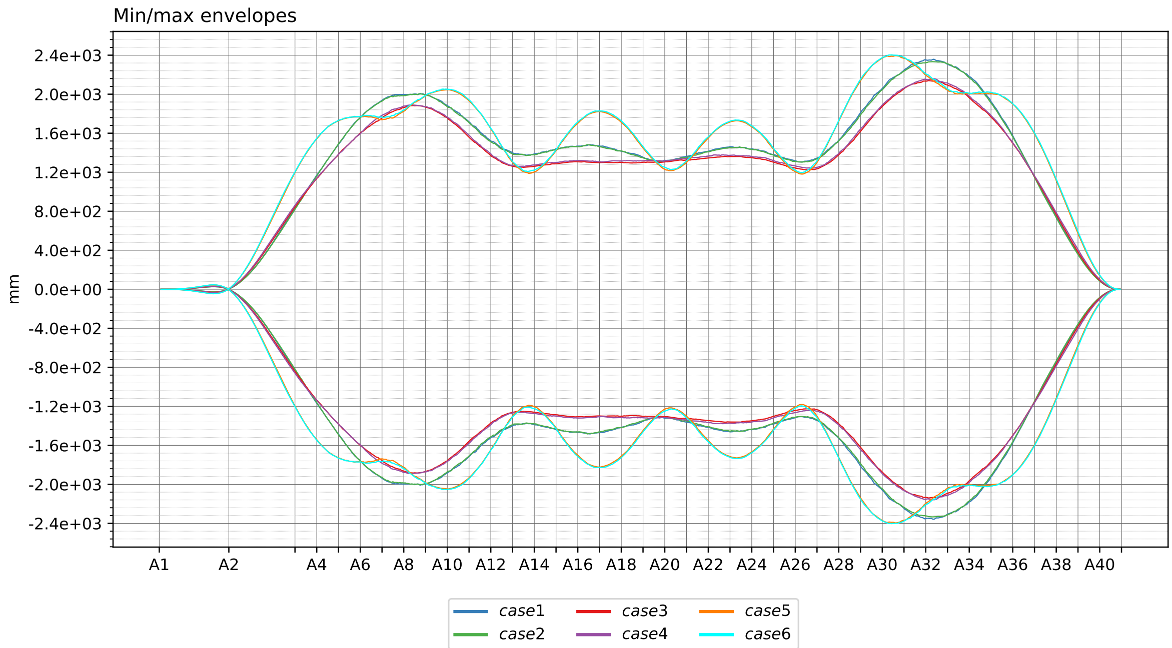

5.1.6 Global Vertical displacement

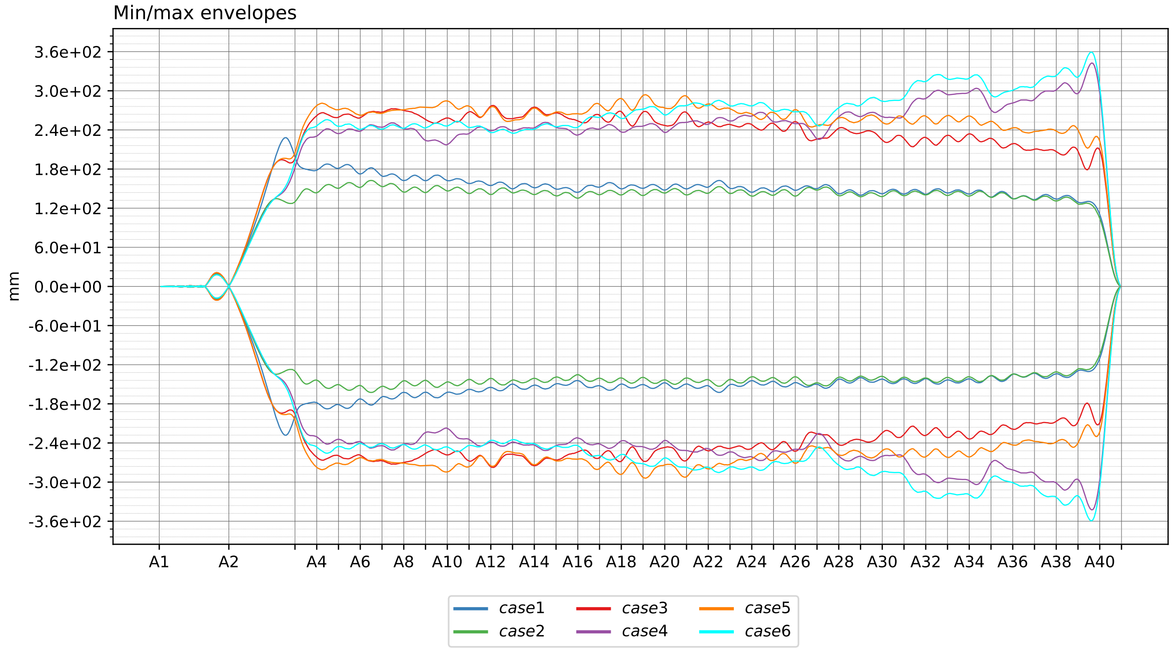

5.1.7 Rotation about vertical axis

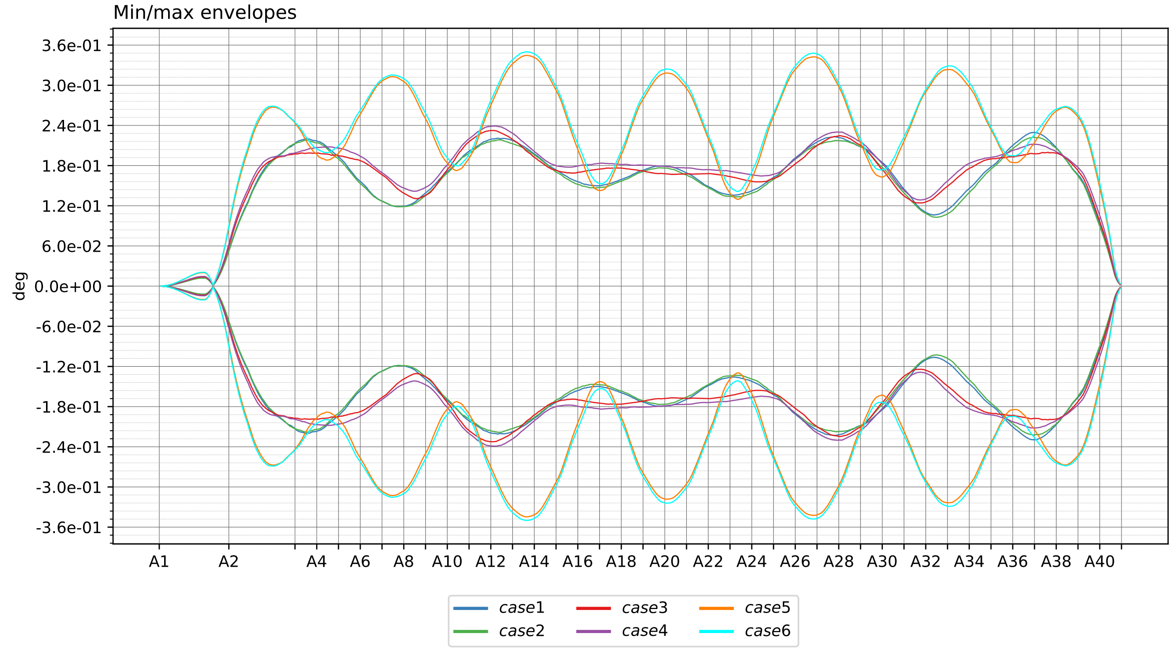

5.1.8 Rotation about transverse axis

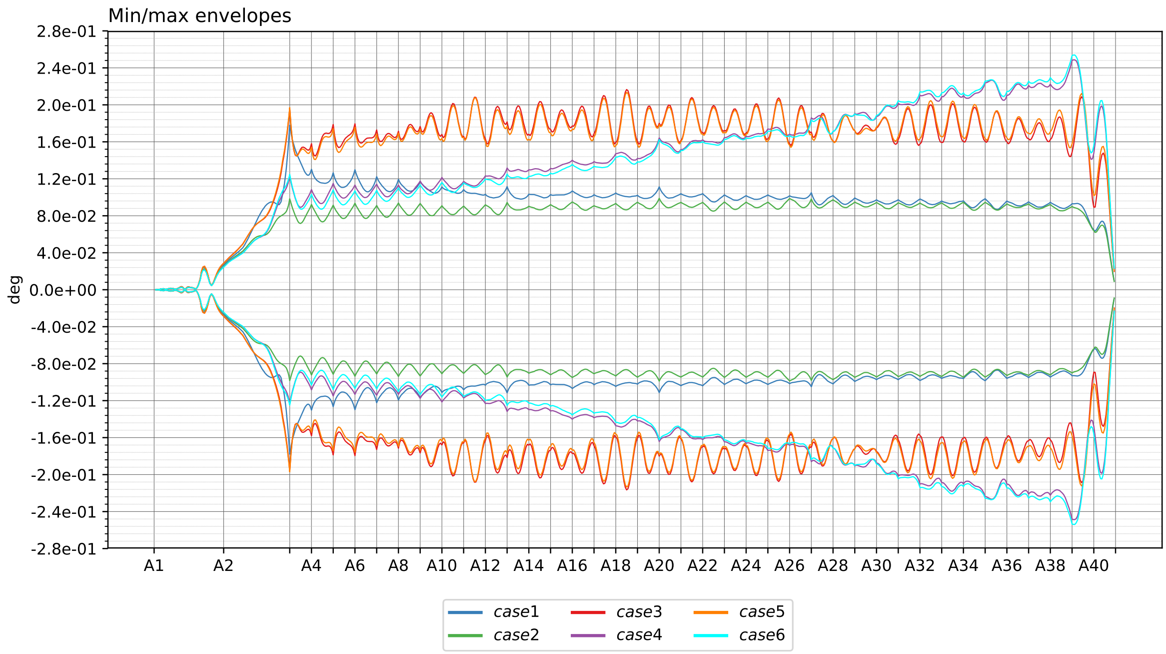

5.1.9 Rotation about bridge axis

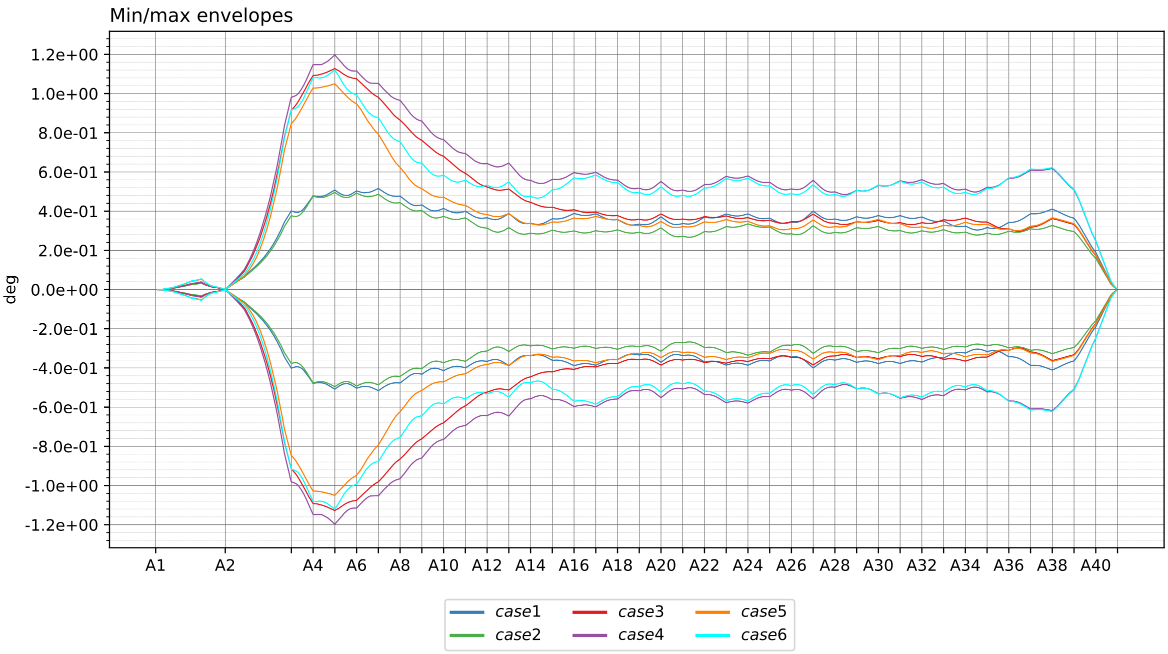

5.1.10 Global Transverse acceleration

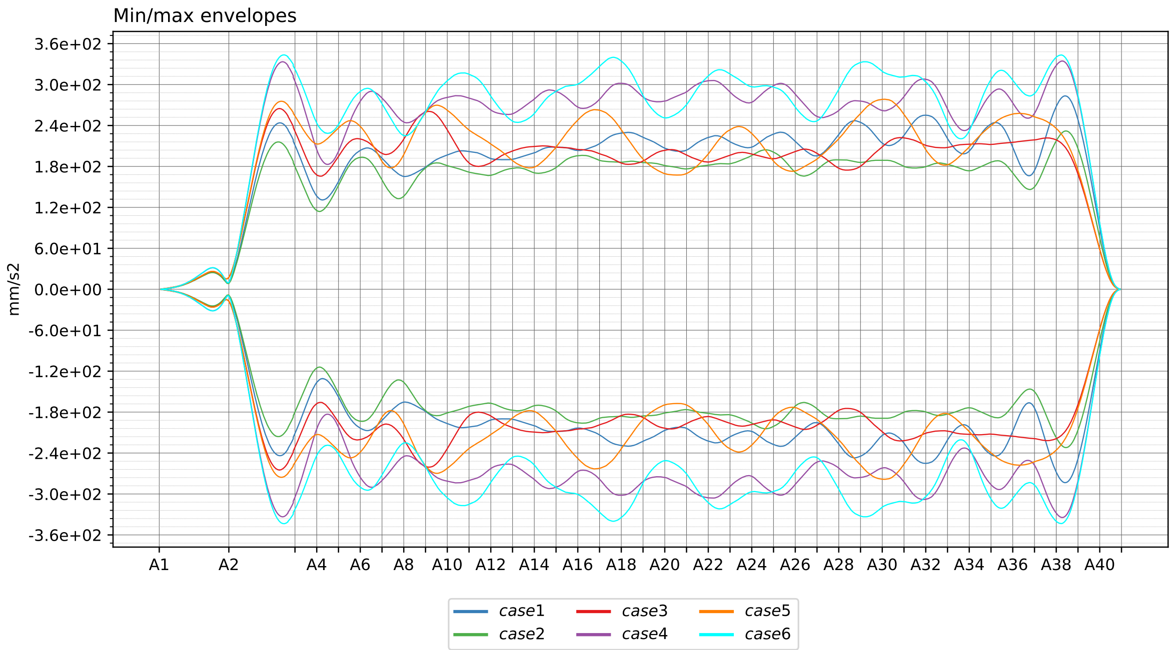

5.1.11 Global Vertical acceleration

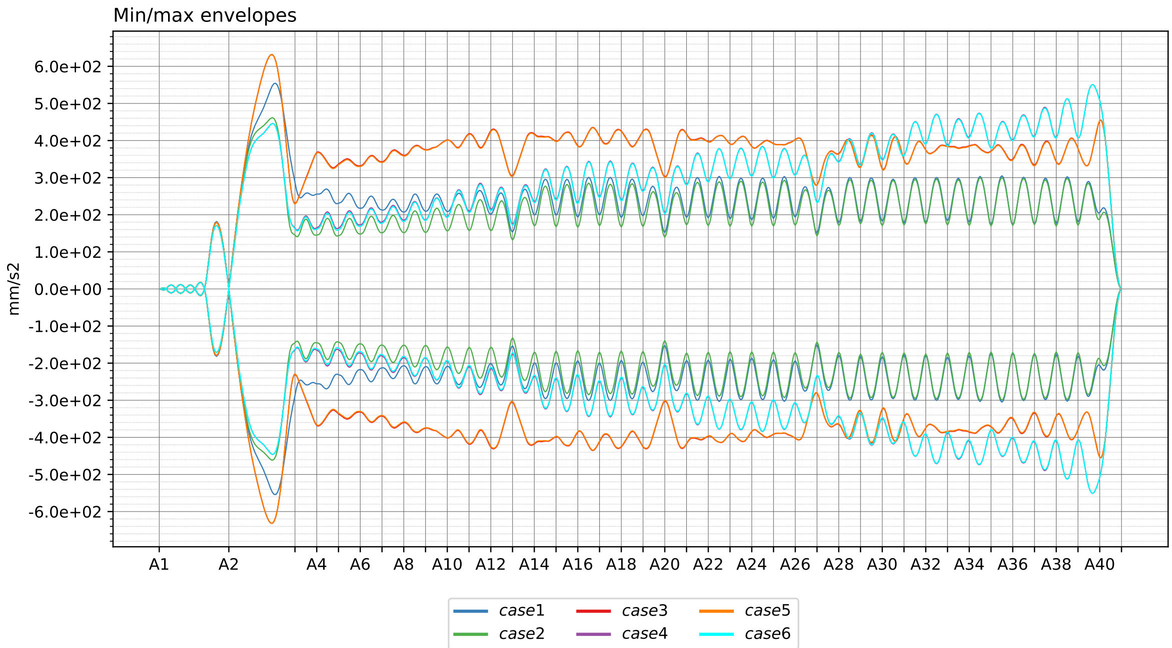

5.2 100 year

5.2.1 Vertical displacement

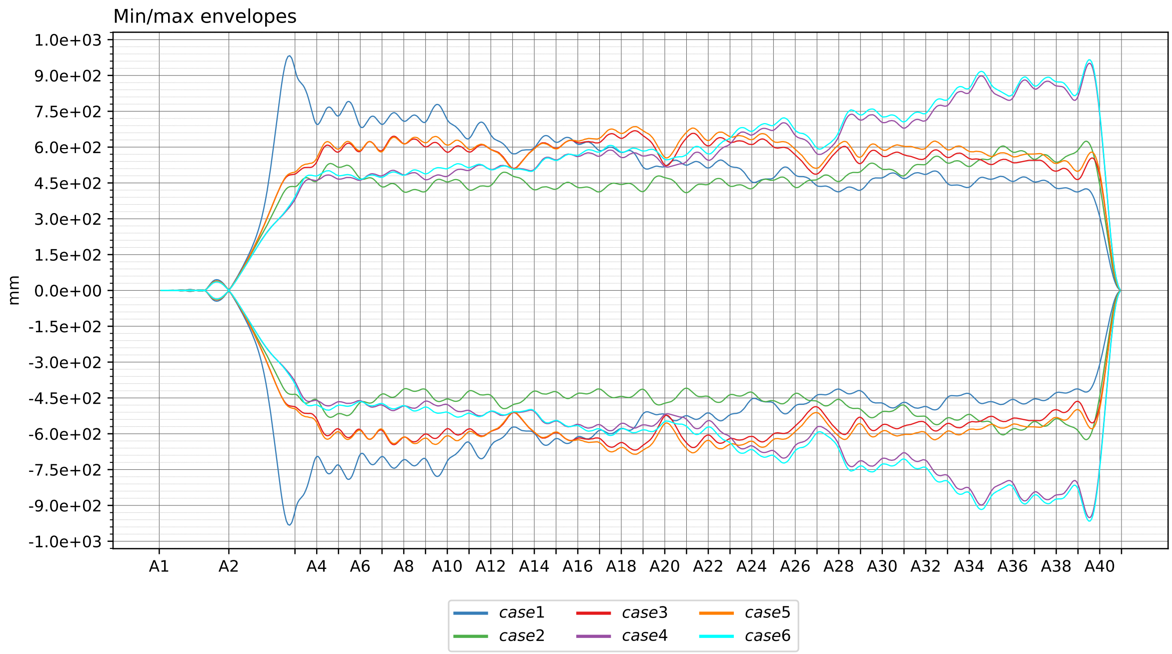

5.2.2 Transverse displacement

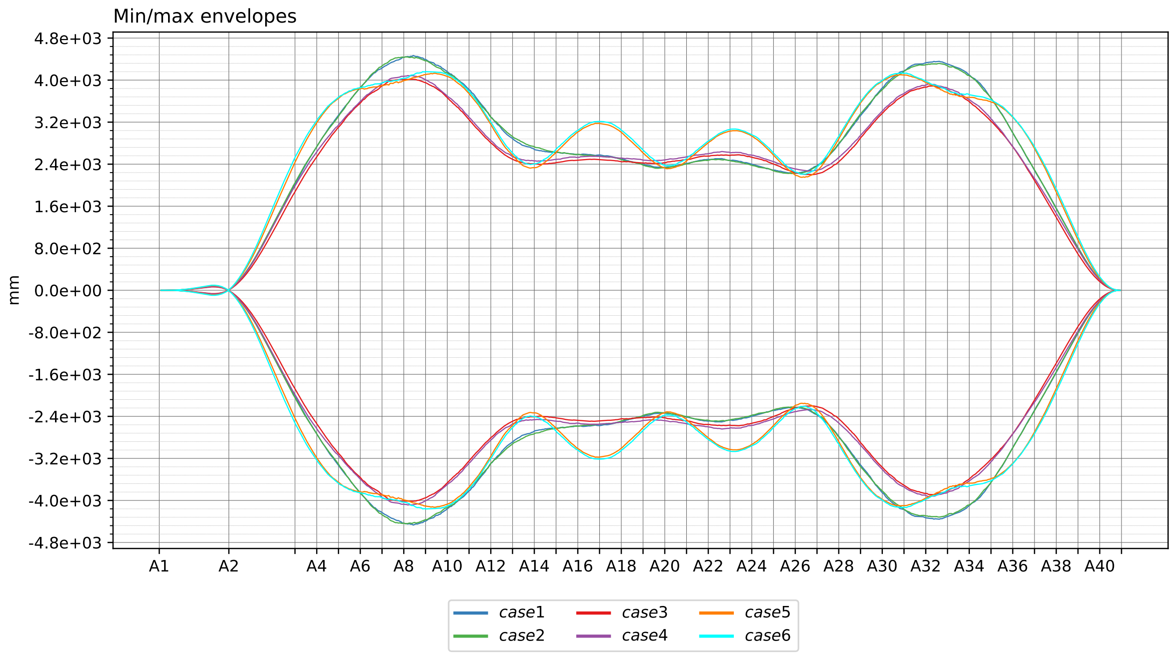

5.2.3 Longitudinal displacement

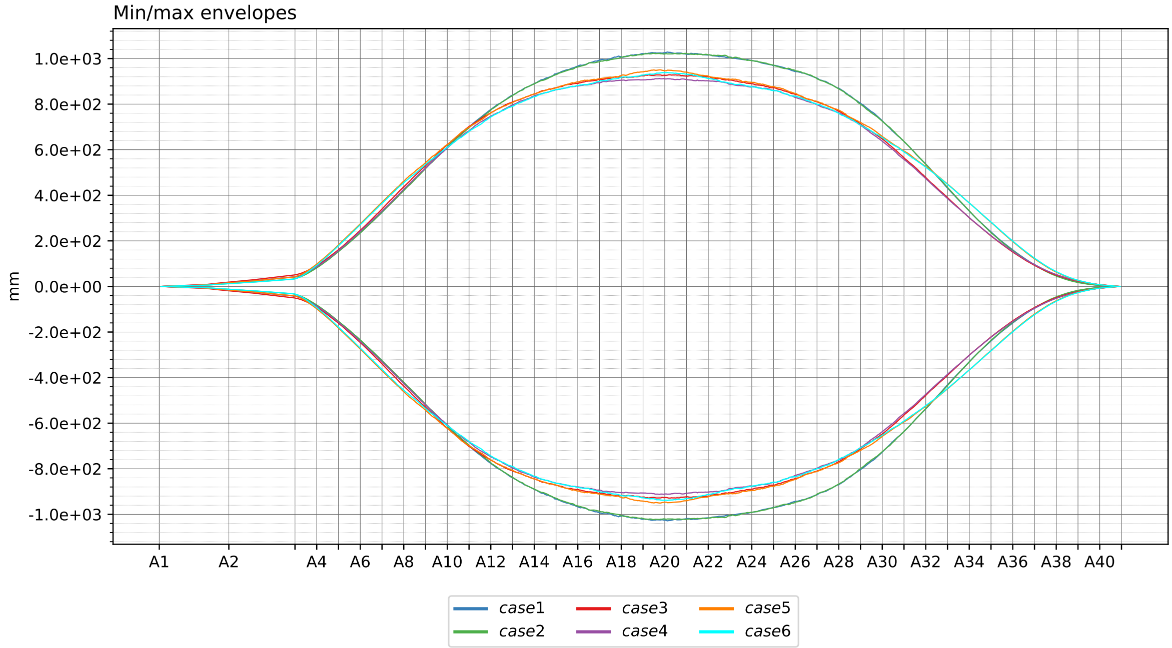

5.2.4 Global Longitudinal displacement

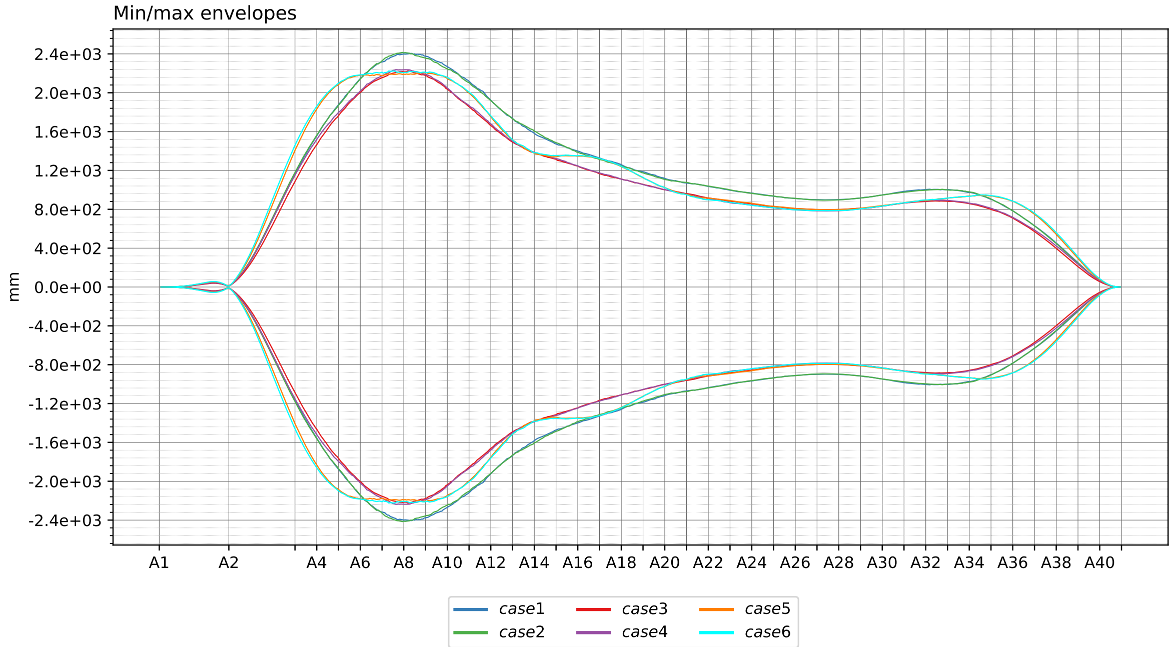

5.2.5 Global Transverse displacement

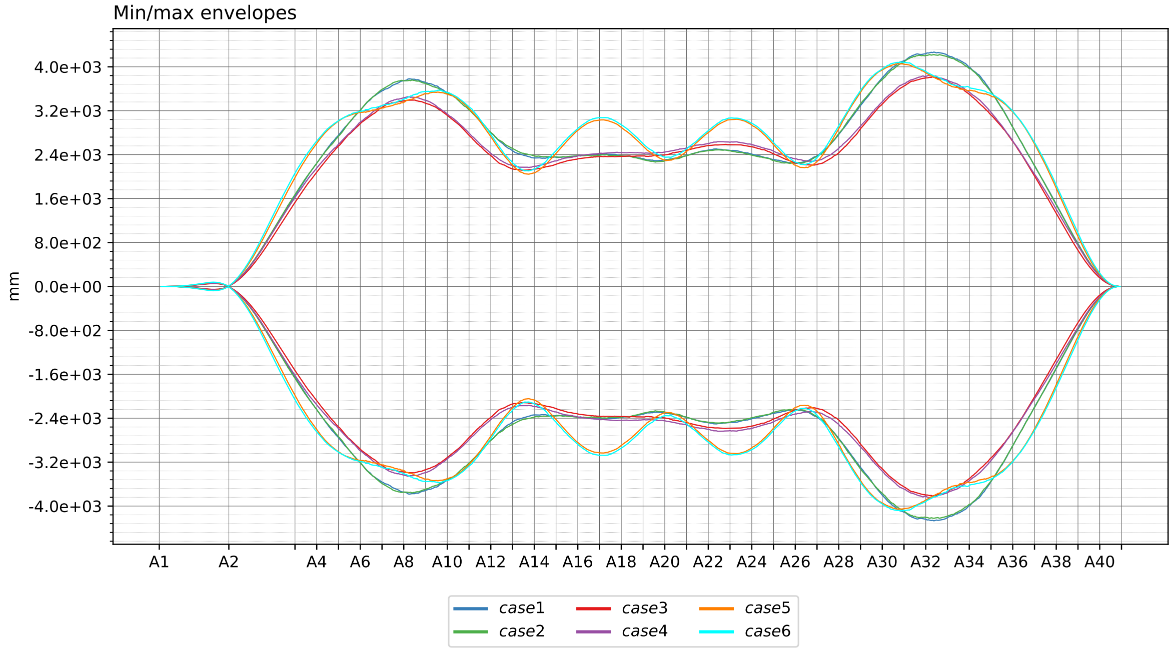

5.2.6 Global Vertical displacement

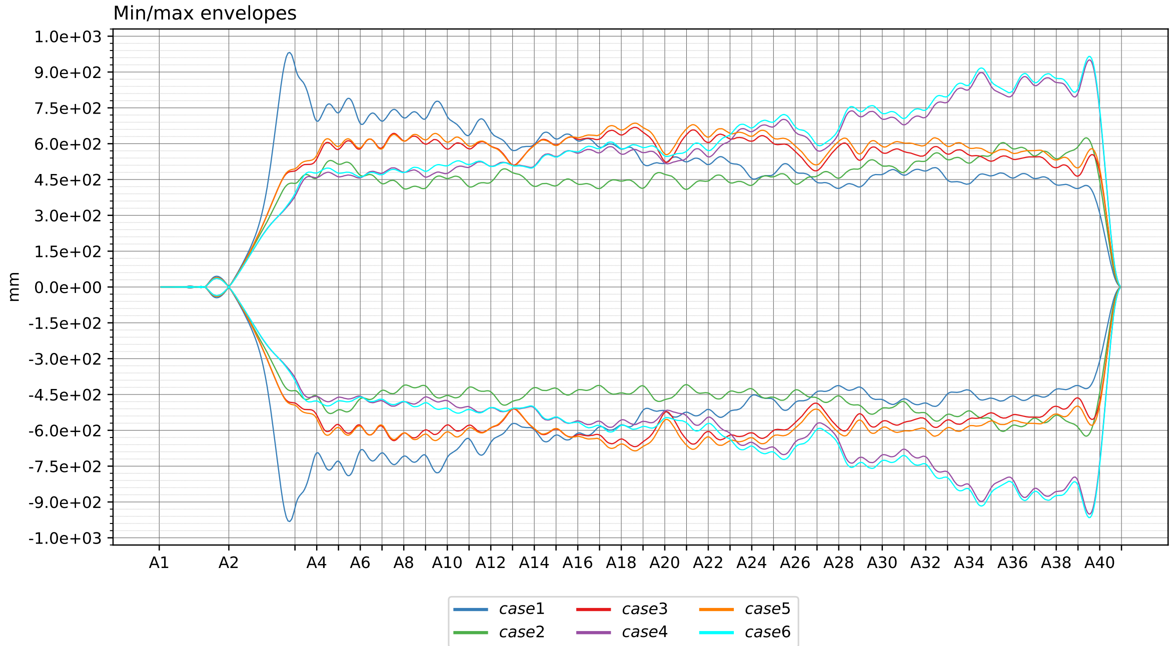

5.2.7 Rotation about vertical axis

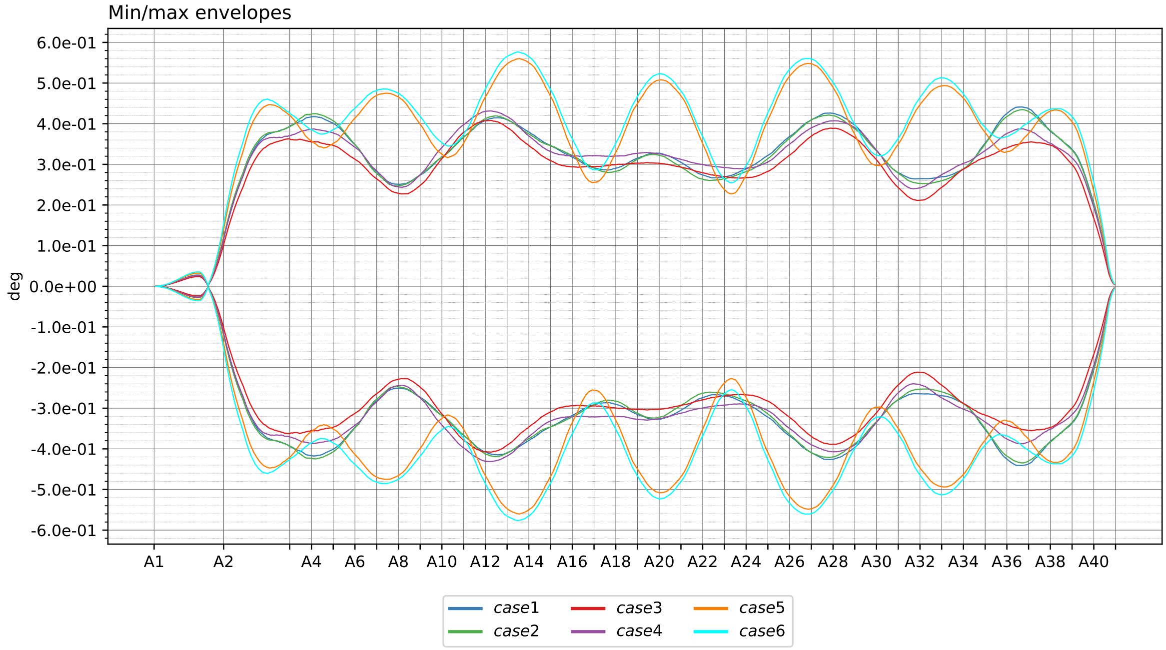

5.2.8 Rotation about transverse axis

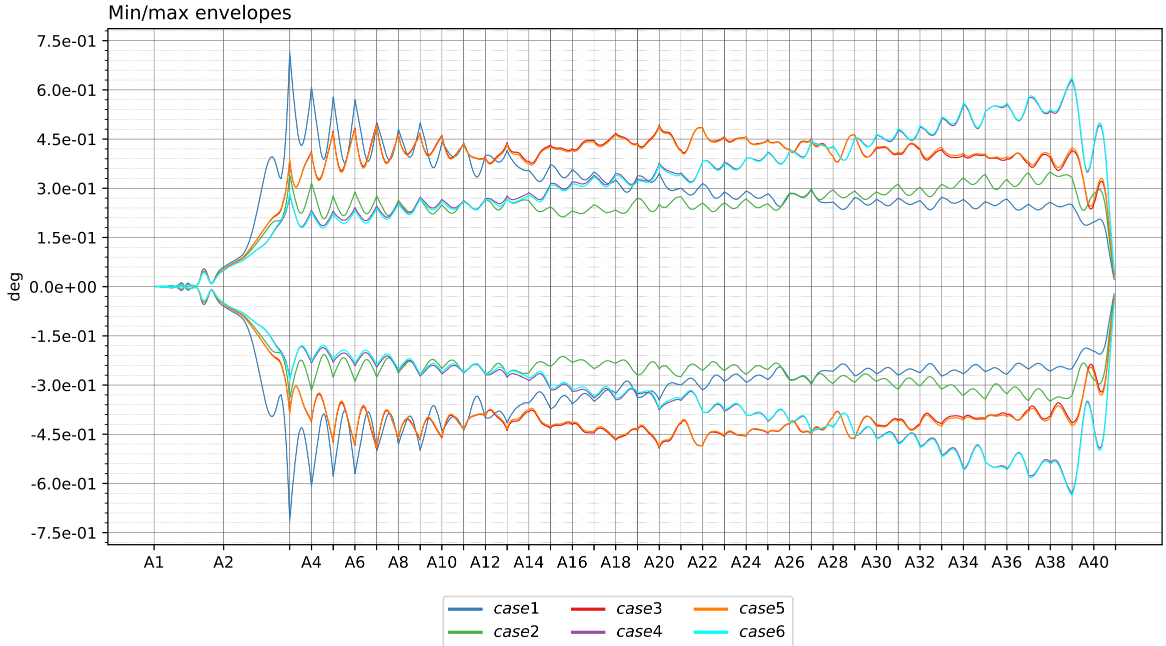

5.2.9 Rotation about bridge axis

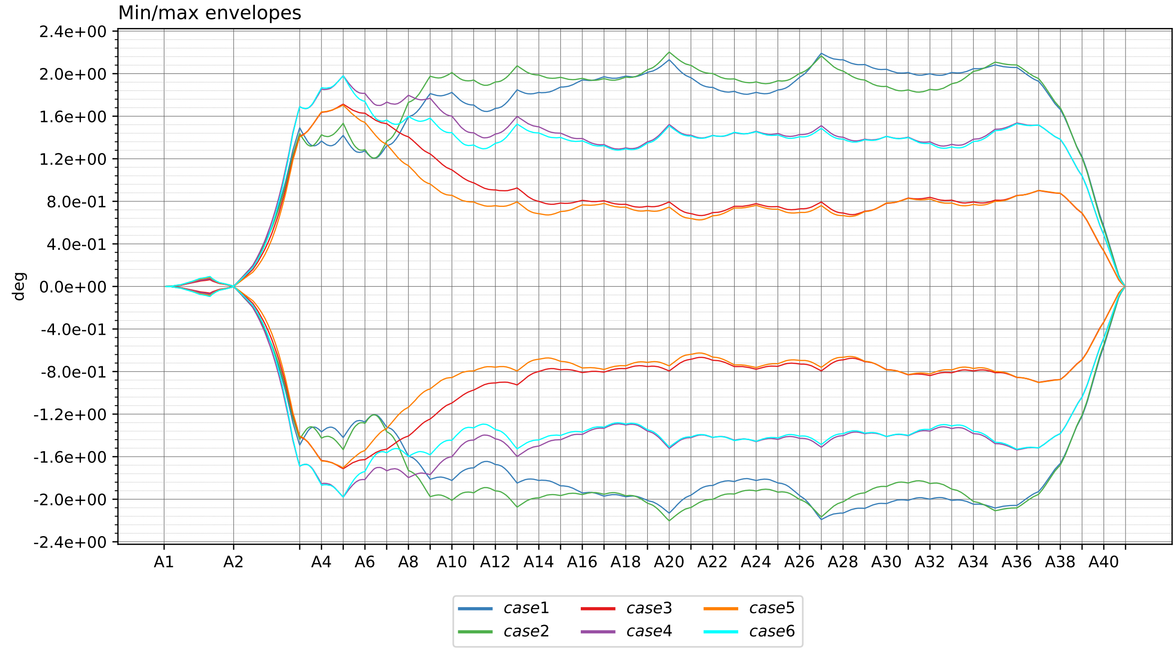

5.2.10 Global Transverse acceleration

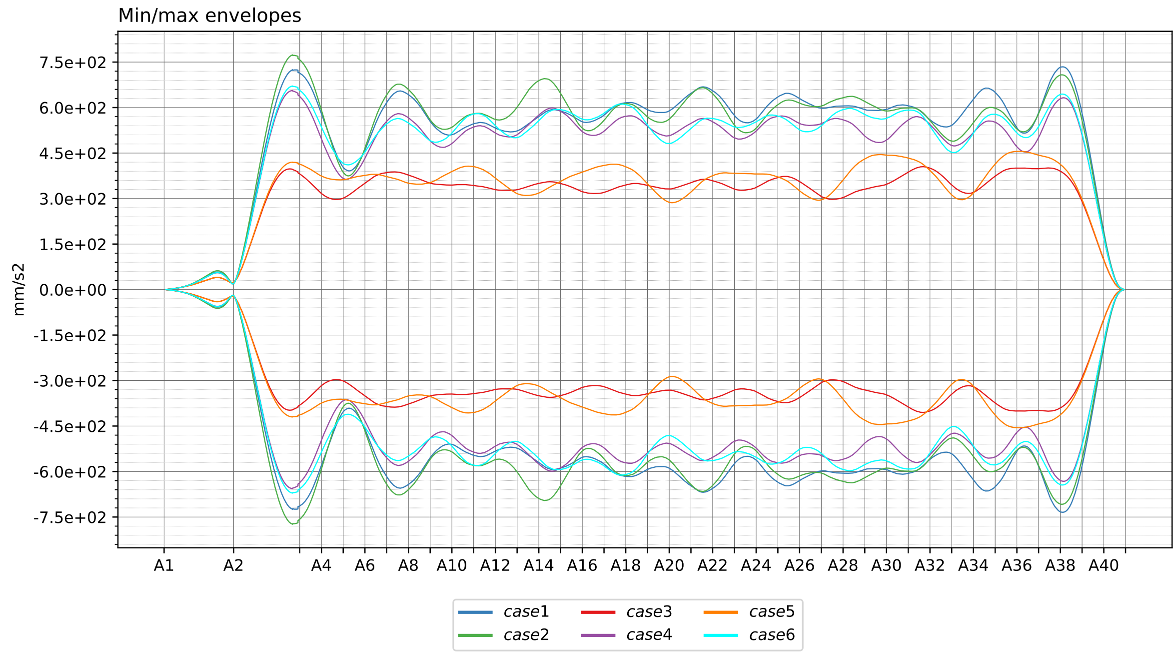

5.2.11 Global Vertical acceleration

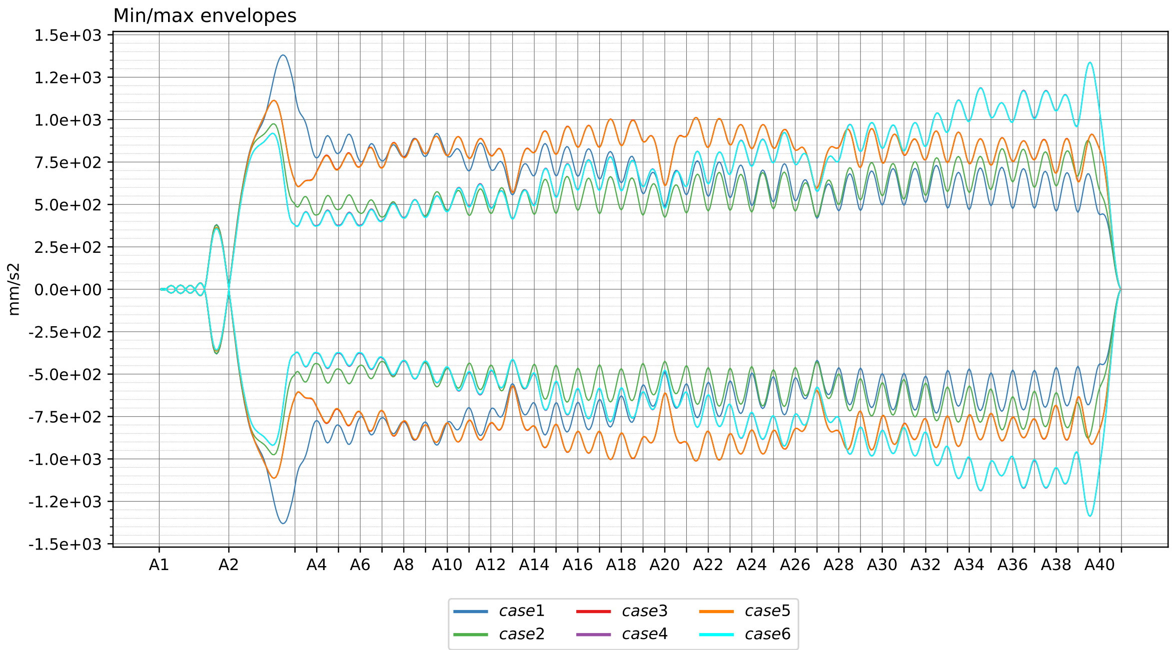

Concept development, floating bridge

E39 Bjørnafjorden

Appendix G – Enclosure 13

10205546-11-NOT-059

Estimation of extreme response using the AUR method

MEMO

PROJECT	**Concept development, floating bridge E39 Bjørnafjorden**	DOCUMENT CODE	10205546-11-NOT-059
CLIENT	Statens vegvesen	ACCESSIBILITY	Restricted
SUBJECT	**Estimation of extreme response using the AUR method**	PROJECT MANAGER	Svein Erik Jakobsen
TO	Statens vegvesen	PREPARED BY	Finn-Idar Grøtta Giske
COPY TO		RESPONSIBLE UNIT	AMC

SUMMARY

This document describes the application of the average upcrossing rate (AUR) method for estimating short-term extreme response. The AUR method can be applied to both Gaussian and non-Gaussian response processes, and does not require a specific simulation time. Compared to the Gumbel method for extreme response, the AUR method utilizes more of the data in the simulated time series, and is thereby expected to be more accurate.

0	29.03.2019	Status 2 issue	F. I. G. Giske	R. M. Larssen	S. E. Jakobsen
REV.	DATE	DESCRIPTION	PREPARED BY	CHECKED BY	APPROVED BY

1 References

[1] Naess A, Moan T. Stochastic Dynamics of Marine Structures. Cambridge: Cambridge University Press; 2013.

2 Background

For the short-term extreme response, we are interested in the maximal value of a stationary stochastic response process during a short-term period, e.g. the 1-hour max value. This short-term max value will be a random variable fully described by its cumulative distribution function (CDF), and characteristic values can be given as e.g. the expected value or a specified percentile of this distribution.

If the stationary response process can be assumed Gaussian, approximate analytical expressions can be derived. For instance, the expected short-term max value is given as

$$\xi_{exp\,max} \approx \mu + \sigma \left\{ \sqrt{2\ln(\nu_\mu T)} + \frac{0.5772}{\sqrt{2\ln(\nu_\mu T)}} \right\},$$

where μ and σ are the mean value and standard deviation of the response process, ν_μ is the average upcrossing rate of the mean value and T is the short-term period. A rough and simple approximation that is commonly used is $\xi_{exp\,max} \approx \mu + 4\sigma$ for a 3-hour short-term period. This corresponds to $\xi_{exp\,max} \approx \mu + 3.7\sigma$ for a short-term period of one hour.

The assumption of a Gaussian response process is usually reasonable for typical response processes of a floating bridge exposed to environmental loads, e.g. the axial force or strong- and weak-axis bending moments. However, if we are interested in the extreme values of Von Mises stress, the assumption of a Gaussian response process is not valid.

Avoiding the assumption of a Gaussian response process, the characteristic extreme values can be estimated by simulating several 1-hour time series of the response and picking out the maximal value in each of the time series. For response due to environmental loads, the asymptotic extreme value distribution is usually of Gumbel type. Based on this observation, a Gumbel distribution can be fitted to the simulated max values, and characteristic values of the extreme response can be obtained. However, such an approach will only utilize a limited amount of the data available in the time series, as only one data point is obtained from each (possibly very time consuming) 1-hour simulation. The simulated time series must also have exactly the same length as the short-term period of interest. Furthermore, even if the asymptotic extreme value distribution is indeed a Gumbel distribution, it may be questionable to assume a Gumbel distribution for moderate levels of the extreme value.

A more flexible method for estimating the short-term extreme response distribution is given by the average upcrossing rate (AUR) method, ref. [1]. This method utilizes more of the data from the simulated time series and is thereby expected to be more accurate. The method does not rely on a specific simulation length, and it has the ability to capture subasymptotic behaviour.

2.1 Theoretical background of the AUR method

The average upcrossing rate (AUR) method, or Naess-Gaidai method, is described in Section 16.6.3 of ref. [1]. The basic assumption is that upcrossings of high levels of a stationary stochastic process $X(t)$ are statistically independent events. This is a good approximation as long as the process is not too narrow banded. Under this assumption, the maximum value $M(T)$ of $X(t)$ during a period of duration T, has a CDF given by

$$F_{M(T)}(\xi) = \mathrm{Prob}[M(T) \leq \xi] = \exp\{-\nu(\xi)T\},$$

where $\nu(\xi)$ is the average upcrossing rate of $X(t)$ for a level ξ.

The average upcrossing rate can be estimated for a given level ξ_i by counting the number of ξ_i-upcrossings from time series of $X(t)$. Estimates $\hat{\nu}(\xi_i)$ can be obtained, along with approximations for the 95% confidence intervals $\left(C^-(\xi_i), C^+(\xi_i)\right)$ as described in ref. [1].

The basic idea of the AUR-method is that for large levels $\xi \geq \xi_0$, the average upcrossing rate is a function of the form

$$\nu(\xi) = q \cdot \exp\{-a(\xi - b)^c\},\ \xi \geq \xi_0,$$

where $a > 0$, $b \leq \xi_0$ and $c > 0$. The parameters q, a, b, c are found by a fitting to observed upcrossing rates $\hat{\nu}(\xi_i)$ for different levels ξ_i. Specifically, the fitting is performed on the log level by minimizing the sum of square errors

$$F(q, a, b, c) = \sum_{i=1}^{N} w_i |\ln \hat{\nu}(\xi_i) - \ln q + a(\xi_i - b)^c|^2$$

where the weights w_i depend on the confidence intervals of the observations as $w_i = (\ln C^+(\xi_i) - \ln C^-(\xi_i))^{-2}$. The optimization is simplified by observing that if b and c are fixed, the problem is given as a linear least squares problem, and the optimal values of $\ln q$ and a are given by simple formulas in terms of b and c. This means that the nonlinear optimization of the square error can be performed with only two variables.

It should be noted that an asymptotic Gumbel distribution for the extreme values corresponds to $c = 1$ in the assumed average upcrossing rate. By assuming a more general class of functions, the ability to capture subasymptotic behaviour is greatly enhanced, cf. ref [1].

It should also be noted that for cases where c should be close to 1, the minimization of the sum of square errors $F(q, a, b, c)$ may give unreasonable results. By inserting $c = 1$ in the above expression for $F(q, a, b, c)$, it is seen that linear least squares gives optimal values for $(\ln q + ab)$ and a, which means that there is an infinite number of solutions. In some cases, this has the strange effect that when $F(q, a, b, c)$ is minimized, we obtain excessively large values of c and excessively small values of a.

One way to overcome the problem of excessively large c-values (and corresponding small a-values) could be to weakly penalize deviations from $c = 1$, based on the assumption of an asymptotic Gumbel distribution. For instance, the sum of square errors could be modified with a factor $(1 + k \cdot |\ln c|)$ for some value k, e.g. $k = 0.5$. The AUR parameters are then obtained by minimizing the modified sum of square errors given by

$$\tilde{F}(q, a, b, c) = (1 + k \cdot |\ln c|) \sum_{i=1}^{N} w_i |\ln \hat{\nu}(\xi_i) - \ln q + a(\xi_i - b)^c|^2.$$

3 Short-term extreme values of Von Mises stress

As an example, we consider ten simulated 1-hour time series of Von Mises stress. The time series are scaled and nondimensionalized by dividing by the sample standard deviation, and the sample mean value is subtracted. This yields ten 1-hour time series *x(t)* which are used as input for the AUR method. One of the ten time series is shown in Figure 3-1. In the case of a Gaussian process, large negative values will be equally common as large positive values. This is clearly not the case in Figure 3-1, so the process is obviously not Gaussian.

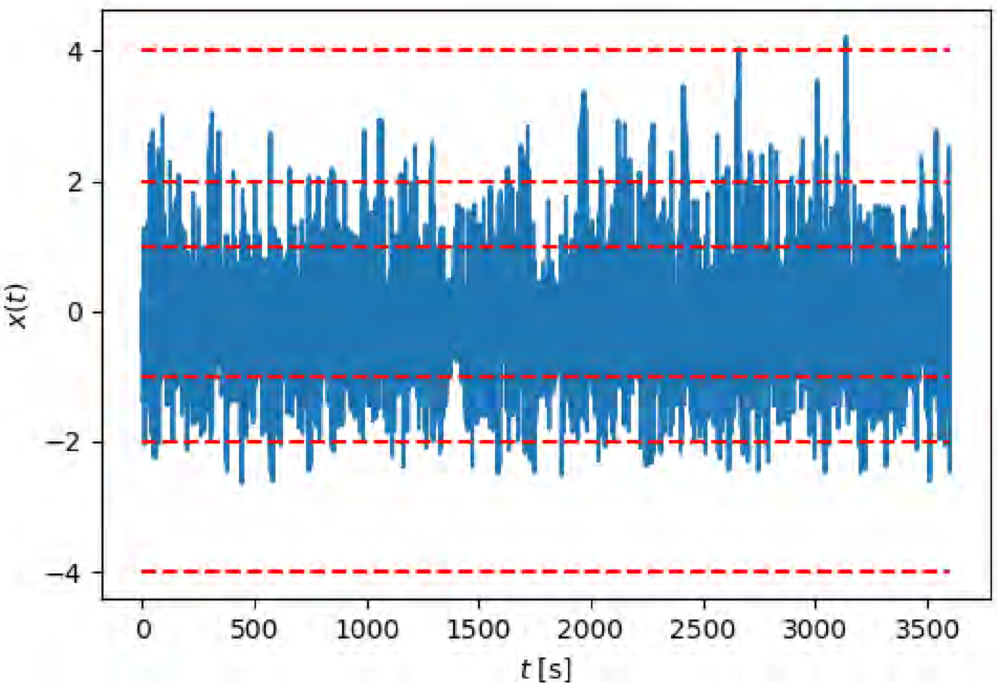

Figure 3-1 One of the ten 1-hour time series used as input for the AUR method.

3.1 Estimating average upcrossing rates and fitting the model

Assuming upcrossings to be independent events above a level $\xi_0 = 1.5$, the average upcrossing rate is estimated at 50 levels ξ_i between 1.5 and 4. In order to improve the estimates of the confidence intervals, the time series are split into 600 s parts. Figure 3-2 shows all ten time series split into a total of 60 time series of duration 600 s. The estimated average upcrossing rates $\hat{\nu}(\xi_i)$ are given in Figure 3-3, along with the 95% confidence intervals $\left(C^-(\xi_i), C^+(\xi_i)\right)$.

Using the estimates $\hat{\nu}(\xi_i)$, the average upcrossing rate model $\nu(\xi) = q \cdot \exp\{-a(\xi - b)^c\}$ for $\xi \geq \xi_0$ is fitted as described in Section 2.1 above (without any modification to the sum of square errors). An estimated 95% confidence band for the average upcrossing rate is obtained by centring the confidence intervals $\left(C^-(\xi_i), C^+(\xi_i)\right)$ around the fitted curve $\nu(\xi_i)$, and then perform the same fitting procedure using the points of the confidence intervals. The obtained model $\nu(\xi)$ is plotted on the log level in Figure 3-4, along with the estimated values $\hat{\nu}(\xi_i)$. The estimated 95% confidence band is also shown. The parameters of the model $\nu(\xi)$ are given by $q = \exp\{-2.624\}\,\mathrm{s}^{-1}, a = 1.394, b = 1.310, c = 1.170$.

From the average upcrossing rate $\nu(\xi)$ the 1-hour extreme value distribution is given as

$$F_{1hr\,max}(\xi) = \exp\{-\nu(\xi) \cdot 3600\text{ s}\} = \exp\{-\exp\{\ln q - a(\xi - b)^c\} \cdot 3600\text{ s}\},\ \ \xi \geq \xi_0.$$

The obtained CDF is displayed in Figure 3-5, along with the estimated 95% confidence band.

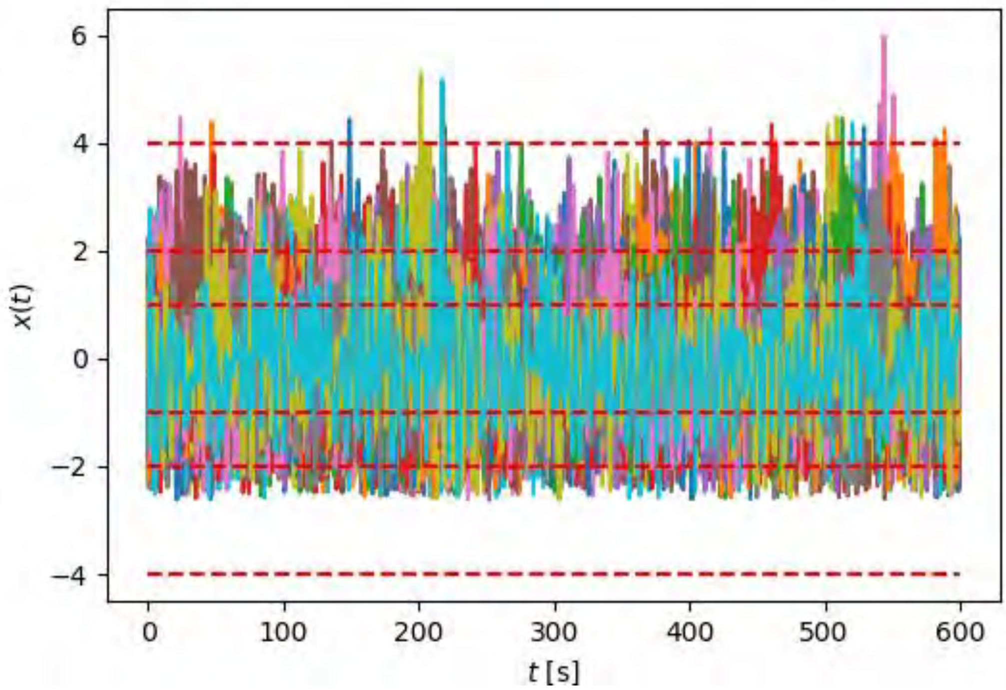

Figure 3-2 All 10 time series split into 600 s parts.

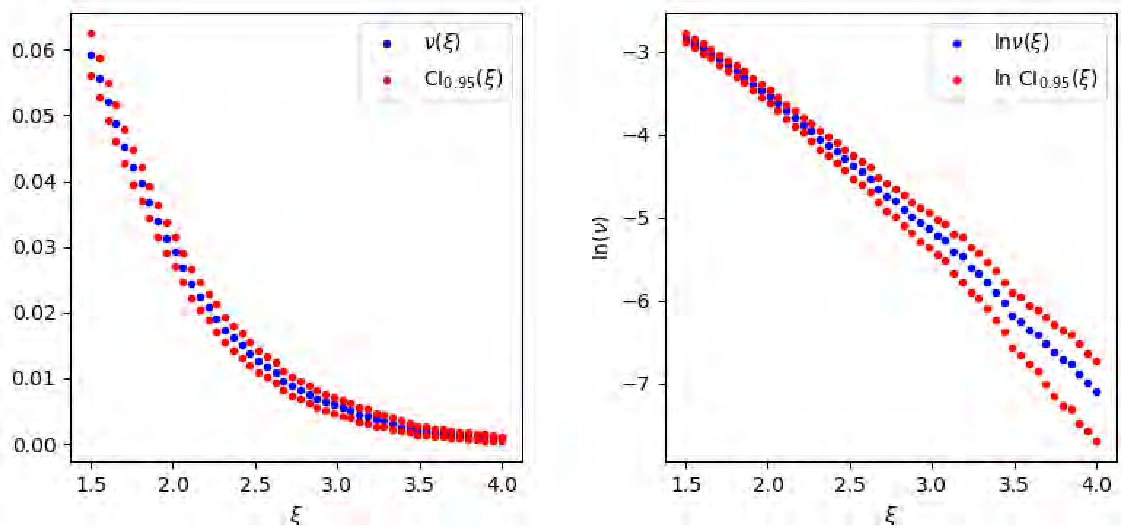

Figure 3-3 Estimated average upcrossing rate along with 95% confidence intervals.

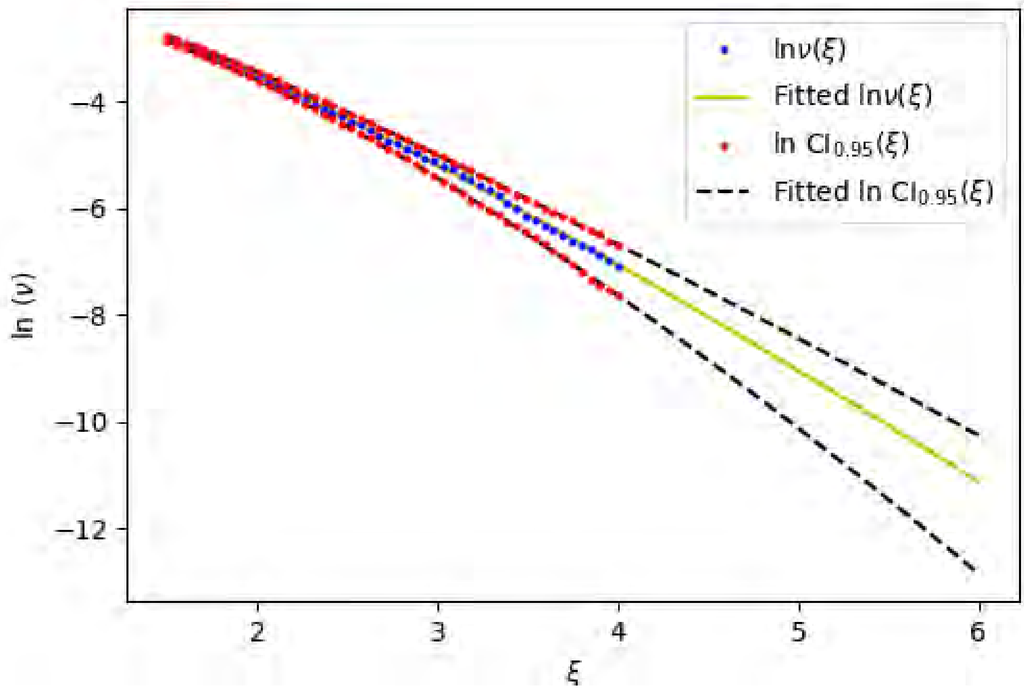

Figure 3-4 The average upcrossing rate model is fitted by minimizing the square error on the log level.

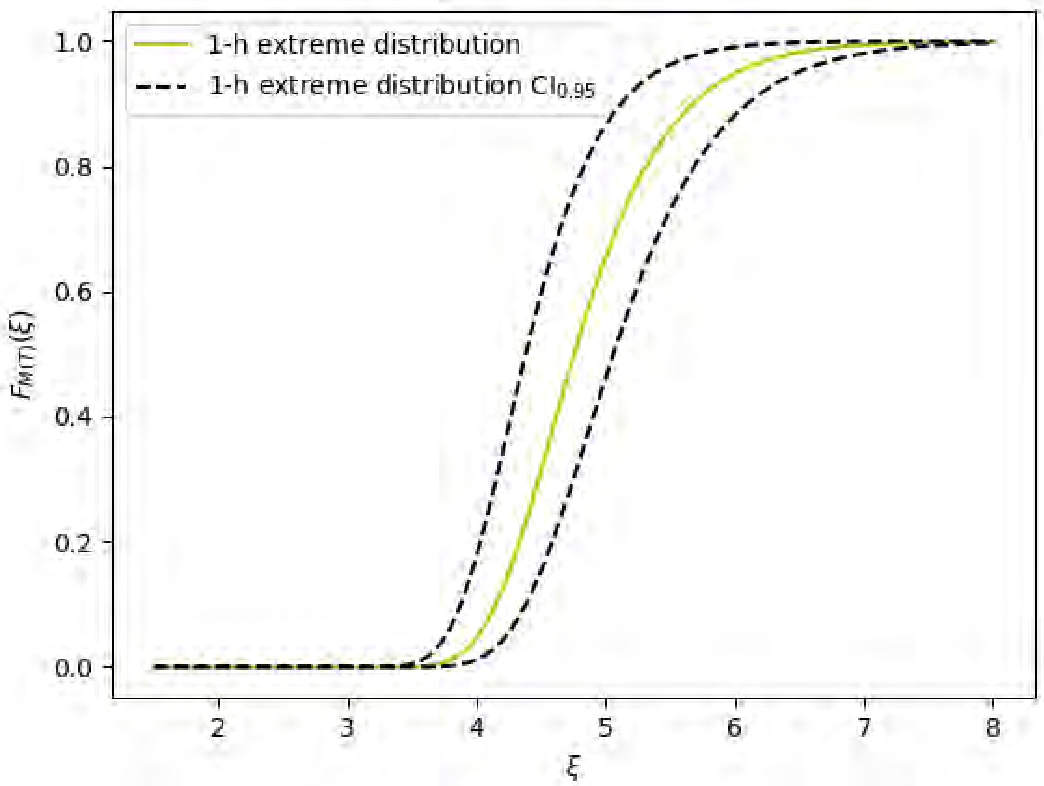

Figure 3-5 The estimated short-term extreme value distribution, along with a 95% confidence band.

3.2 Calculating characteristic values of the extreme response

Using the expression for the 1-hour extreme value distribution, a level ξ_p with a specified non-exceedance probability p is given by

$$\xi_p = b + \left[\frac{1}{a}\left(\ln q - \ln\left[-\frac{\ln p}{3600\ \mathrm{s}}\right]\right)\right]^{1/c}.$$

For instance, the median value and the 90-percentile are obtained by taking $p = 0.5$ and $p = 0.9$ respectively.

The expected value for the 1-hour max can be calculated by the following integral:

$$\xi_{exp\ max} = \int_0^\infty [1 - F_{1hr\ max}(\xi)]d\xi = \xi_0 + \int_{\xi_0}^\infty [1 - F_{1hr\ max}(\xi)]d\xi$$

This expression is based on the assumption that $F_{1hr\ max}(\xi) = 0$ for $\xi < \xi_0$, which is reasonable as long as the value of ξ_0 is not chosen excessively large.

Alternatively, the expected value can be obtained by simulating from the extreme value distribution and taking the sample mean, i.e.

$$\xi_{exp\ max} \approx \frac{1}{N}\sum_{i=1}^{N} \xi_{p_i},$$

where p_i are drawn from the uniform distribution on the interval [0,1) and N is a large number, e.g. $N = 100\ 000$. Since the obtained extreme value distribution is defined only for $\xi \geq \xi_0$, ξ_{p_i} is given as

$$\xi_{p_i} = \begin{cases} b + \left[\frac{1}{a}\left(\ln q - \ln\left[-\frac{\ln p_i}{3600\ \mathrm{s}}\right]\right)\right]^{1/c}, & p_i \geq F_{1hr\ max}(\xi_0), \\ \xi_0, & p_i < F_{1hr\ max}(\xi_0). \end{cases}$$

This corresponds to assuming $F_{1hr\ max}(\xi) = 0$ for $\xi < \xi_0$. When using this approach, the coefficient of variation (CoV) is easily estimated as

$$CoV \approx \frac{\text{sample mean}}{\text{sample standard deviation}} = \frac{\xi_{exp\ max}}{\sqrt{\frac{1}{N-1}\sum_{i=1}^{N}\left(\xi_{p_i} - \xi_{exp\ max}\right)^2}}.$$

For the case considered in Section 3.1 the expected max is found to be $\xi_{expected\ max} = 4.851$ and the 90-percentile is $\xi_{0.9} = 5.672$. The value of the expected max appears reasonable, as the mean of the maximal values in the ten time series is 4.623. The 90-percentile represents the value that is exceeded on average once in ten 1-hour time series, and it is actually the case for the ten time series that exactly one of them has a maximal value larger than $\xi_{0.9} = 5.672$.

3.3 Modified AUR method

As mentioned in Section 2.1, there are some cases where the AUR method may give unreasonable values for the AUR parameters. What happens is that the fitting to the average upcrossing rate can be marginally improved by steadily increasing the value of c, such that the obtained value for c becomes too large. The corresponding value of a then becomes unnaturally small. For extreme value distributions that are asymptotically Gumbel, the value of c should typically be around the range 0.5-3.

The unreasonable values are better explained with an example. Again, we consider ten simulated 1-hour time series of Von Mises stress, which are scaled and nondimensionalized in the same way as before. The considered time series are shown in Figure 3-6, and the observed upcrossing rates are shown in Figure 3-7. The observed log upcrossing rate (to the right in Figure 3-7) appears to be close to linear, and we would expect a value of c close to 1. However, with a large value of c and a corresponding small value of a, the fit can be marginally improved. The fitted model is shown in Figure 3-8, and the resulting parameter values are $q = \exp\{10.61\}\,\mathrm{s}^{-1}, a = 3.685 \cdot 10^{-137}, b = -562.6, c = 50.00$ (An upper bound $c = 50.0$ is set for the parameter c). The fit is then close to linear for values of ξ close to the observed range, but when we look at larger values of ξ, as shown in Figure 3-9, we see that $\ln \nu(\xi)$ curves downwards. If the real asymptotic extreme value distribution is a Gumbel distribution, this corresponds to an underestimation of the upcrossing rate, and thereby an underestimation of the extreme values. In addition, in Figure 3-9 the lower bound of the confidence band has reasonable parameter values ($c = 1.10$) such that it intersects the estimated upcrossing rate.

Using the penalty approach described in Section 2.1, with the modified sum of square errors $\tilde{F}(q, a, b, c)$, the parameter values obtained are $q = \exp\{-0.8601\}\,\mathrm{s}^{-1}, a = 0.7600, b = -0.7142, c = 1.267$. The fitted average upcrossing rate is shown in Figure 3-10. Visually, the fit is just as good as in Figure 3-8, so the improvement of the fit with larger values of c was only marginal. However, for larger values of ξ as shown in Figure 3-11 it is seen that the fitted model appears more reasonable than in Figure 3-9.

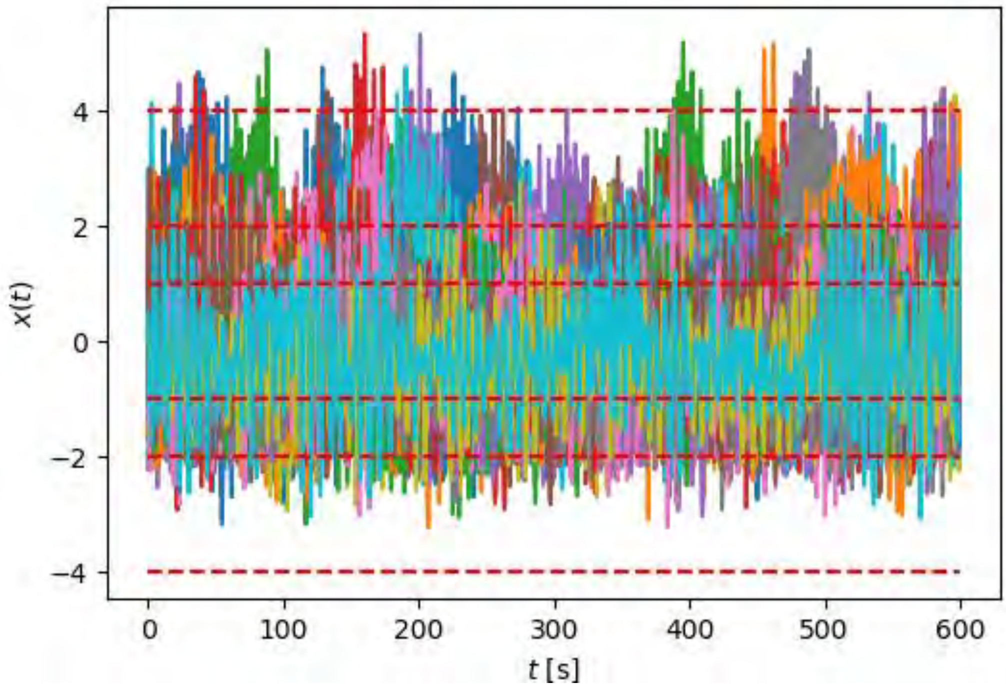

Figure 3-6 The 10 time series (split into 600 s parts) for which the AUR method gives unreasonable parameter values.

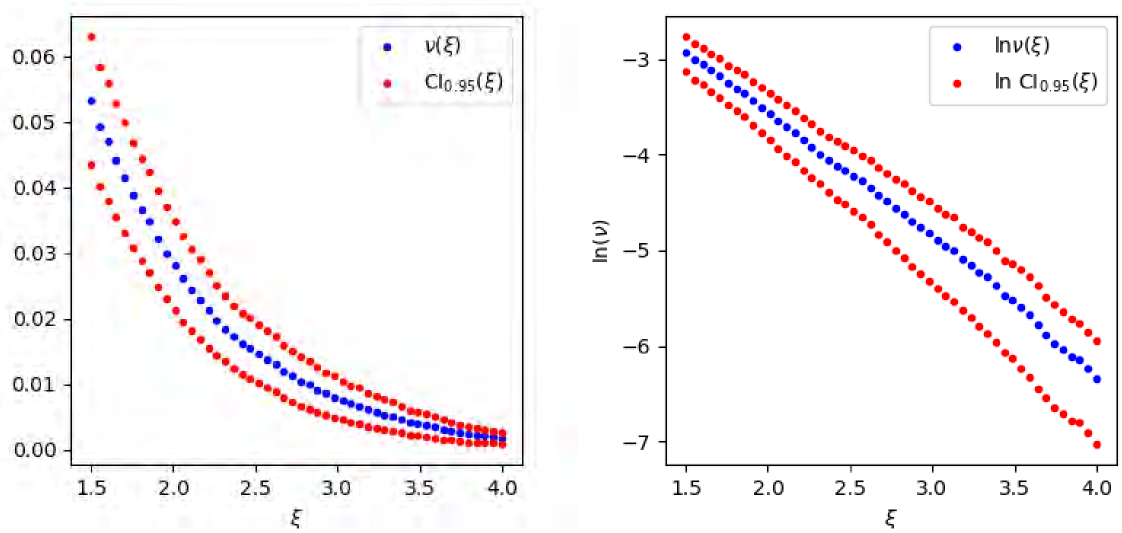

Figure 3-7 Estimated average upcrossing rate along with 95% confidence intervals.

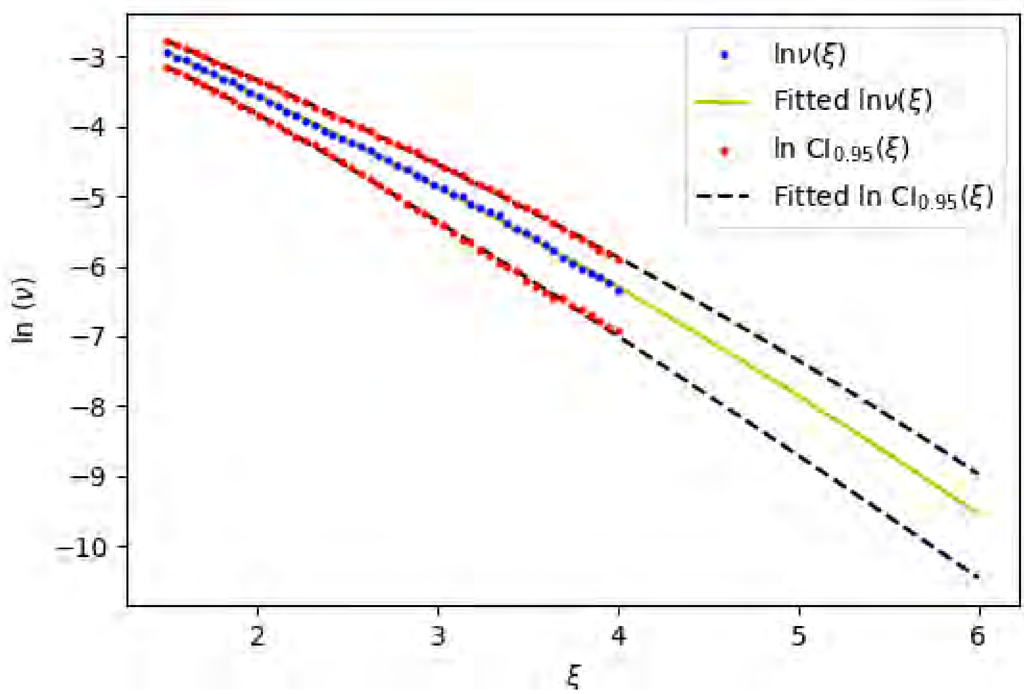

Figure 3-8 The fitted average upcrossing rate model.

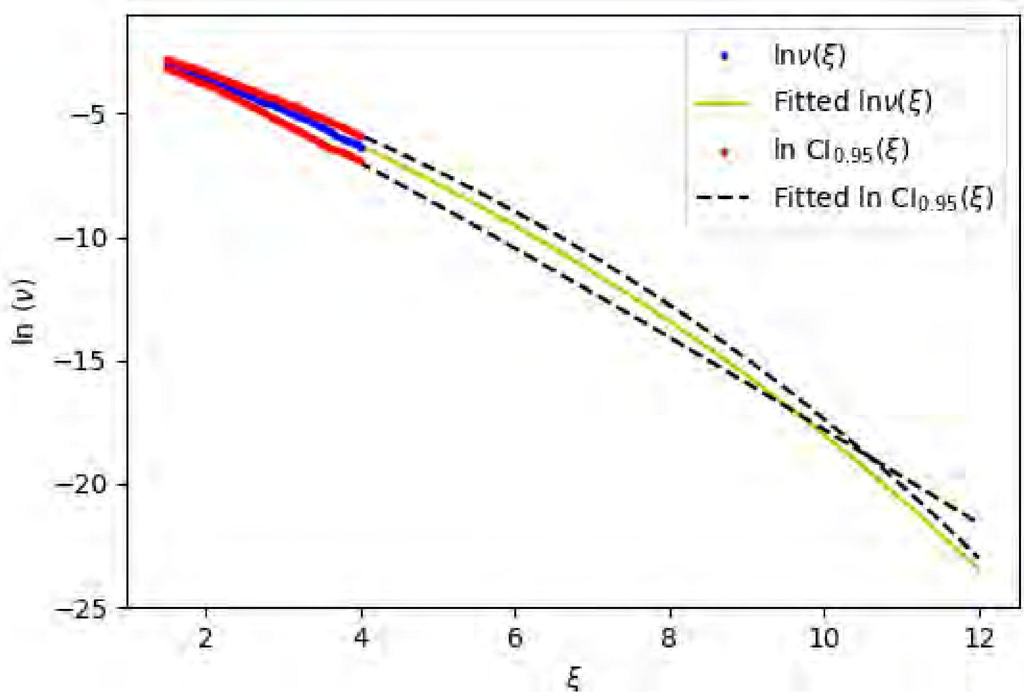

Figure 3-9 The fitted average upcrossing rate model for a larger range of ξ.

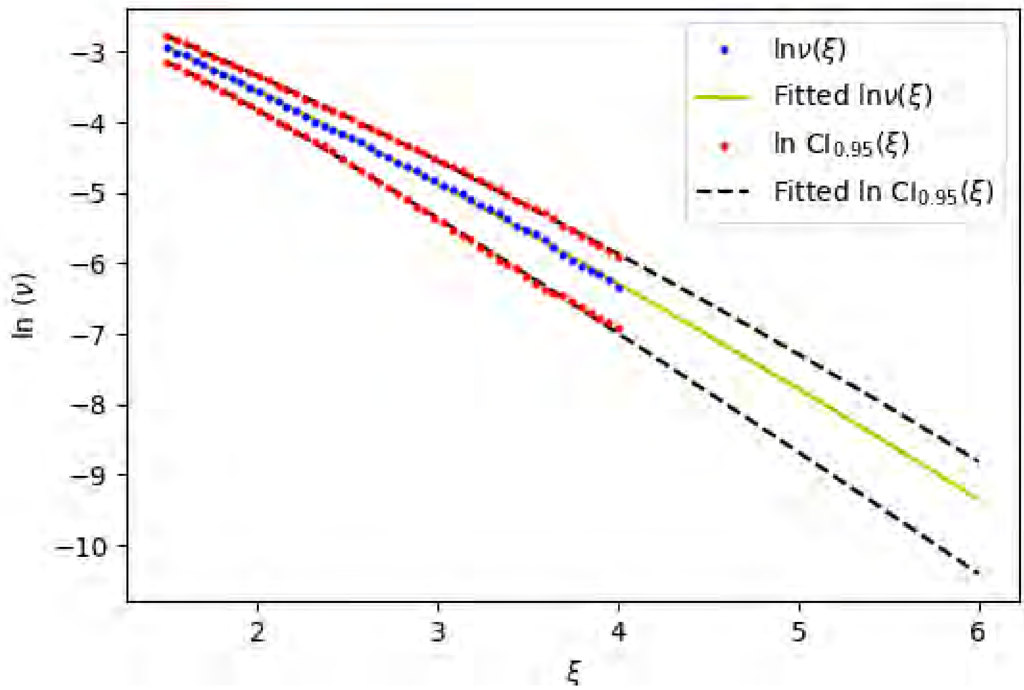

Figure 3-10 The fitted average upcrossing rate model when the AUR method is modified with a penalty strategy to obtain reasonable values for the distribution parameters.

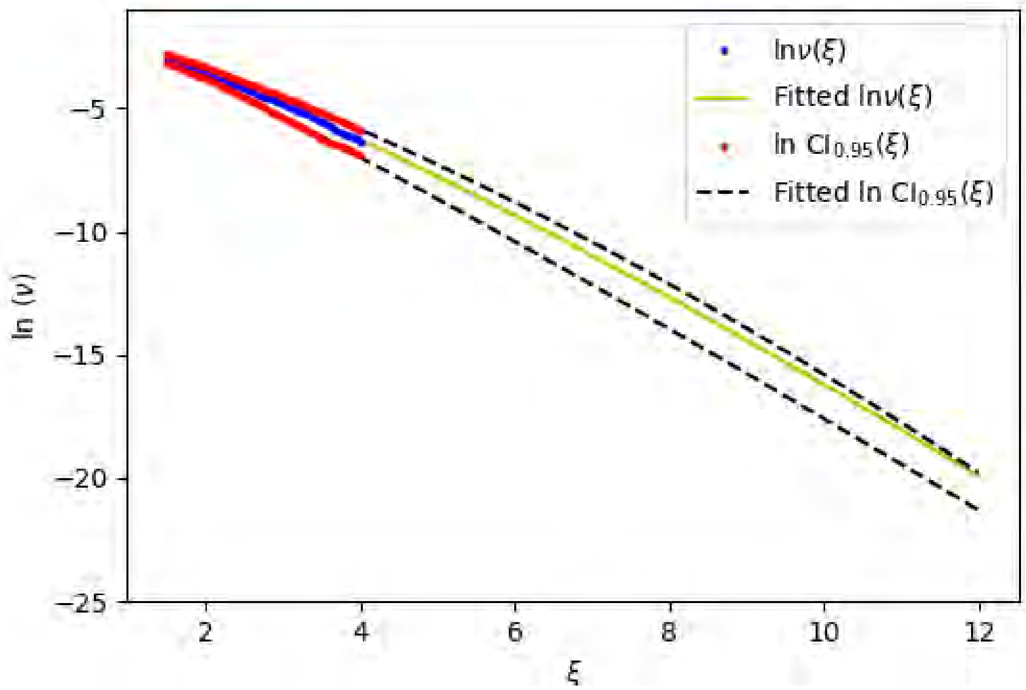

Figure 3-11 The fitted average upcrossing rate model for a larger range of ξ when the AUR method is modified with a penalty strategy to obtain reasonable values for the distribution parameters.

3.4 Short-term extreme values using different numbers of time series

The extreme value estimation was performed for the case considered in Sections 3.1 and 3.2, using a varying number N of the ten time series. The penalty approach was applied in order to ensure reasonable results also for small N. In Table 3-1 the resulting estimates are given for the expected max and the 90-percentile. Figure 3-12 shows the fitted average upcrossing rate (on the log level) for the ten cases. It appears that using a small number of time series, the average upcrossing rate is underestimated, resulting in underestimation of the characteristic extreme response values. This is coincidental, however, which can be seen in Table 3-2 where the time series are included in the reverse order. It is also noted that the 95% confidence intervals are quite wide even when all ten time series are used. If a more accurate estimation of the extreme values is required, more data than ten 1-hour time series should be used. Still, rough estimates of the extreme values are obtained from the first few time series.

Table 3-1 Estimated characteristic values of the extreme response along with 95% confidence intervals for a varying number of time series.

Number of time series	Estimated expected max	Expected max 95% confidence interval	Estimated 90-percentile	90-percentile 95% confidence interval
1	4.193	(3.582, 4.959)	4.724	(3.944, 5.759)
2	4.130	(3.696, 4.427)	4.635	(4.059, 5.010)
3	4.300	(3.769, 4.773)	4.873	(4.143, 5.526)
4	4.268	(3.871, 4.649)	4.800	(4.268, 5.326)
5	4.333	(3.936, 4.644)	4.915	(4.376, 5.320)
6	4.433	(4.084, 4.699)	5.056	(4.590, 5.389)
7	4.599	(4.141, 4.956)	5.311	(4.657, 5.795)
8	4.635	(4.223, 4.952)	5.366	(4.780, 5.792)
9	4.917	(4.479, 5.248)	5.783	(5.174, 6.218)
10	4.859	(4.463, 5.178)	5.685	(5.137, 6.109)

Table 3-2 Estimated characteristic values of the extreme response along with 95% confidence intervals when the time series are included in the reverse order as in Table 3-1 and Figure 3-12.

Number of time series	Estimated expected max	Expected max 95% confidence interval	Estimated 90-percentile	90-percentile 95% confidence interval
1	4.891	(3.728, 6.383)	5.660	(4.116, 7.719)
2	5.398	(4.569, 5.963)	6.385	(5.319, 7.066)
3	5.275	(4.579, 5.715)	6.245	(5.322, 6.773)
4	5.298	(4.616, 5.772)	6.293	(5.360, 6.896)
5	5.247	(4.675, 5.661)	6.223	(5.444, 6.751)
6	5.155	(4.668, 5.517)	6.110	(5.458, 6.569)
7	5.080	(4.616, 5.431)	5.999	(5.372, 6.447)
8	5.034	(4.596, 5.377)	5.935	(5.340, 6.382)
9	4.874	(4.465, 5.200)	5.693	(5.127, 6.125)
10	4.859	(4.463, 5.178)	5.685	(5.137, 6.109)

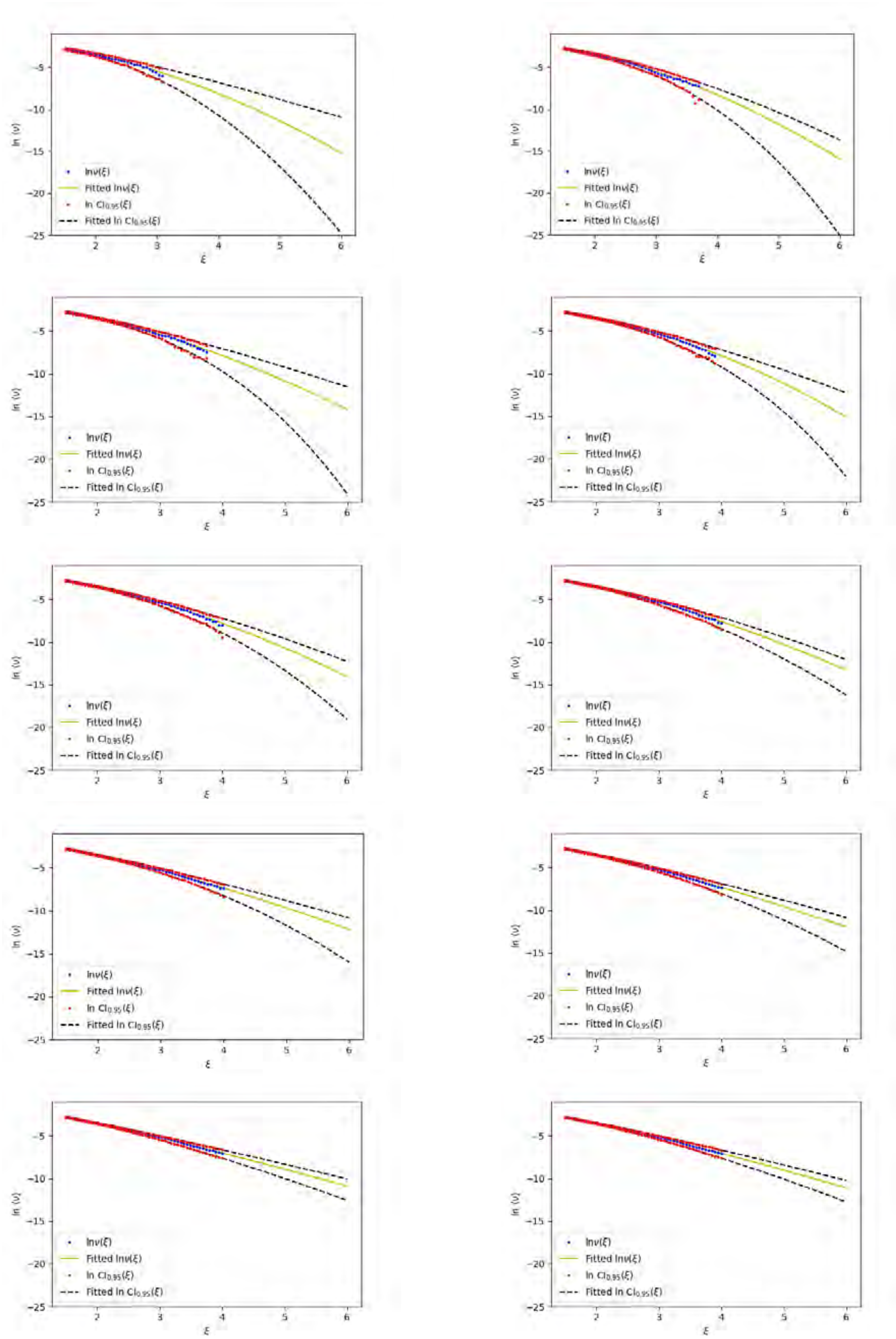

Figure 3-12 Fitted average upcrossing rate using 1 (upper left), 2 (upper right) and up to 10 (lower right) of the time series.

4 Short-term extreme values of Von Mises stress along the bridge

Using ten simulated 1-hour time series of Von Mises stress at 751 different points along the bridge, the AUR method is compared with the Gumbel method. The time series at each point is scaled and nondimensionalized by dividing by the sample standard deviation, and the sample mean value is subtracted before the methods are applied. Specifically, a time series $y(t)$ of Von Mises stress is transformed to a time series $x(t) = \left(y(t) - \mu_y\right)/\sigma_y$, where μ_y and σ_y are the sample mean and standard deviation respectively. The methods are then applied to $x(t)$, and characteristic values are obtained. Finally, the characteristic values are transformed back to characteristic values for Von Mises stress. The expected max, for instance, is obtained as $\mu_y + \sigma_y \xi_{exp\,max}$.

The most straightforward version of the Gumbel method is the method of moments (MoM). When MoM is used, the mean value and standard deviation of the assumed Gumbel distribution are estimated using the sample mean $\mu_{\max}$ and sample standard deviation $\sigma_{\max}$ of the ten max values from the simulated time series. The estimates of the expected max and the 90-percentile are then obtained as $\mu_{\max}$ and $\mu_{\max} + 1.3\sigma_{\max}$ respectively. Alternatively, a Gumbel distribution can be fitted to the ten max values using the maximum likelihood (ML) method, and characteristic values are obtained from the fitted distribution.

The estimates of expected 1-hour max and the 90-percentile are shown in Figure 4-1 and Figure 4-2 respectively. The results obtained using the AUR method are compared with the results obtained by the Gumbel methods (MoM and ML). In this case, we see that there is very little difference between the two variants of the Gumbel method. We see that there is good agreement between the AUR method and the Gumbel methods. However, for some cases the results are somewhat different. This could be due to a violation of the assumption of independent upcrossings for the AUR method, in which case the AUR method will give conservative estimates.

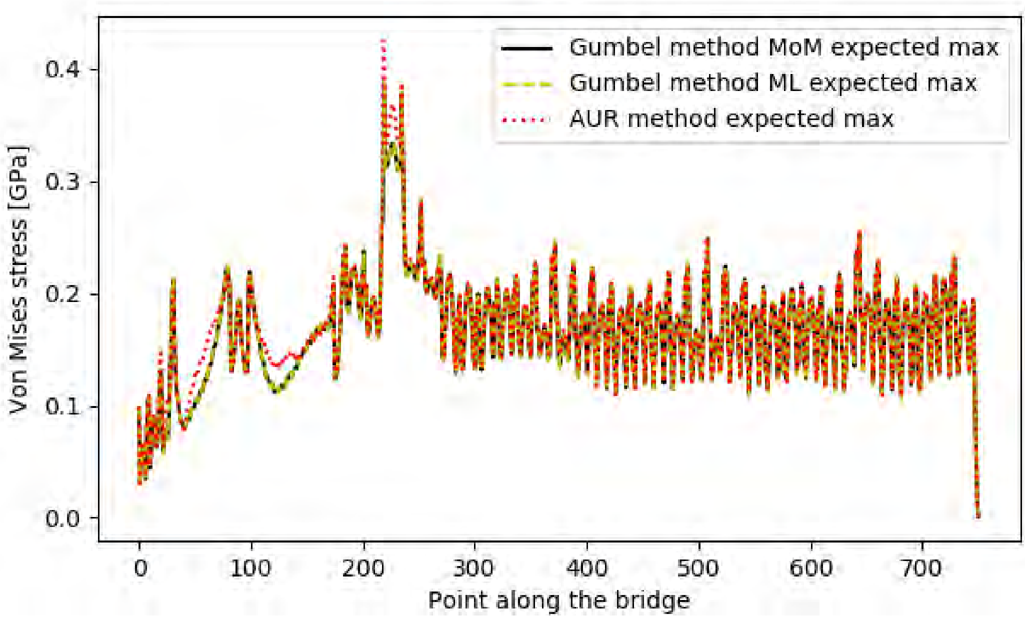

Figure 4-1 Expected max values obtained from the AUR method are compared with the estimates obtained by the two variants of the Gumbel methods.

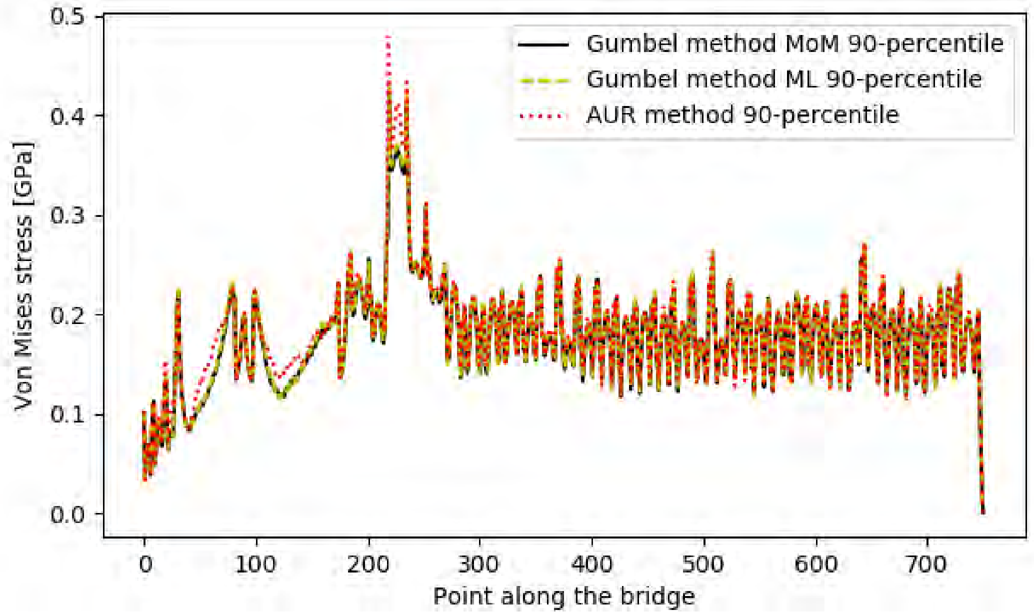

Figure 4-2 90-percentiles obtained from the AUR method are compared with the estimates obtained by the two variants of the Gumbel methods.

5 Short-term extreme values of axial force and strong axis bending moment

Considering ten simulated 1-hour time series of axial force and strong axis bending moments at 751 different points along the bridge, we investigate the performance of the AUR method for response processes that with a good approximation can be considered Gaussian. The estimates of expected 1-hour max is compared for the AUR method, the Gumbel method and the Gaussian approximation. The method of moments (MoM) and maximum likelihood (ML) variants of the Gumbel method are explained in Section 4. Assuming that the response process is Gaussian, the expected short-term max value is given as

$$\xi_{exp\ max} \approx \mu + \sigma \left\{ \sqrt{2\ln(\nu_\mu T)} + \frac{0.5772}{\sqrt{2\ln(\nu_\mu T)}} \right\},$$

where μ and σ are the mean value and standard deviation of the response process, ν_μ is the average upcrossing rate of the mean value and $T = 1$ hour is the short-term period. This expression can be roughly approximated by $\xi_{exp\ max} \approx \mu + 3.7\sigma$ for a short-term period of one hour.

The estimates of expected 1-hour max for the different methods are shown in Figure 5-1 and Figure 5-3 for axial force and strong axis bending moments respectively. The estimates of the corresponding expected 1-hour minimum values are shown in Figure 5-2 and Figure 5-4. We see that there is generally very good agreement between the different methods. However, it appears that the AUR method and the Gaussian approximations give slightly larger extreme values than the Gumbel methods.

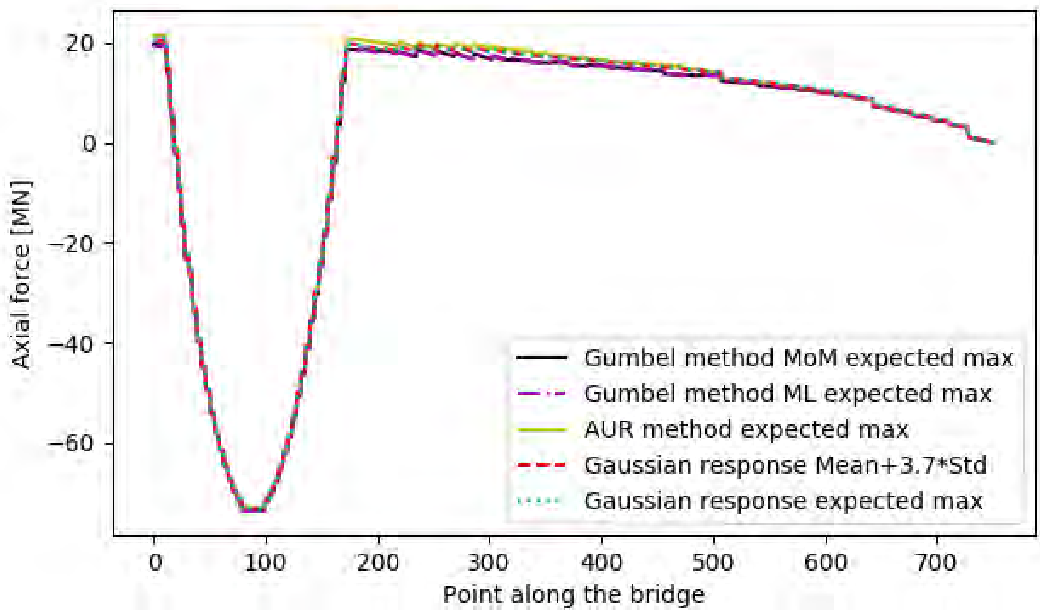

Figure 5-1 Estimates of the expected 1-hour max for the axial force.

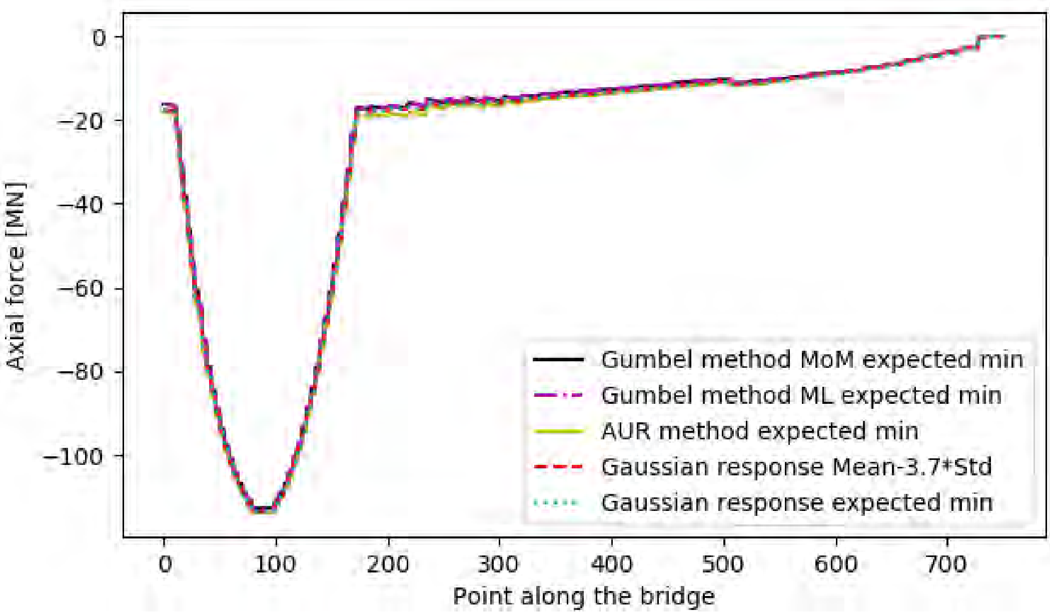

Figure 5-2 Estimates of the expected 1-hour min for the axial force.

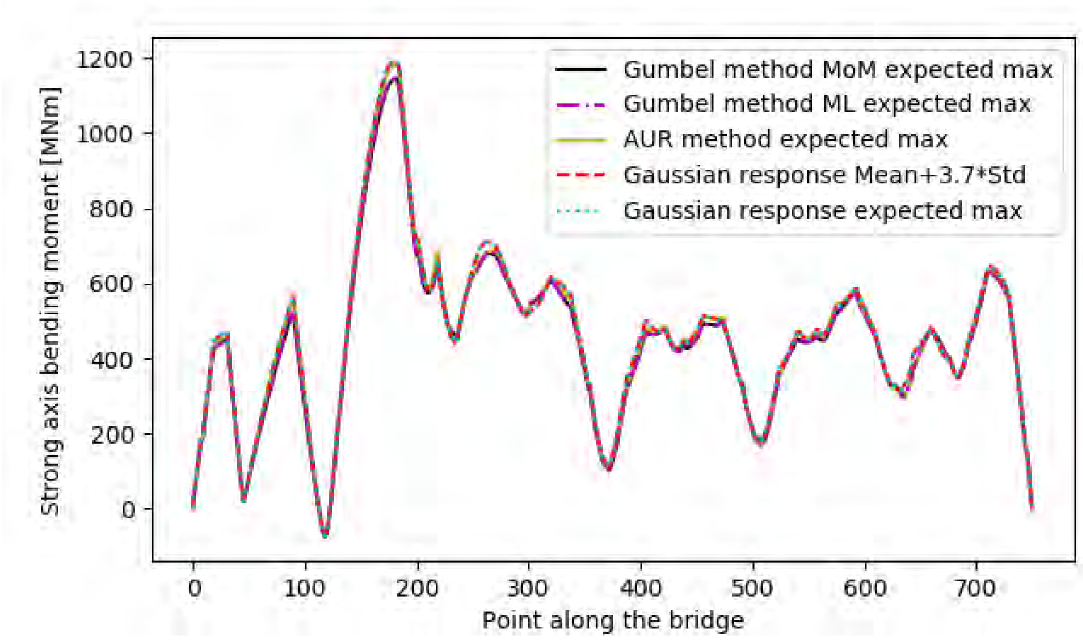

Figure 5-3 Estimates of the expected 1-hour max for the strong axis bending moment.

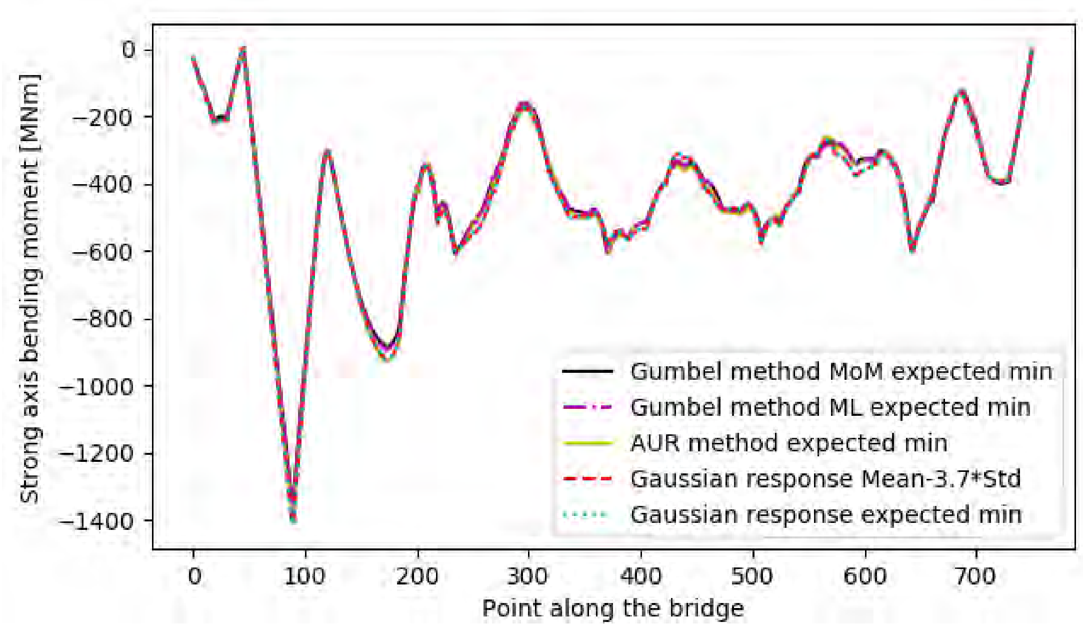

Figure 5-4 Estimates of the expected 1-hour min for the strong axis bending moment.

Concept development, floating bridge

E39 Bjørnafjorden

Appendix G – Enclosure 14

10205546-11-NOT-088

Variable static loads

AAS-JAKOBSEN COWI Multiconsult
JOHS HOLT AkerSolutions entail NGI DISSING+WEITLING architecture a|s mossmaritime

MEMO

PROJECT	**Concept development, floating bridge E39 Bjørnafjorden**	DOCUMENT CODE	10205546-11-NOT-088
CLIENT	Statens vegvesen	ACCESSIBILITY	Restricted
SUBJECT	**AMC status 2 – Variable static loads**	PROJECT MANAGER	Svein Erik Jakobsen
TO	Statens vegvesen	PREPARED BY	Henric Thompsson
COPY TO		RESPONSIBLE UNIT	AMC

SUMMARY

This memo contains a description of the thermal and traffic loads and how they are implemented in the analyses. The analyses are performed in RM Bridge and are calculated on a linear elastic full-scale beam model.

The traffic loads are dependent of the loaded length. This is accounted for in RM Bridge by the influence line method for all displacements and force components where the loaded length is chosen as influence length (distance between zero points). In case of favourable long sections of the influence line an equivalent triangular function with the fictitious load length is evaluated. This fictitious length is the base of an equivalent triangle calculated as the integral area divided by the peak value of the treated influence section. The loaded length on which the load intensity is based on is chosen as the minimum length of the actual influence length and the base of the equivalent triangle for that section.

The carriageway width give six notational lanes and one footway and bicycle lane having in total seven lanes. There are two traffic situations evaluated in the analysis; either the heaviest traffic lanes placed to the left (west side) or the heaviest traffic lanes placed to the right (east side) of the carriageway.

The thermal loads are calculated according to NS-EN 1991-1-5 and based on the max/min air temperatures with 100 years return period. The thermal loads consists of the uniformly temperature and the linear gradient over the cross-section. In addition to these load cases a temperature difference of the stay cables and the bridge is included.

0	29.03.2019	Status 2 issue	Henric Thompsson	Per Norum Larsen	Svein Erik Jakobsen
REV.	DATE	DESCRIPTION	PREPARED BY	CHECKED BY	APPROVED BY

TABLE OF CONTENTS

1 Introduction

The four different concepts K11, K12, K13 and K14 are evaluated at this stage. The static analyses are performed in RM Bridge Enterprise, version 11.03.16. The static loads prescribed in this memo are the traffic loads and thermal loads.

2 Loads

2.1 Traffic loading

2.1.1 Vertical traffic loading

According to Design basis the carriage way is portioned as in Figure 2-1. The traffic loading accounts for traffic also placed on the shoulders giving in total six notational lanes 3 meters wide each and one footway and bicycle lane having in total seven traffic lanes. In the analyses the corresponding lanes are labelled/numbered as in Figure 2-2 having Lane 1 to the left (west side).

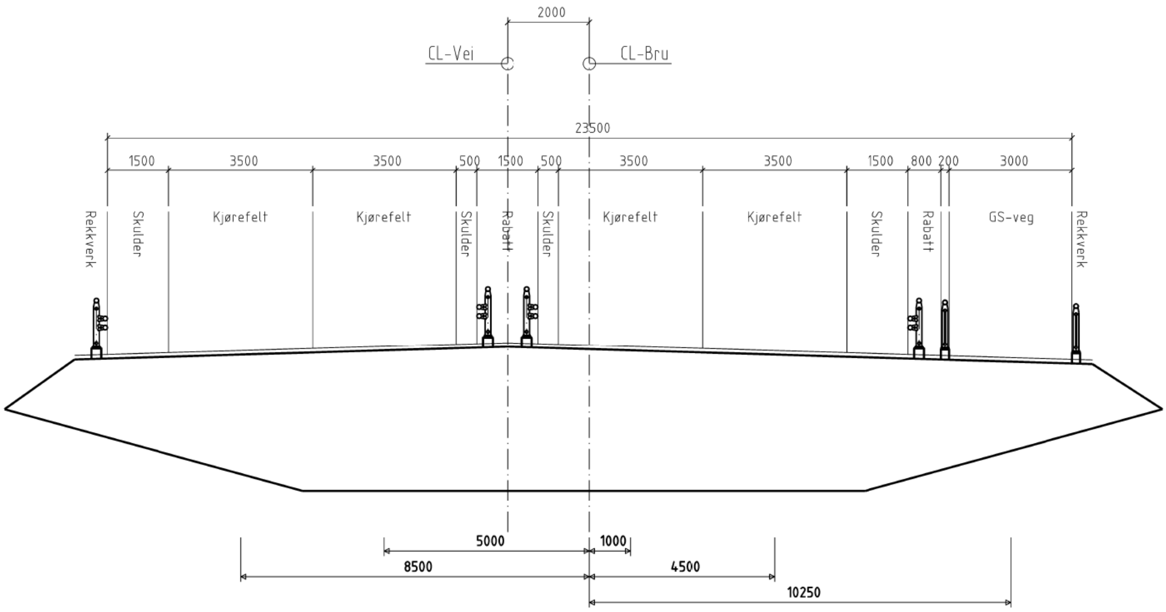

Figure 2-1 The bridge deck partitioning due to traffic related functions

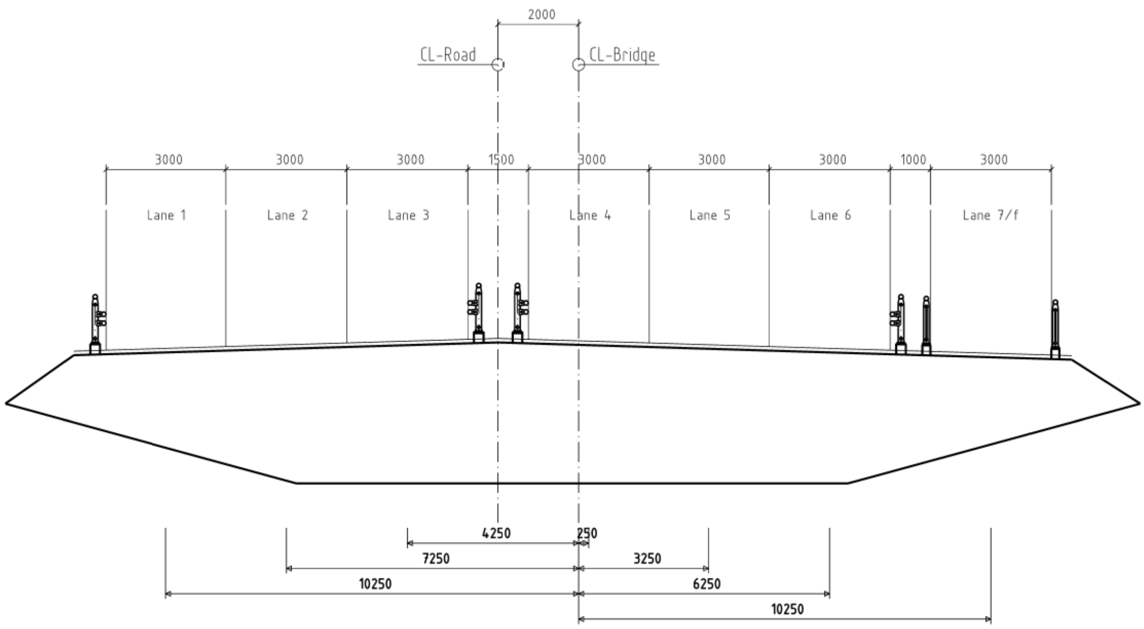

Figure 2-2 Lane numbering and eccentricities relative CL bridge girder

The traffic load intensity depends on the loaded length. The loaded length correction factors are according to Table 2-1 giving the traffic loads as inTable 2-2.

Table 2-1 Correction factors for traffic load combinations depending on the actual loading length

		Loaded length L		
		L≤200m (1)	200m<L<1000m (2)	L≥1000m (2)
Tandem system (TS)				
- Notational lane i=1,2 and 3:	α_{Qi}	1.0	1.0	1.0
Uniformly distributed loads (UDL system)				
- Notational lane i=1:	α_{q1}	0.6	Linear interpolation	0.5
- Notational lane i>1:	α_{qi}	1.0	Linear interpolation	1.0
- Remaining area:	α_{qr}	1.0	Linear interpolation	0.0
Footways and cycle tracks				
- Footway and cycle track:	α_{fk}	0.5 (3)	Linear interpolation	0.125 (4)

(1) Load model LM1, [NS-EN 1991-2:2003+NA:2010, Section NA.4.3.2]

(2) Forskrift for trafikklast på bruer, ferjekaier og andre bærende konstruksjoner i det offentlige vegnettet

(3) Combination factor together with characteristic traffic LM1 loads [NS-EN 1991-2:2003+NA:2010, Table NA.4.4a]

(4) Combination factor 0.5 (3) combined with correction factor 0.25 [2]

Table 2-2 Traffic loads depend on the actual loaded length

	Loaded length L								
	L<200m			200m<L<1000m			L>1000m		
	Lane width: w_l [m]	TS: $\alpha_{Qi}*Q_{ik}$ [kN]	UDL: $\alpha_{qi}*q_{ik}$ [kN/m^2]	Lane width: w_l [m]	TS: $\alpha_{Qi}*Q_{ik}$ [kN]	UDL: $\alpha_{qi}*q_{ik}$ [kN/m^2] (1)	Lane width: w_l [m]	TS: $\alpha_{Qi}*Q_{ik}$ [kN]	UDL: $\alpha_{qi}*q_{ik}$ [kN/m^2]
Notational lane 1	3	2x300	5.4	3	2x300	4.950	3	2x300	4.5
Notational lane 2	3	2x200	2.5	3	2x200	2.500	3	2x200	2.5
Notational lane 3	3	2x100	2.5	3	2x100	2.500	3	2x100	2.5
Notational lane 4	3		2.5	3		2.500	3		2.5
Notational lane 5	3		2.5	0			0		
Notational lane 6	3		2.5	0			0		
Remaining area	0		2.5	6		1.250	6		0
Footway and cycle track	3		2.5	3		1.563	3		0.625
$\Sigma\alpha_Q*Q_k$ or $\Sigma w_l*\alpha_q*q_k$		1200	61.2		1200	49.538		1200	37.875

(1) Linear interpolation between L=200m and L=1000m. For comparison reasons L is chosen 600m

According to «Forskrift for trafikklast på bruer, ferjekaier og andre bærende konstruksjoner i det offentlige vegnettet» there is a shift in number of notational lanes at loaded length L=200m. For loaded length L<=200m there are six notational lanes and above L>200m the number of notational lanes are equal the given number of traffic lanes, i.e. four traffic lanes. The other two lanes area threated as "remaining area". There are two traffic situations evaluated in the analysis; either the heaviest traffic lanes placed to the left or the heaviest traffic lanes placed to the right. The left-adjusted traffic load situation is illustrated in Figure 2-3 and Figure 2-4. The right-adjusted is not shown but is the other way around having Lane 6 as notational lane 1, lane 5 as notational lane 2 etc.

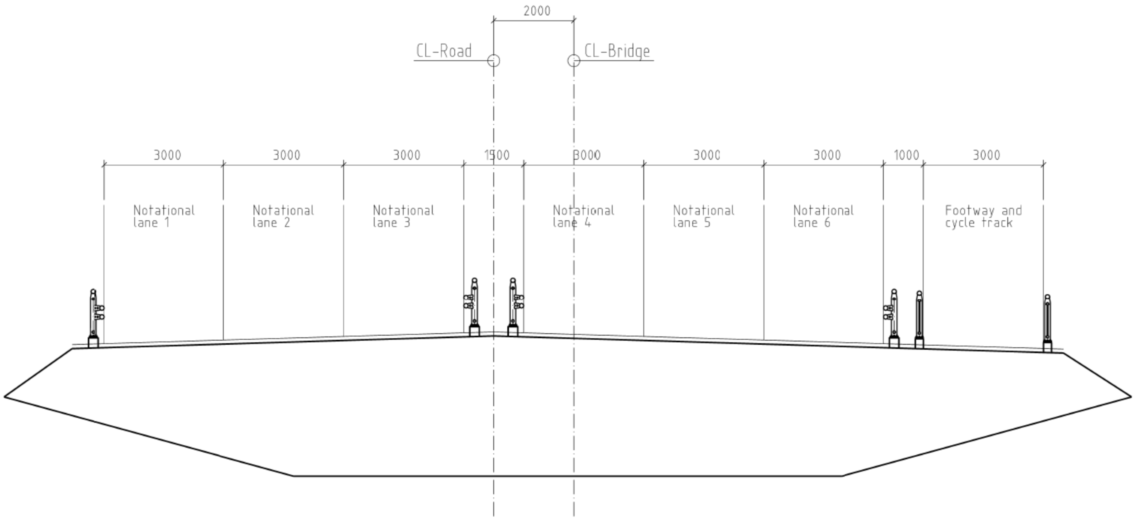

Figure 2-3 The bridge deck partitioning into notational lanes for loaded length L<=200m. The notational lane numbering order depend on the traffic situation that gives the most unfavourable effects. The lane numbering order above is for the left adjusted traffic situation

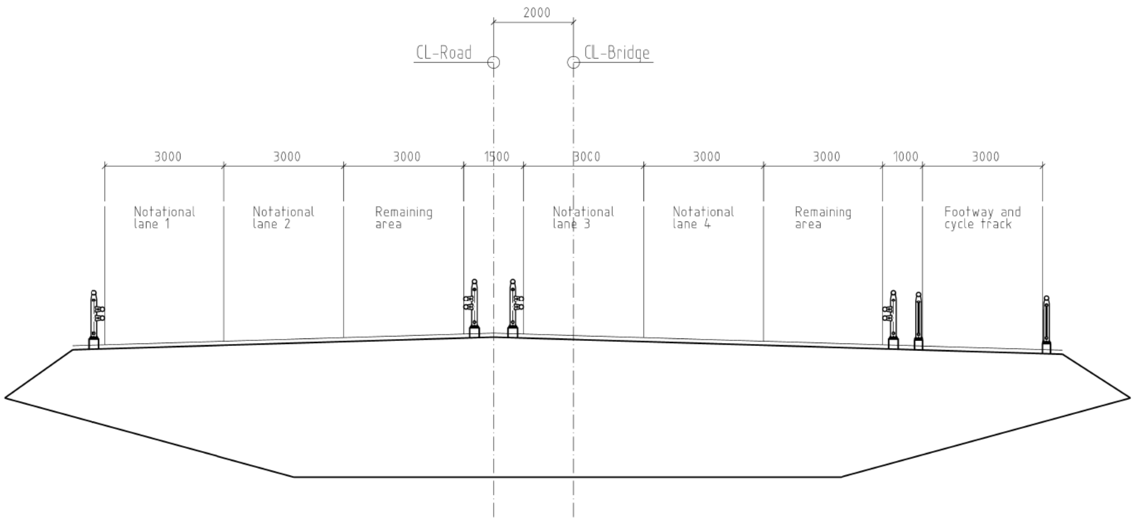

Figure 2-4 The bridge deck partitioning into notational lanes and remaining area for loaded length L>200m. The notational lane numbering order depend on the traffic situation that gives the most unfavourable effects. The lane numbering order above is for the left adjusted traffic situation

2.1.2 Horizontal traffic loading

Horizontal traffic loading such as braking and centrifugal forces are neglected in the analyses.

2.2 Temperature loading

According to MetOcean Design basis the max air temperature for 100-years return period is Tmax=33°C and min air temperature Tmin=-17°C. The temperature load combinations are according to NS-EN 1991-1-5.

For the steel bridge girder the following temperatures are included in the analyses:

Table 2-3 Temperature loading on steel bridge girder

		Temperature [°C]	Reference
Max temperature	Tmax	33	R=100years, [MetOcean Design basis - rev1, table 22]
Min temperature	Tmin	-17	R=100years, [MetOcean Design basis - rev1, table 22]
Installation temperature	T0	10	[NS-EN 1991-1-5, chapter NA.A.1(3)]
Upper representative air temperature	T_emax	49	Type 1 (Tmax+16°C), [NS-EN 1991-1-5, Figure NA.6.1]
Lower representative air temperature	T_emin	-20	Type 1 (Tmin-3°C), [NS-EN 1991-1-5, Figure NA.6.1]
Max temperature contraction	ΔT_Ncon	30	T0-T_emin, [NS-EN-1-5, eq. (6.1)]
Max temperature expansion	ΔT_Nexp	39	T_emax-T0, [NS-EN-1-5, eq. (6.2)]
Temperature gradient, linear variation over the cross-section (warmer topside)	ΔT_Mheat	12.6	Type 1 (0.7*18°C), [NS-EN 1991-1-5, table NA.6.1 and NA.6.2]
Temperature gradient, linear variation over the cross-section (warmer bottom side)	ΔT_Mcool	15.6	Type 1 (1.2*13°C), [NS-EN 1991-1-5, table NA.6.1 and NA.6.2]
Future temperature increase	ΔT_fut	2	Future increase on Tmax, [Designbasis MetOcean, rev1]
Temperature differences on stay cables	ΔT_cables	10	[NS-EN 1991-1-5, chapter 6.1.6]

For the concrete bridge girder the following temperatures are included in the analyses:

Table 2-4 Temperature loading on concrete bridge girder

		Temperature [°C]	Reference
Max temperature	Tmax	33	R=100years, [MetOcean Design basis - rev1, table 22]
Min temperature	Tmin	-17	R=100years, [MetOcean Design basis - rev1, table 22]
Installation temperature	T0	10	[NS-EN 1991-1-5, chapter NA.A.1(3)]
Upper representative air temperature	T_emax	30	Type 3 (Tmax-3°C), [NS-EN 1991-1-5, Figure NA.6.1]
Lower representative air temperature	T_emin	-9	Type 3 (Tmin+8°C), [NS-EN 1991-1-5, Figure NA.6.1]
Max temperature contraction	ΔT_Ncon	19	T0-T_emin, [NS-EN-1-5, eq. (6.1)]
Max temperature expansion	ΔT_Nexp	20	T_emax-T0, [NS-EN-1-5, eq. (6.1)]
Temperature gradient, linear variation over the cross-section (warmer topside)	ΔT_Mheat	7	Type 3 (0.7*10°C), [NS-EN 1991-1-5, table NA.6.1 and NA.6.2]
Temperature gradient, linear variation over the cross-section (warmer bottom side)	ΔT_Mcool	5	Type 3 (1*5°C), [NS-EN 1991-1-5, table NA.6.1 and NA.6.2]
Future temperature increase	ΔT_fut	2	Future increase on Tmax, [Designbasis MetOcean, rev1]
Temperature differences on stay cables	ΔT_cables	10	[NS-EN 1991-1-5, chapter 6.1.6]

In addition the uniformly expansion and contraction temperature loadings they are also combined with the linearly variation over the cross-section according to NS-EN 1991-1-5, chapter NA.6.1.5.

3 RM Bridge analysis

3.1 General information about the concepts

The four bridge models are illustrated in Table 3-1.

Table 3-1 RM Bridge models for the four concepts K11, K12, K13 and K14

K11	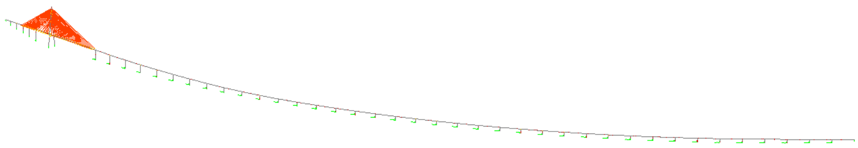
K12	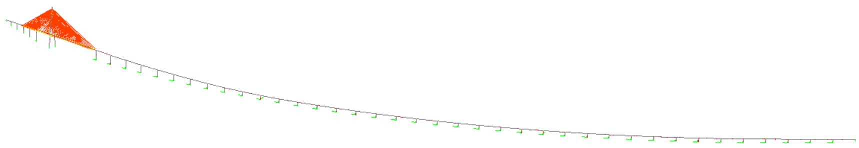
K13	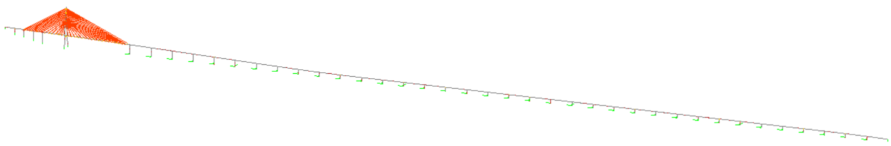
K14	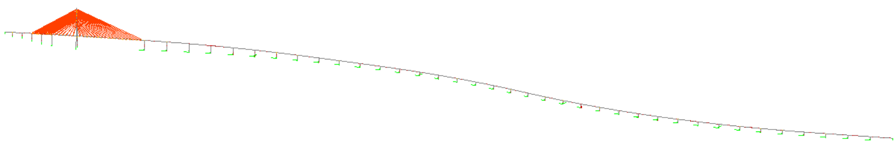

3.1.1 Beam element numbering

Table 3-2 Beam and Cable element numbering in RM Bridge for K11, K12, K13 and K14

	K11 - Beam elements			K12 - Beam elements			K13 - Beam elements			K14 - Beam elements		
	Start	End	Step	Start	End	Step	Start	End	Step	Start	End	Step
Bridge girder												
- High bridge	101	192	1	101	192	1	105	192	1	101	192	1
- (Concrete)	101	138	1	101	138	1	105	138	1	101	138	1
- (Steel)	139	192	1	139	192	1	139	192	1	139	192	1
- Floating bridge	251	858	1	251	858	1	251	826	1	251	842	1
Pier, viaduct												
- Pier A1-A	2101	2104	1	2101	2104	1	2101	2104	1	2101	2104	1
- Pier A1-B	2201	2204	1	2201	2204	1	2201	2204	1	2201	2204	1
- Pier A1-C	2301	2304	1	2301	2304	1	2301	2304	1	2301	2304	1
- Pier A1-D	2401	2404	1	2401	2404	1	2401	2404	1	2401	2404	1
- Pier A1-E	2501	2504	1	2501	2504	1	2501	2504	1	2501	2504	1
Pier, floating bridge												
- Pier A3	4031	4038	1	4031	4038	1	4031	4038	1	4031	4038	1
- Pier A4	4041	4048	1	4041	4048	1	4041	4048	1	4041	4048	1
- Pier A5	4051	4056	1	4051	4056	1	4051	4056	1	4051	4056	1
- Pier A6	4061	4066	1	4061	4066	1	4061	4066	1	4061	4066	1
- Pier A7	4071	4076	1	4071	4076	1	4071	4076	1	4071	4076	1
- Pier A8	4081	4086	1	4081	4086	1	4081	4086	1	4081	4086	1
- Pier A9	4091	4094	1	4091	4094	1	4091	4094	1	4091	4094	1
- Pier A10	4101	4104	1	4101	4104	1	4101	4104	1	4101	4104	1
- Pier A11	4111	4112	1	4111	4112	1	4111	4112	1	4111	4112	1
- Pier A12	4121	4122	1	4121	4122	1	4121	4122	1	4121	4122	1
- Pier A13	4131	4132	1	4131	4132	1	4131	4132	1	4131	4132	1
- Pier A14	4141	4142	1	4141	4142	1	4141	4142	1	4141	4142	1
- Pier A15	4151	4152	1	4151	4152	1	4151	4152	1	4151	4152	1
- Pier A16	4161	4162	1	4161	4162	1	4161	4162	1	4161	4162	1
- Pier A17	4171	4172	1	4171	4172	1	4171	4172	1	4171	4172	1
- Pier A18	4181	4182	1	4181	4182	1	4181	4182	1	4181	4182	1
- Pier A19	4191	4192	1	4191	4192	1	4191	4192	1	4191	4192	1
- Pier A20	4201	4202	1	4201	4202	1	4201	4202	1	4201	4202	1
- Pier A21	4211	4212	1	4211	4212	1	4211	4212	1	4211	4212	1
- Pier A22	4221	4222	1	4221	4222	1	4221	4222	1	4221	4222	1
- Pier A23	4231	4232	1	4231	4232	1	4231	4232	1	4231	4232	1
- Pier A24	4241	4242	1	4241	4242	1	4241	4242	1	4241	4242	1
- Pier A25	4251	4252	1	4251	4252	1	4251	4252	1	4251	4252	1
- Pier A26	4261	4262	1	4261	4262	1	4261	4262	1	4261	4262	1
- Pier A27	4271	4272	1	4271	4272	1	4271	4272	1	4271	4272	1
- Pier A28	4281	4282	1	4281	4282	1	4281	4282	1	4281	4282	1
- Pier A29	4291	4292	1	4291	4292	1	4291	4292	1	4291	4292	1
- Pier A30	4301	4302	1	4301	4302	1	4301	4302	1	4301	4302	1
- Pier A31	4311	4312	1	4311	4312	1	4311	4312	1	4311	4312	1
- Pier A32	4321	4322	1	4321	4322	1	4321	4322	1	4321	4322	1
- Pier A33	4331	4332	1	4331	4332	1	4331	4332	1	4331	4332	1
- Pier A34	4341	4342	1	4341	4342	1	4341	4342	1	4341	4342	1
- Pier A35	4351	4352	1	4351	4352	1	4351	4352	1	4351	4352	1
- Pier A36	4361	4362	1	4361	4362	1	4361	4362	1	4361	4362	1
- Pier A37	4371	4372	1	4371	4372	1	4371	4372	1	4371	4372	1
- Pier A38	4381	4382	1	4381	4382	1	4381	4382	1	4381	4382	1
- Pier A39	4391	4392	1	4391	4392	1				4391	4392	1
- Pier A40	4401	4402	1	4401	4402	1						
Pontoon, floating bridge												
- Pontoon A3	5031	5034	1	5031	5034	1	5031	5034	1	5031	5034	1
- Pontoon A4	5041	5044	1	5041	5044	1	5041	5044	1	5041	5044	1
- Pontoon A5	5051	5054	1	5051	5054	1	5051	5054	1	5051	5054	1
- Pontoon A6	5061	5064	1	5061	5064	1	5061	5064	1	5061	5064	1
- Pontoon A7	5071	5074	1	5071	5074	1	5071	5074	1	5071	5074	1
- Pontoon A8	5081	5084	1	5081	5084	1	5081	5084	1	5081	5084	1
- Pontoon A9	5091	5094	1	5091	5094	1	5091	5094	1	5091	5094	1
- Pontoon A10	5101	5104	1	5101	5104	1	5101	5104	1	5101	5104	1
- Pontoon A11	5111	5114	1	5111	5114	1	5111	5114	1	5111	5114	1
- Pontoon A12	5121	5124	1	5121	5124	1	5121	5124	1	5121	5124	1
- Pontoon A13	5131	5134	1	5131	5134	1	5131	5134	1	5131	5134	1
- Pontoon A14	5141	5144	1	5141	5144	1	5141	5144	1	5141	5144	1
- Pontoon A15	5151	5154	1	5151	5154	1	5151	5154	1	5151	5154	1
- Pontoon A16	5161	5164	1	5161	5164	1	5161	5164	1	5161	5164	1
- Pontoon A17	5171	5174	1	5171	5174	1	5171	5174	1	5171	5174	1
- Pontoon A18	5181	5184	1	5181	5184	1	5181	5184	1	5181	5184	1
- Pontoon A19	5191	5194	1	5191	5194	1	5191	5194	1	5191	5194	1
- Pontoon A20	5201	5204	1	5201	5204	1	5201	5204	1	5201	5204	1
- Pontoon A21	5211	5214	1	5211	5214	1	5211	5214	1	5211	5214	1
- Pontoon A22	5221	5224	1	5221	5224	1	5221	5224	1	5221	5224	1
- Pontoon A23	5231	5234	1	5231	5234	1	5231	5234	1	5231	5234	1
- Pontoon A24	5241	5244	1	5241	5244	1	5241	5244	1	5241	5244	1
- Pontoon A25	5251	5254	1	5251	5254	1	5251	5254	1	5251	5254	1
- Pontoon A26	5261	5264	1	5261	5264	1	5261	5264	1	5261	5264	1
- Pontoon A27	5271	5274	1	5271	5274	1	5271	5274	1	5271	5274	1
- Pontoon A28	5281	5284	1	5281	5284	1	5281	5284	1	5281	5284	1
- Pontoon A29	5291	5294	1	5291	5294	1	5291	5294	1	5291	5294	1
- Pontoon A30	5301	5304	1	5301	5304	1	5301	5304	1	5301	5304	1
- Pontoon A31	5311	5314	1	5311	5314	1	5311	5314	1	5311	5314	1
- Pontoon A32	5321	5324	1	5321	5324	1	5321	5324	1	5321	5324	1
- Pontoon A33	5331	5334	1	5331	5334	1	5331	5334	1	5331	5334	1
- Pontoon A34	5341	5344	1	5341	5344	1	5341	5344	1	5341	5344	1
- Pontoon A35	5351	5354	1	5351	5354	1	5351	5354	1	5351	5354	1
- Pontoon A36	5361	5364	1	5361	5364	1	5361	5364	1	5361	5364	1
- Pontoon A37	5371	5374	1	5371	5374	1	5371	5374	1	5371	5374	1
- Pontoon A38	5381	5384	1	5381	5384	1	5381	5384	1	5381	5384	1
- Pontoon A39	5391	5394	1	5391	5394	1				5391	5394	1
- Pontoon A40	5401	5404	1	5401	5404	1						
Pylon, A2												
- Lower Leg, right	3101	3108	1	3101	3108	1	3101	3108	1	3101	3108	1
- Upper Leg, right	3110	3125	1	3110	3125	1	3110	3125	1	3110	3125	1
- Lower Leg, left	3201	3208	1	3201	3208	1	3201	3208	1	3201	3208	1
- Upper Leg, Left	3210	3225	1	3210	3225	1	3210	3225	1	3210	3225	1
- Spire	3301	3308	1	3301	3308	1	3301	3308	1	3301	3308	1
- Cross-beam	3401	3402	1	3401	3402	1	3401	3402	1	3401	3402	1
Cables												
- Back span, right	21011	21181	10	21011	21181	10	21011	21181	10	21011	21181	10
- Back span, left	22011	22181	10	22011	22181	10	22011	22181	10	22011	22181	10
- Main span, right	23011	23181	10	23011	23181	10	23011	23181	10	23011	23181	10
- Main span, left	24011	24181	10	24011	24181	10	24011	24181	10	24011	24181	10

Table 3-3 Spring element numbering in RM Bridge for K11, K12, K13 and K14

	K11 - Spring elements			K12 - Spring elements			K13 - Spring elements			K14 - Spring elements		
	Start	End	Step	Start	End	Step	Start	End	Step	Start	End	Step
Bridge girder												
- High bridge	13100	(Abutment, start)		13100	(Abutment, start)		13100	(Abutment, start)		13100	(Abutment, start)	
	31191	(Connection, high/floating)		31191	(Connection, high/floating)		31191	(Connection, high/floating)		31191	(Connection, high/floating)	
- Floating bridge	13200	(Abutment, end)		13200	(Abutment, end)		13200	(Abutment, end)		13200	(Abutment, end)	
Pier, viaduct												
- Pier A1-A	12100	(Foundation - Pier A1-A)		12100	(Foundation - Pier A1-A)		12100	(Foundation - Pier A1-A)		12100	(Foundation - Pier A1-A)	
- Pier A1-B	12200	(Foundation - Pier A1-B)		12200	(Foundation - Pier A1-B)		12200	(Foundation - Pier A1-B)		12200	(Foundation - Pier A1-B)	
- Pier A1-C	12300	(Foundation - Pier A1-C)		12300	(Foundation - Pier A1-C)		12300	(Foundation - Pier A1-C)		12300	(Foundation - Pier A1-C)	
- Pier A1-D	12400	(Foundation - Pier A1-D)		12400	(Foundation - Pier A1-D)		12400	(Foundation - Pier A1-D)		12400	(Foundation - Pier A1-D)	
- Pier A1-E	12500	(Foundation - Pier A1-E)		12500	(Foundation - Pier A1-E)		12500	(Foundation - Pier A1-E)		12500	(Foundation - Pier A1-E)	
Pontoon, floating bridge	Stiff-Vertical	Stiff-Roll	Water plane	Stiff-Vertical	Stiff-Roll	Water plane	Stiff-Vertical	Stiff-Roll	Water plane	Stiff-Vertical	Stiff-Roll	Water plane
- Pontoon A3	50103	50203	30030	50103	50203	30030	50103	50203	30030	50103	50203	30030
- Pontoon A4	50104	50204	30040	50104	50204	30040	50104	50204	30040	50104	50204	30040
- Pontoon A5	50105	50205	30050	50105	50205	30050	50105	50205	30050	50105	50205	30050
- Pontoon A6	50106	50206	30060	50106	50206	30060	50106	50206	30060	50106	50206	30060
- Pontoon A7	50107	50207	30070	50107	50207	30070	50107	50207	30070	50107	50207	30070
- Pontoon A8	50108	50208	30080	50108	50208	30080	50108	50208	30080	50108	50208	30080
- Pontoon A9	50109	50209	30090	50109	50209	30090	50109	50209	30090	50109	50209	30090
- Pontoon A10	50110	50210	30100	50110	50210	30100	50110	50210	30100	50110	50210	30100
- Pontoon A11	50111	50211	30110	50111	50211	30110	50111	50211	30110	50111	50211	30110
- Pontoon A12	50112	50212	30120	50112	50212	30120	50112	50212	30120	50112	50212	30120
- Pontoon A13	50113	50213	30130	50113	50213	30130	50113	50213	30130	50113	50213	30130
- Pontoon A14	50114	50214	30140	50114	50214	30140	50114	50214	30140	50114	50214	30140
- Pontoon A15	50115	50215	30150	50115	50215	30150	50115	50215	30150	50115	50215	30150
- Pontoon A16	50116	50216	30160	50116	50216	30160	50116	50216	30160	50116	50216	30160
- Pontoon A17	50117	50217	30170	50117	50217	30170	50117	50217	30170	50117	50217	30170
- Pontoon A18	50118	50218	30180	50118	50218	30180	50118	50218	30180	50118	50218	30180
- Pontoon A19	50119	50219	30190	50119	50219	30190	50119	50219	30190	50119	50219	30190
- Pontoon A20	50120	50220	30200	50120	50220	30200	50120	50220	30200	50120	50220	30200
- Pontoon A21	50121	50221	30210	50121	50221	30210	50121	50221	30210	50121	50221	30210
- Pontoon A22	50122	50222	30220	50122	50222	30220	50122	50222	30220	50122	50222	30220
- Pontoon A23	50123	50223	30230	50123	50223	30230	50123	50223	30230	50123	50223	30230
- Pontoon A24	50124	50224	30240	50124	50224	30240	50124	50224	30240	50124	50224	30240
- Pontoon A25	50125	50225	30250	50125	50225	30250	50125	50225	30250	50125	50225	30250
- Pontoon A26	50126	50226	30260	50126	50226	30260	50126	50226	30260	50126	50226	30260
- Pontoon A27	50127	50227	30270	50127	50227	30270	50127	50227	30270	50127	50227	30270
- Pontoon A28	50128	50228	30280	50128	50228	30280	50128	50228	30280	50128	50228	30280
- Pontoon A29	50129	50229	30290	50129	50229	30290	50129	50229	30290	50129	50229	30290
- Pontoon A30	50130	50230	30300	50130	50230	30300	50130	50230	30300	50130	50230	30300
- Pontoon A31	50131	50231	30310	50131	50231	30310	50131	50231	30310	50131	50231	30310
- Pontoon A32	50132	50232	30320	50132	50232	30320	50132	50232	30320	50132	50232	30320
- Pontoon A33	50133	50233	30330	50133	50233	30330	50133	50233	30330	50133	50233	30330
- Pontoon A34	50134	50234	30340	50134	50234	30340	50134	50234	30340	50134	50234	30340
- Pontoon A35	50135	50235	30350	50135	50235	30350	50135	50235	30350	50135	50235	30350
- Pontoon A36	50136	50236	30360	50136	50236	30360	50136	50236	30360	50136	50236	30360
- Pontoon A37	50137	50237	30370	50137	50237	30370	50137	50237	30370	50137	50237	30370
- Pontoon A38	50138	50238	30380	50138	50238	30380	50138	50238	30380	50138	50238	30380
- Pontoon A39	50139	50239	30390	50139	50239	30390				50139	50239	30390
- Pontoon A40	50140	50240	30400	50140	50240	30400						
Pylon, A2												
- Lower Leg, right	32010	(Foundation, right pylon leg)		32010	(Foundation, right pylon leg)		32010	(Foundation, right pylon leg)		32010	(Foundation, right pylon leg)	
- Upper Leg, right	32020	(Foundation, left pylon leg)		32020	(Foundation, left pylon leg)		32020	(Foundation, left pylon leg)		32020	(Foundation, left pylon leg)	
- Lower Leg, left	32011	(Right vert. supp. of MG on Pylon)		32011	(Right vert. supp. of MG on Pylon)		32011	(Right vert. supp. of MG on Pylon)		32011	(Right vert. supp. of MG on Pylon)	
- Upper Leg, Left	32012	(Left vert. supp. of MG on Pylon)		32012	(Left vert. supp. of MG on Pylon)		32012	(Left vert. supp. of MG on Pylon)		32012	(Left vert. supp. of MG on Pylon)	
- Spire	32111	(Hor. supp. of MG on Pylon)		32111	(Hor. supp. of MG on Pylon)		32111	(Hor. supp. of MG on Pylon)		32111	(Hor. supp. of MG on Pylon)	
- Cross-beam												
Mooring lines												
- Mooring A8				40081			40081			40081		
- Mooring A16				40161			40161			40161		
- Mooring A24				40241			40241			40241		
- Mooring A32				40321			40321			40321		

3.2 Traffic analysis in RM Bridge

In RM Bridge the loaded length (in RM referred to QLEN) is chosen as the minimum of the actual influence length (sum of contributing parts between zero points in the influence line) or the sum of equivalent triangular bases calculated based on the peak influence value and the integrated area for each contributing influence parts of the influence line. The load intensity is then based on this calculated loaded length but applies on the whole influence length between zero-points (not only on the calculated loaded length). This procedure applies for all leading displacement and force components in the traffic load combination.

An example is given below for the torque moment in the bridge girder at axis 19 (RM element 507, pnt.1) for Lane 1 as notational lane 1 and the uniformly distributed load (varies between 16.2kN/m and 13.5kN/m). The load intensity for the green part is in RM calculated to 14.663kN/m. By hand this can be calculated as $QLEN = \left(\frac{14.663kN}{m} - \frac{16.2kN}{m}\right) \cdot \left(\frac{1000m - 200m}{\frac{13.5kN}{m} - \frac{16.2kN}{m}}\right) + 200m = 655.55m$ which also is indicated in the upper plot in Table 3-4. This load is then applied on the whole green part of the lower plot of the influence line.

Table 3-4 Example, torque in bridge girder at axis 19.

Equivalent loaded length (base of equivalent triangle):
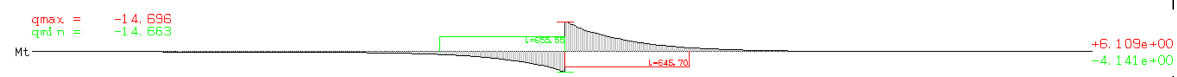
Influence length between zero-points in the influence line:
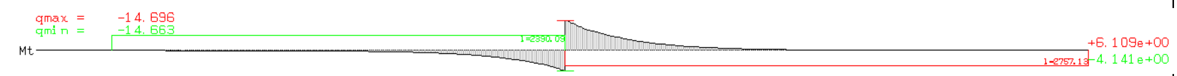

If one instead studying the roll in the bridge girder for the same lane and load train the calculated loaded length is smaller than the influence lines but still longer then 1000m, hence the lower bound traffic loads apply for this check, see Table 3-5.

Table 3-5 Example, roll about bridge girder at axis 19.

Equivalent loaded length (base of equivalent triangle):
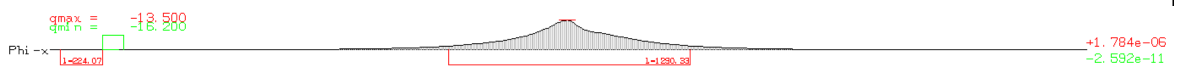
Influence length between zero-points in the influence line:
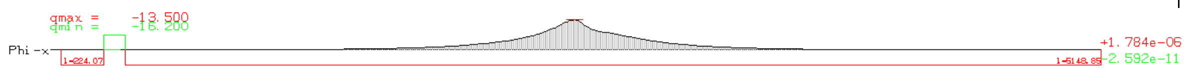

An other example is given below in Table 3-6 for the same section (axis 19) and lane and load train but for the weak axis moment (Mz). The load intensity corresponding to the red parts are

$$q(QLEN) = \frac{16.2kN}{m} + \frac{\frac{13.5kN}{m} - \frac{16.2kN}{m}}{1000m - 200m} \cdot (249.27m + 249.57m - 200m) = \frac{15.191kN}{m}$$

which is the same as calculated in the RM module. One can also observe that the green parts have a total loaded length longer than 1000m (QLEN=2107.15m+2475.02m+~77m+m>1000m) but the used load intensity is 14.137kN/m which indicates that the loaded length is based on the equivalent triangle bases which in sum is calculated to QLEN=811.29m. This influence line among the other force and displacement components at this section can also be found in Figure 3-5.

Table 3-6 Example, weak axis bending in bridge girder at axis 19.

Equivalent loaded length (base of equivalent triangle): 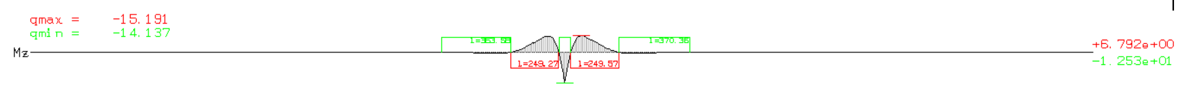
Influence length between zero-points in the influence line: 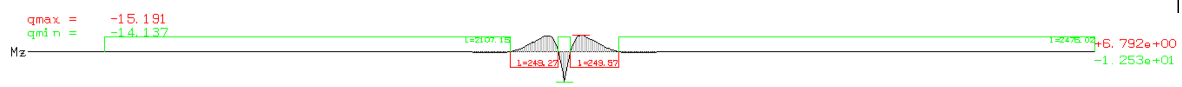

3.2.1 Load trains

The variable load intensity depending on the loaded length is defined with a load function, see Table 3-8 and Figure 3-1. The following Load trains are evaluated:

Table 3-7 Load trains in RM

Load train number	Load train type	Load	Load function
11	TS, no.lane 1:	2x300kN	
12	TS, no.lane 2:	2x200kN	
13	TS, no.lane 3:	2x100kN	
21	UDL, no.lane 1:	Var. 16.2 to 13.5kN/m	q1(qlen)
22	UDL, no.lane 2:	Var. 7.5 to 7.5kN/m	q2(qlen)
23	UDL, no.lane 3:	Var. 7.5 to 0kN/m	q3(qlen)
24	UDL, no.lane 4:	Var. 7.5 to 7.5kN/m	q4(qlen)
25	UDL, no.lane 5:	Var. 7.5 to 7.5kN/m	q5(qlen)
26	UDL, no.lane 6:	Var. 7.5 to 0kN/m	q6(qlen)
27	UDL, footway:	Var. 7.5 to 1.875kN/m	qf(qlen)
121	UDL, no.lane 1 (200m):	16.2kN/m	
122	UDL, no.lane 2 (200m):	7.5kN/m	
123	UDL, no.lane 3 (200m):	7.5kN/m	
124	UDL, no.lane 4 (200m):	7.5kN/m	
125	UDL, no.lane 5 (200m):	7.5kN/m	
126	UDL, no.lane 6 (200m):	7.5kN/m	
127	UDL, footway (200m):	7.5kN/m	
31	UDL, no.lane 1 (1000m):	13.5kN/m	
32	UDL, no.lane 2 (1000m):	7.5kN/m	
33	UDL, no.lane 3 (1000m):	7.5kN/m	
34	UDL, no.lane 4 (1000m):	7.5kN/m	
35	UDL, no.lane 5 (1000m):	0kN/m	
36	UDL, footway (1000m):	1.875kN/m	

Table 3-8 Load functions – load intensity depending on loaded length in each notational lane

	Lane nr:	#1		#2		#3		#4		#5		#6		#7	Sum:	
	Load length	q	Q	q	Q	q	Q	q	Q	q	Q	q	Q	q	q	Q
Heaviest traffic to the left	0	16.200	600	7.500	400	7.500	200	7.500	0	7.500	0	7.500	0	7.500	61.200	1200
	200	16.200	600	7.500	400	7.500	200	7.500	0	7.500	0	7.500	0	7.500	61.200	1200
	400	15.525	600	7.500	400	5.625	0	7.500	200	7.500	0	5.625	0	6.094	55.369	1200
	600	14.850	600	7.500	400	3.750	0	7.500	200	7.500	0	3.750	0	4.688	49.538	1200
	800	14.175	600	7.500	400	1.875	0	7.500	200	7.500	0	1.875	0	3.281	43.706	1200
	1000	13.500	600	7.500	400	0.000	0	7.500	200	7.500	0	0.000	0	1.875	37.875	1200
	5000	13.500	600	7.500	400	0.000	0	7.500	200	7.500	0	0.000	0	1.875	37.875	1200
Heaviest traffic to the right	0	7.500	0	7.500	0	7.500	0	7.500	200	7.500	400	16.200	600	7.500	61.200	1200
	200	7.500	0	7.500	0	7.500	0	7.500	200	7.500	400	16.200	600	7.500	61.200	1200
	400	5.625	0	7.500	0	7.500	200	5.625	0	7.500	400	15.525	600	6.094	55.369	1200
	600	3.750	0	7.500	0	7.500	200	3.750	0	7.500	400	14.850	600	4.688	49.538	1200
	800	1.875	0	7.500	0	7.500	200	1.875	0	7.500	400	14.175	600	3.281	43.706	1200
	1000	0.000	0	7.500	0	7.500	200	0.000	0	7.500	400	13.500	600	1.875	37.875	1200
	5000	0.000	0	7.500	0	7.500	200	0.000	0	7.500	400	13.500	600	1.875	37.875	1200

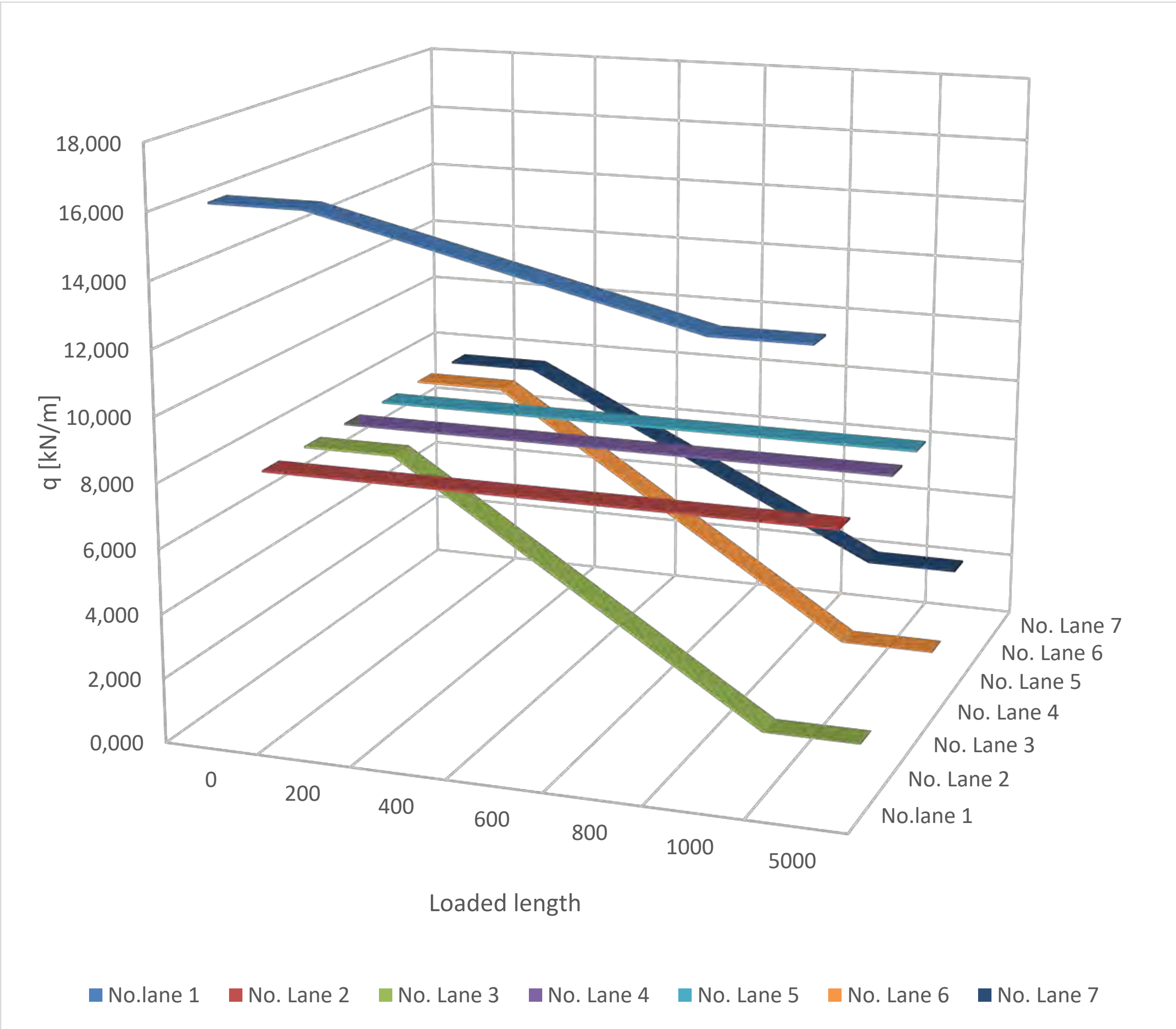

Figure 3-1 Load function - load intensity depending on loaded length in each notational lane

3.2.2 Traffic load combinations

Combinations rules

SupAndSup - Conditional adding of the result values of an envelope to the contents of the treated superposition file (if they are unfavorable).

SupOrSup - Conditional replacement of the current envelope result values by the result values of the envelope being superimposed (if they are more unfavorable).

Traffic loading, loaded length dependent traffic loading

Table 3-9 Left-adjusted traffic loading – single load train and lane sup-files

Lane	Lane number in RM	Load train number in RM	Sup-file
1	101	21	ln1-qlen-L-q1.sup
		11	ln1-qlen-L-P1.sup
2	102	22	ln2-qlen-L-q2.sup
		12	ln2-qlen-L-P2.sup
3	103	23	ln3-qlen-L-q3.sup
		13	ln3-qlen-L-P3.sup
4	104	24	ln4-qlen-L-q4.sup
		13	ln4-qlen-L-P3.sup
5	105	25	ln5-qlen-L-q5.sup
6	106	26	ln6-qlen-L-q6.sup
7/f	107	27	lnf-qlen-L-qf.sup

To account for the shift in number of notational lanes the tandem load 3 shifts from lane 3 to lane 4. To account for this the tandem load is placed both on lane 3 and 4 and the most unfavourable response is included in the traffic load combination, see Table 3-10.

Table 3-10 Left-adjusted traffic loading - Tandem load 3 placed both on lane 3 and 4. Unfavourable response from the two are used in the combination

Sup-file	Combination rule	Sup-file
ln34-qlen-L-P3.sup	SupOrSup	ln3-qlen-L-P3.sup
	SupOrSup	ln4-qlen-L-P3.sup

Table 3-11 Left-adjusted traffic loading – Load length dependent traffic loading

Sup-file	Combination rule	Sup-file
Q-Trf-qlen-L.sup	SupAndSup	ln1-qlen-L-q1.sup
	SupAndSup	ln1-qlen-L-P1.sup
	SupAndSup	ln2-qlen-L-q2.sup
	SupAndSup	ln2-qlen-L-P2.sup
	SupAndSup	ln3-qlen-L-q3.sup
	SupAndSup	ln34-qlen-L-P3.sup
	SupAndSup	ln4-qlen-L-q4.sup
	SupAndSup	ln5-qlen-L-q5.sup
	SupAndSup	ln6-qlen-L-q6.sup
	SupAndSup	lnf-qlen-L-qf.sup

Table 3-12 Right-adjusted traffic loading – single load train and lane sup-files

Lane number	Load train	Sup-file
106	21	ln6-qlen-R-q1.sup
106	11	ln6-qlen-R-P1.sup
105	22	ln5-qlen-R-q2.sup
105	12	ln5-qlen-R-P2.sup
104	23	ln4-qlen-R-q3.sup
104	13	ln4-qlen-R-P3.sup
103	24	ln3-qlen-R-q4.sup
103	13	ln3-qlen-R-P3.sup
102	25	ln2-qlen-R-q5.sup
101	26	ln1-qlen-R-q6.sup
107	27	lnf-qlen-R-qf.sup

To account for the shift in notational lanes the tandem load 3 shifts from lane 3 to lane 4. To account for this the tandem load is placed both on lane 3 and 4 and the most unfavourable response is included in the traffic load combination, see Table 3-13.

Table 3-13 Right-adjusted traffic loading - Tandem load 3 placed both on lane 3 and 4. Unfavourable response from the two are used in the combination

Sup-file	Combination rule	Sup-file
ln34-qlen-R-P3.sup	SupOrSup	ln3-qlen-R-P3.sup
	SupOrSup	ln4-qlen-R-P3.sup

Table 3-14 Right-adjusted traffic loading – Load length dependent traffic loading

Sup-file	Combination rule	Sup-file
Q-Trf-qlen-R.sup	SupAndSup	ln6-qlen-R-q1.sup
	SupAndSup	ln6-qlen-R-P1.sup
	SupAndSup	ln5-qlen-R-q2.sup
	SupAndSup	ln5-qlen-R-P2.sup
	SupAndSup	ln4-qlen-R-q3.sup
	SupAndSup	ln34-qlen-R-P3.sup
	SupAndSup	ln3-qlen-R-q4.sup
	SupAndSup	ln2-qlen-R-q5.sup
	SupAndSup	ln1-qlen-R-q6.sup
	SupAndSup	lnf-qlen-R-qf.sup

The total response from the load length dependent traffic loading is the most unfavourable traffic situation of the left- and right-adjusted traffic situations:

Table 3-15 Load length dependent traffic loading

Sup-file	Combination rule	Sup-file
Q-Trf.sup	SupOrSup	Q-Trf-qlen-L.sup
	SupOrSup	Q-Trf-qlen-R.sup

Traffic loading, loaded length L<200m

The same procedure as for the load length dependent traffic loading applies for this traffic load situation. Instead of using the load train 20-series the 120- series is used, see Table 3-7. This situation have no restrictions on the load length or intensity. The response is stored in sup-file Q-Trf-200m-inf.sup. This loading situation is an upper bound of the traffic loading and is included for verification only.

Traffic loading, loaded length l>1000m

The same procedure as for the load length dependent traffic loading applies for this traffic load situation. Instead of using the load train 20-series the 30-series is used, see Table 3-7. This situation have no restrictions on the load length or intensity. The response is stored in sup-file Q-Trf-1000m.sup. This loading situation is a lower bound of the traffic loading and is included for verification only.

3.2.3 Typical influence lines

The influence lines plotted here is for the K11 bridge concept and for Lane 1 and load train 21. There are no major differences between the different concepts.

Bridge girder

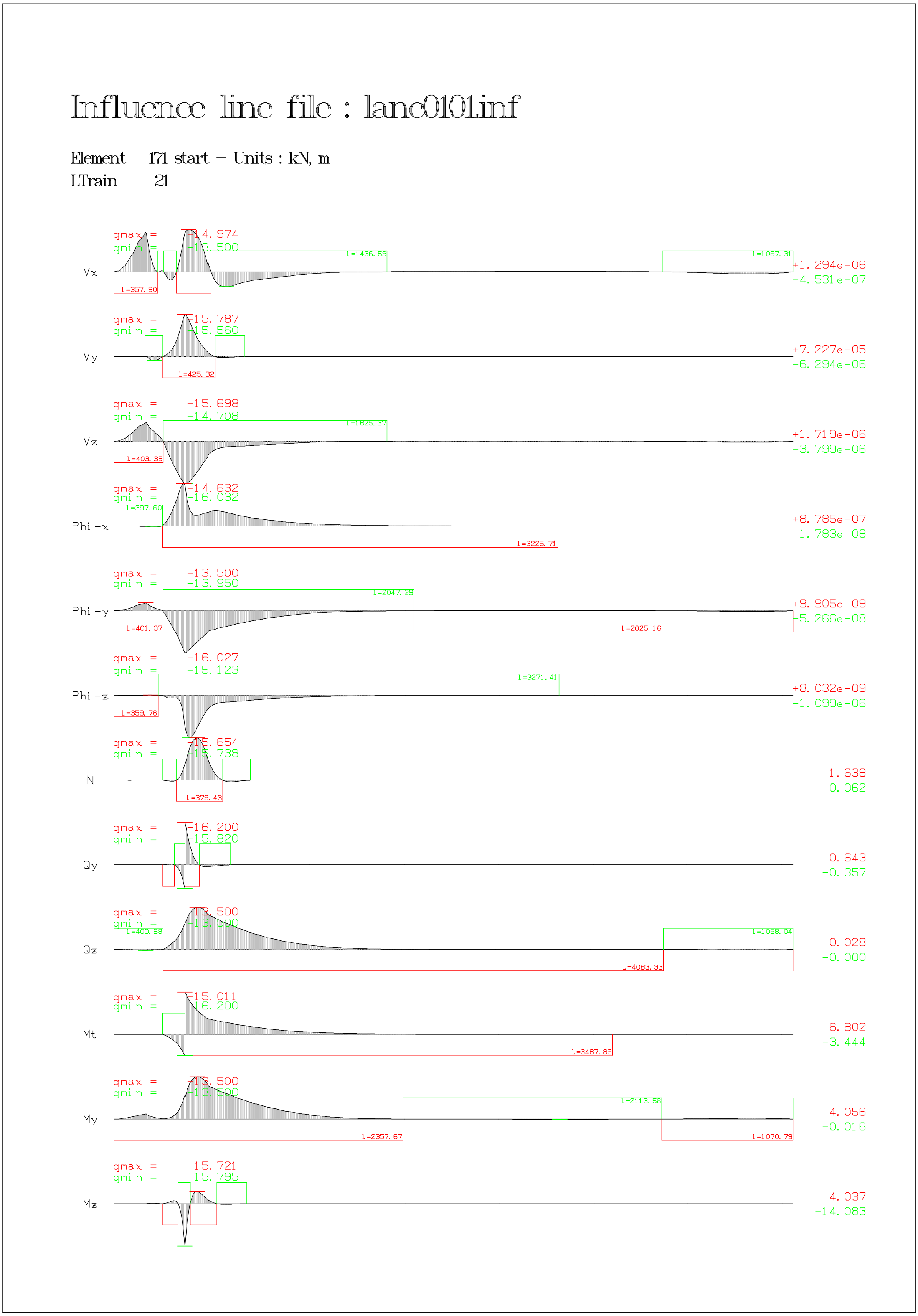

Figure 3-2 Influence lines for lane 1, load train 21 – Bridge girder section in front span high-bridge (between axis 2 and 3)

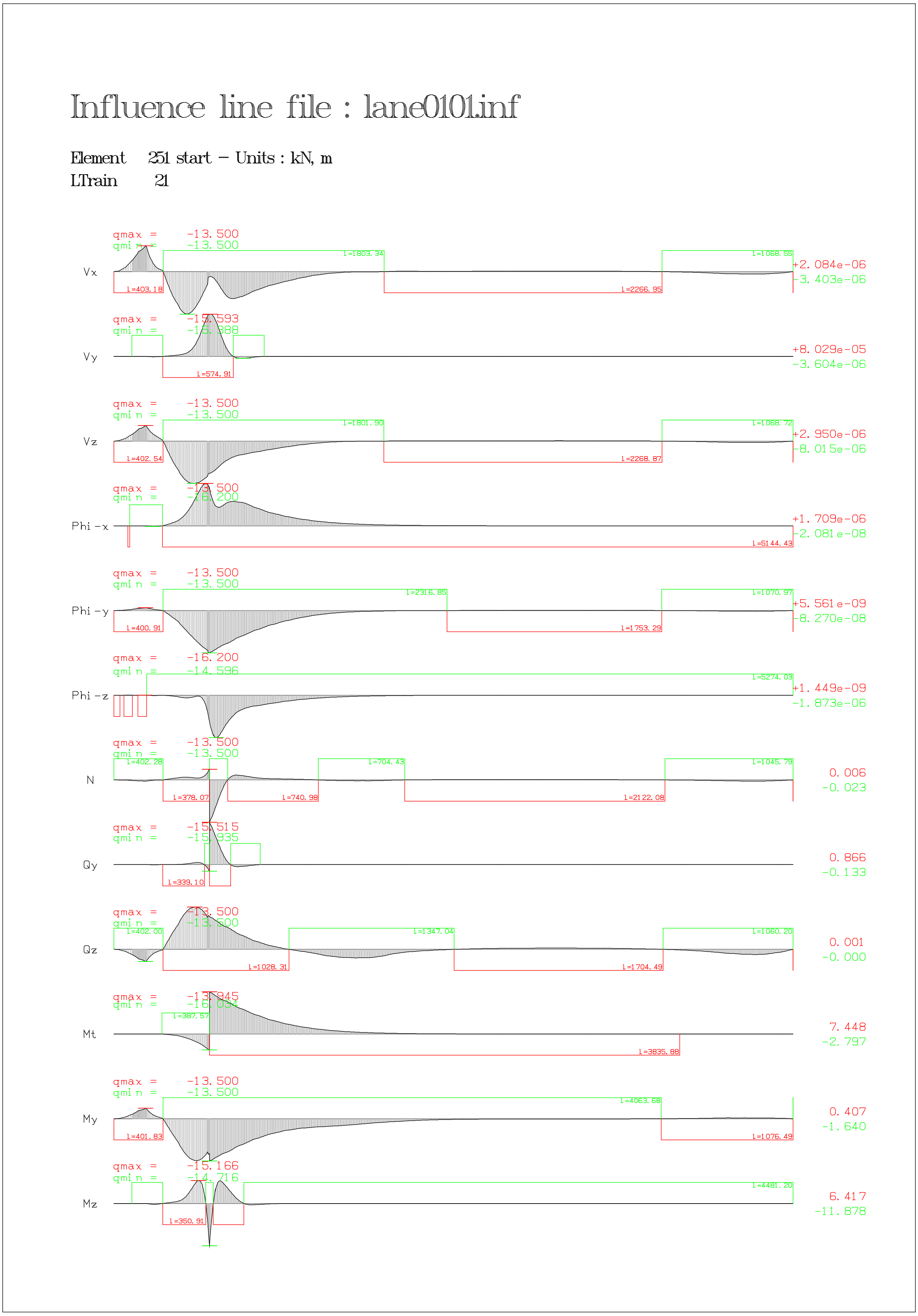

Figure 3-3 Influence lines for lane 1, load train 21 – Bridge girder support section at axis 3

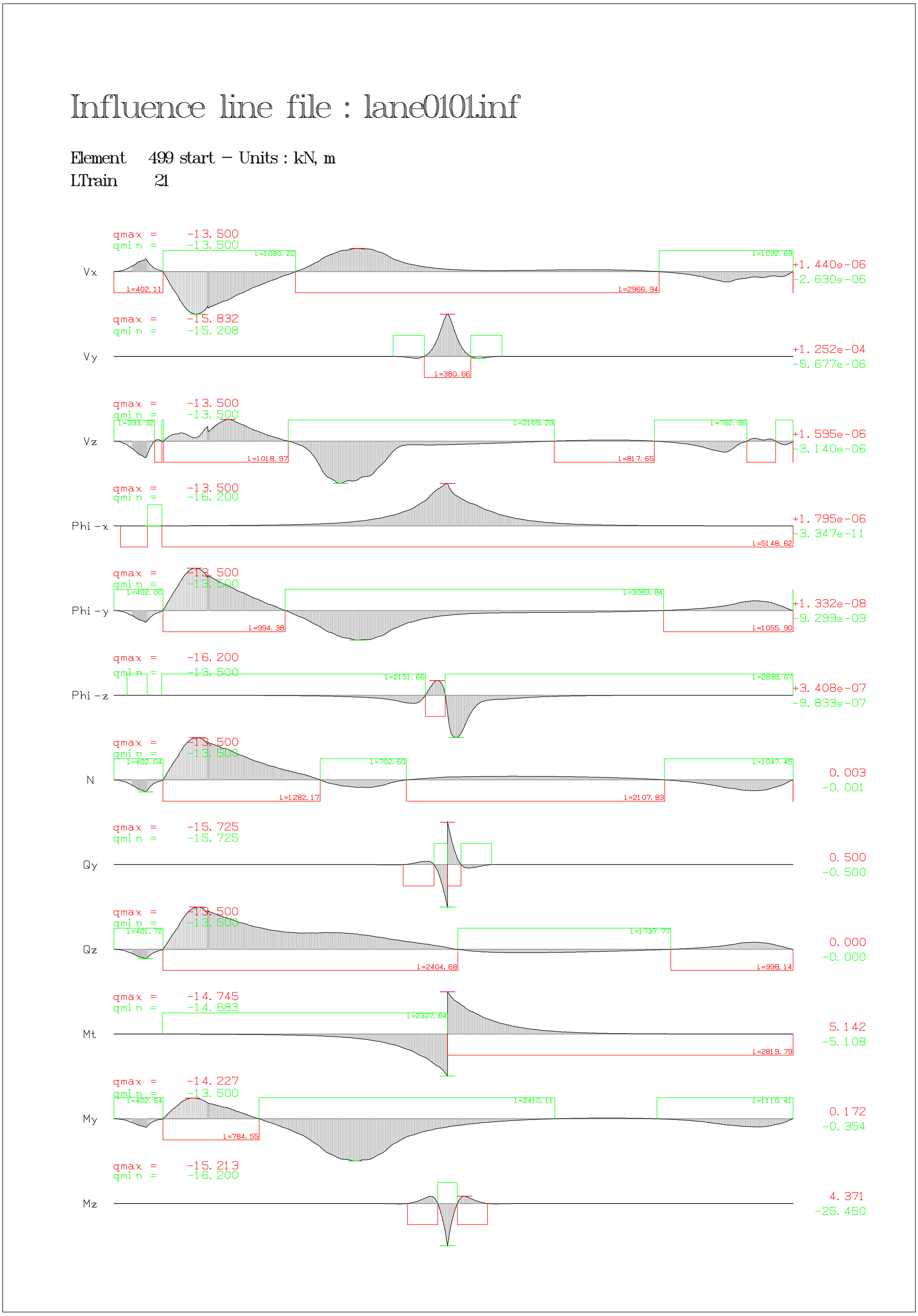

Figure 3-4 Influence lines for lane 1, load train 21 – Bridge girder span section between axis 18 and 19

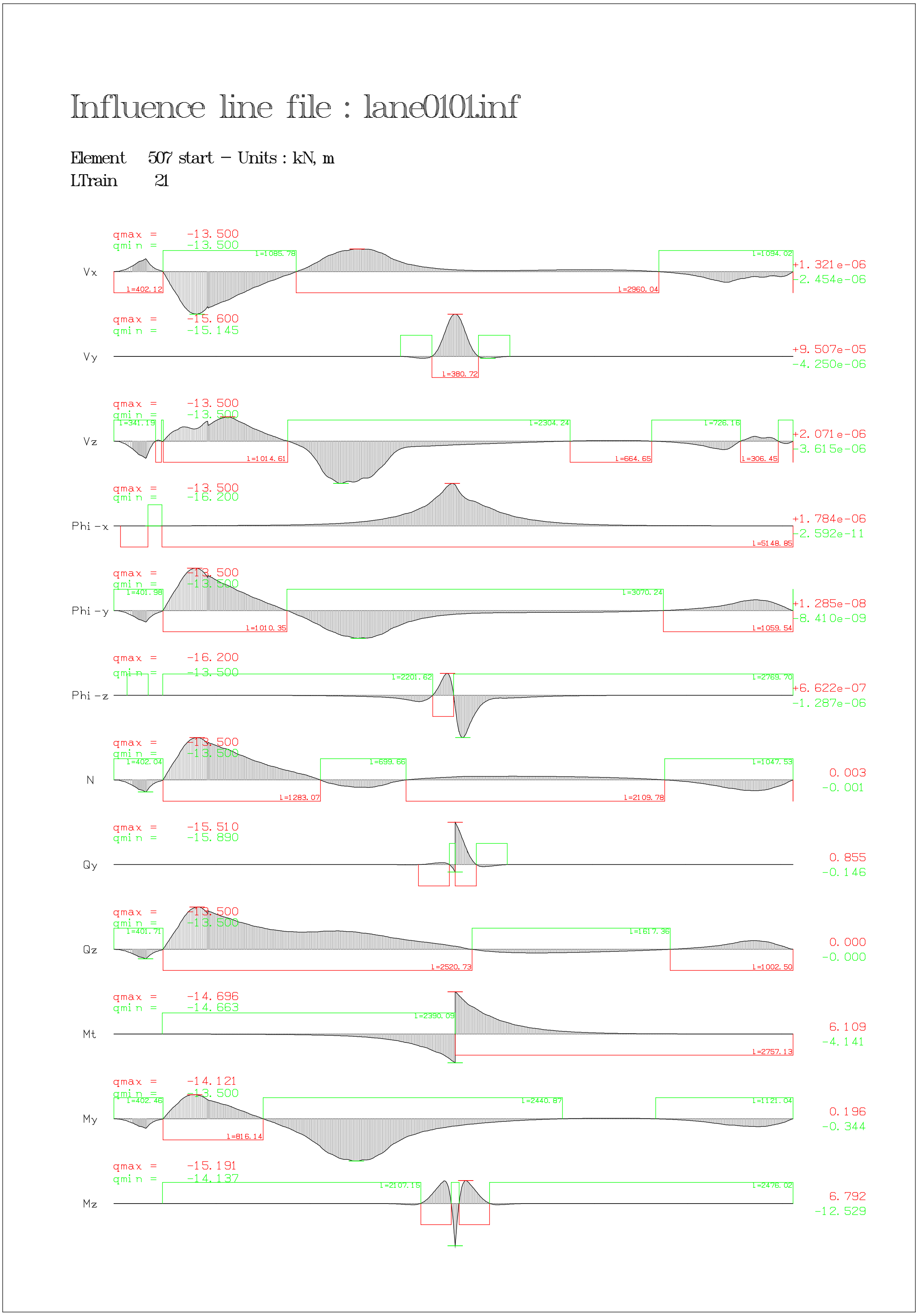

Figure 3-5 Influence lines for lane 1, load train 21 – Bridge girder support section at axis 19

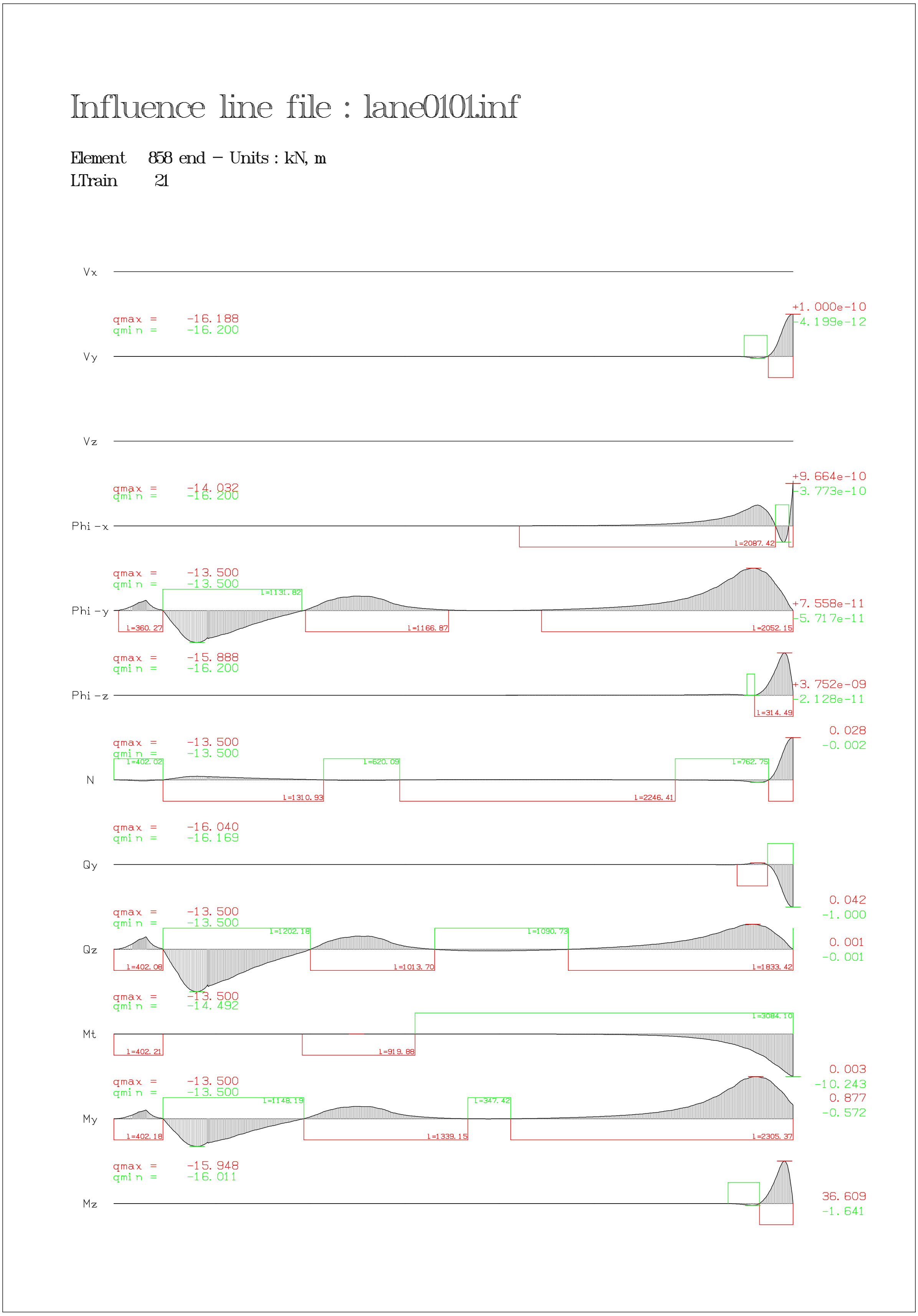

Figure 3-6 Influence lines for lane 1, load train 21 – Bridge girder support section at axis 41 (north abutment)

Pylon

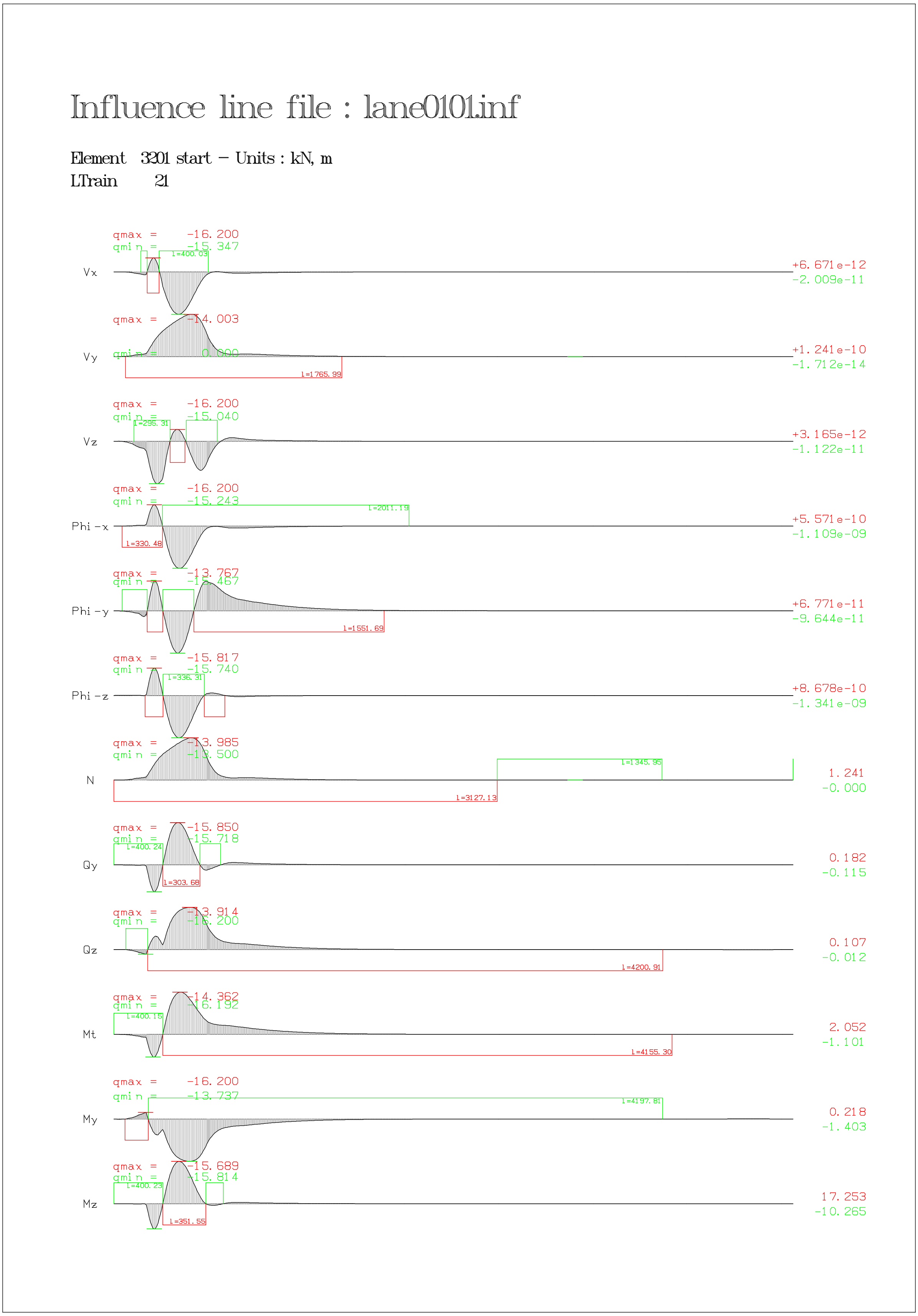

Figure 3-7 Influence lines for lane 1, load train 21 – Pylon, lower west leg at the foundation level

Stay cables

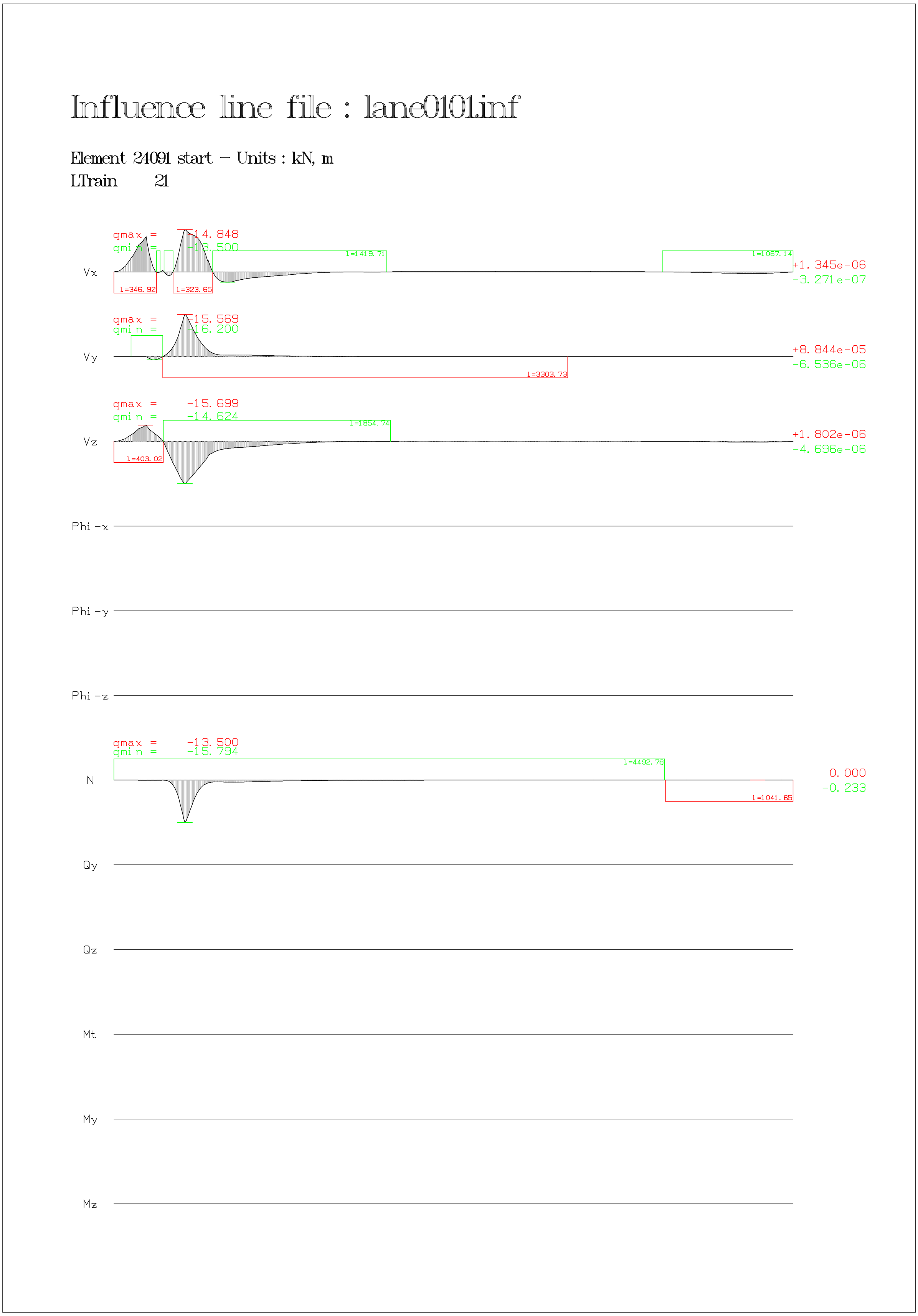

Figure 3-8 Influence lines for lane 1, load train 21 – The mid stay cable in front span, west cable plane

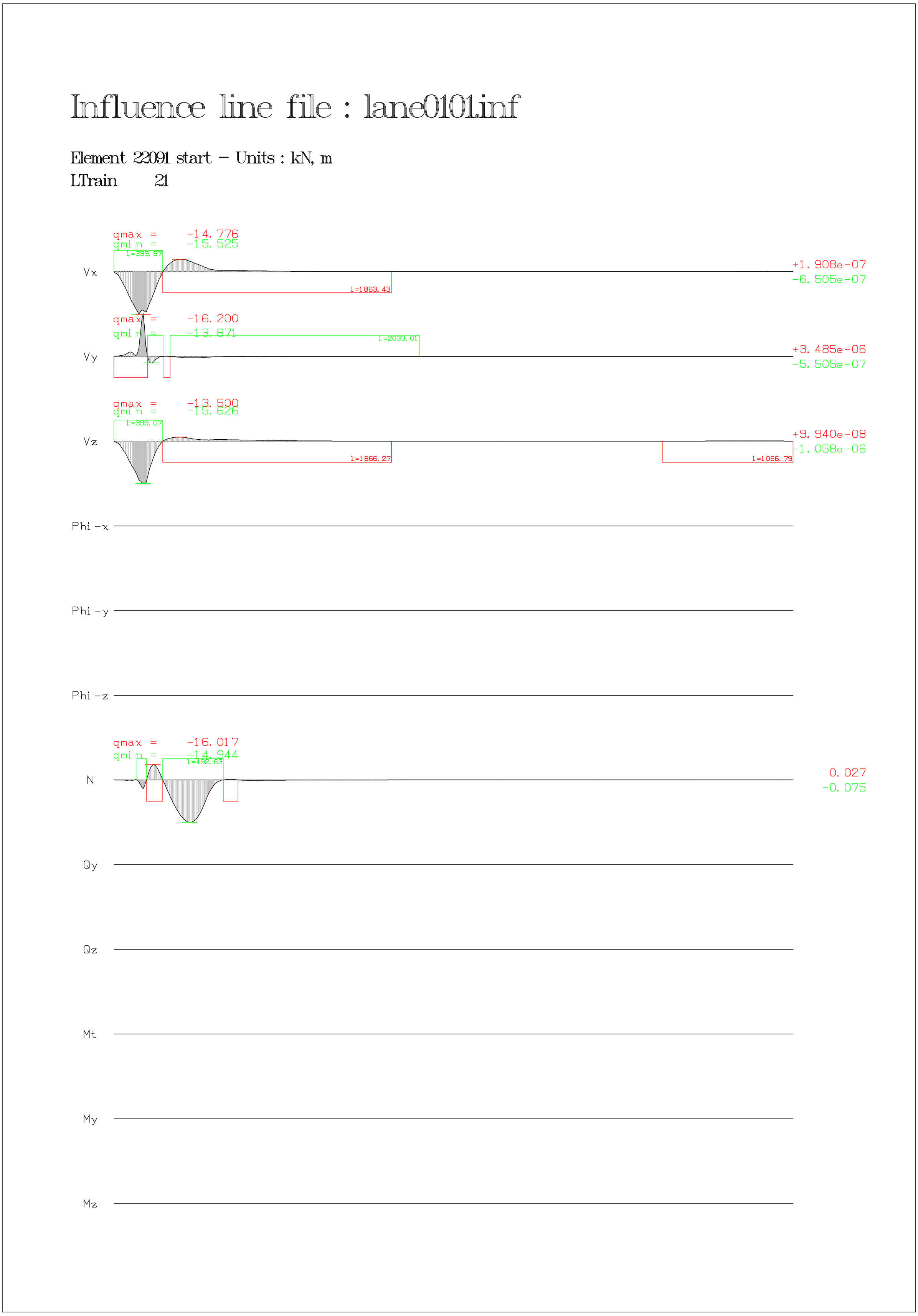

Figure 3-9 Influence lines for lane 1, load train 21 – The mid stay cable in back span, west cable plane